INTERSTELLAR SCINTILLATION OF PULSARS AT 327 MHZ

By

V. BALASUBRAMANIAN

Tata Institute of Fundamental Research
Homi Bhabha Road, Bombay 400 005, India

A Thesis
Submitted for the Ph.D. degree
of the
University of Bombay

May 1979

SYNOPSIS

Pulsars are a new class of galactic objects discovered a decade ago. Their pulsed radio emission is characterised by very regular repetition rates. However, their amplitudes show erratic fluctuations, over time scales ranging from less than a second (i.e. pulse to pulse fluctuations) to several days or longer. The intensity fluctuations with time scales of several minutes are explainable as arising from scintillations due to irregularities in electron density of the interstellar (IS) medium between the observer and the source. These interstellar scintillations (ISS) are characterised by very narrow bandwidths - a few to several hundred kilohertz - over which the intensities are correlated. In contrast to the above, the intrinsic intensity variations - like the pulse to pulse fluctuations with time scales on the order of a few seconds or less - are correlated over several hundred megahertz. In this thesis we describe the observations and analysis of intensity fluctuations of 33 pulsars observed at 327 MHz with the Ooty Radio Telescope.

The theory of ISS of radio waves, as applicable to an extended IS medium model is reviewed in Chapter II. The theory is based on the coherence function approach using Markov approximation. In particular, we have discussed the effect of receiver bandwidth on the observable characteristics of ISS, considering two different models, Gaussian and Kolmogorov spectral models, of the spectrum of irregularities in the interstellar space. Further, a method has been developed by which one can detect the existence or otherwise of intrinsic intensity fluctuations with time scales similar to those produced by ISS.

In Chapter III we describe the salient features of the receiver system used, the observational procedures and the techniques adopted for data reduction, including those used for correcting the data for receiver noise. The observational parameters relevant to intensity fluctuations are defined in this chapter.

Details of the methods used for deducing ISS parameters like decorrelation frequency, scintillation index and scintillation bandwidth from the parameters of the observed intensity fluctuations are given in Chapter IV. These methods incorporate corrections for effects due to the finite bandwidth of the receiver and intensity variations intrinsic to the source. The probable bias in the measurements of these parameters by earlier workers without incorporating these corrections is also pointed out. It is shown that if finite bandwidth effects are not corrected for, the error in the estimates of decorrelation frequency could be 25 per cent or more for values of decorrelation frequency comparable to the receiver bandwidth. We give estimates of the statistical uncertainties on the observed correlations of intensities at different radio frequencies and describe how these uncertainties lead to practical difficulties in distinguishing between Gaussian and Kolmogorov spectral models of the irregularities in the IS medium.

The results obtained from our observations are presented in Chapter V. The decorrelation frequencies for 22 pulsars have been derived. The observationally determined cross correlations of intensities at different frequencies are compared with those predicted from theoretical models. Observational evidence is found for the presence of intrinsic intensity fluctuations with time scales comparable to those due to ISS. It is shown that such fluctuations exist in many pulsars, complicating the elucidation of features of ISS. The dependence of decorrelation frequency on dispersion measure has been investigated using only the definite measurements of the former parameter for 13 pulsars. This systematic observational determination of decorrelation frequencies, free from the finite bandwidth effects and intrinsic fluctuations, shows that the dependence of decorrelation frequency on dispersion measure is steeper than that expected from theoretical models of the irregularities in the IS

medium, even for pulsars of dispersion measure less than 20 pc. cm^{-3}. Earlier investigators had found evidence for this steep dependence only for high dispersion measures (> 70) using measurements on scattering broadening of pulse shapes. Such a steep dependence is at variance with both Gaussian and Kolmogorov models of spectra of irregularities in the IS medium. We summarise the arguments - based on this discrepancy between theory and observations - leading to the conclusion of inhomogeneity of the IS medium.

Measurements of the scintillation bandwidth have been carried out for pulsars in the dispersion measure range 4.8 to 158 pc. cm^{-3}. These show absence of any trend in the relationship between scintillation bandwidth and dispersion measure. This is ascribed to any one or all of the following three reasons: (i) presence of intrinsic intensity variations with time scales similar to those due to ISS as have been deduced by us for several pulsars, (ii) the assumption of frozen scintillation pattern being untenable, as has been found from the two-station observations of ISS of pulsars which makes it difficult to estimate scale sizes of spatial intensity correlations from the observed temporal spectra of intensity fluctuations, (iii) inhomogeneity of the medium. We also point out that the linear dependence of scintillation bandwidth on dispersion measure noted by earlier investigators of ISS spectra, could be an artifact due to either the presence of intrinsic intensity variations with ISS-like time scales in some pulsars or large statistical uncertainties in the determination of the scintillation bandwidths.

Estimates of rms fluctuation in electron density derived from the observed values of decorrelation frequency, using both Gaussian and Kolmogorov spectral models are presented in the last part of Chapter V. Notable from these estimates is the inference of a region of strong fluctuations in electron density in the direction of the pulsar PSR 1642-03. The other interesting conclusion is based on estimates of the ratio of the

rms fluctuation to the average value of electron densities, obtained under the framework of the Kolmogorov model. These estimates show that the electron density distribution in the general IS medium is nonuniform, leading to the picture of a 'clumpy' aggregation of electrons in the medium. This picture of the IS medium is in consonance with that obtained from optical and other observations of the IS medium.

In the last chapter we summarise our results, point out shortcomings of using pulsars for determining the nature of the electron density irregularity spectrum of the interstellar medium and indicate possible improvements for future observations.

Statements required by the University

Statement No.(1) required under 0.770

I hereby declare that the work described in this thesis has not been submitted to this or any other university or body for a degree, diploma or any other academic award.

Statement No.(2) required under 0.771

The work reported in this thesis is based on new observations of several pulsars at 327 MHz. It has led to clear cut evidence for the first time, for the existence of intrinsic intensity fluctuations in many pulsars, with time scales similar to the fluctuations produced by interstellar scintillations (ISS). Systematic observational determination of values of the ISS parameter, decorrelation frequency has been carried out by us for several pulsars using methods which incorporate corrections for the effects of both intrinsic intensity variations and finite bandwidth of the receiver. In the determination of decorrelation frequencies by earlier workers both of these corrections have not been fully accounted for. Based on the present determination of the values of decorrelation frequency we infer the clumpiness of the distribution of electrons in the interstellar medium. Other parameters of ISS, like scintillation bandwidth and scintillation indices have also been observationally estimated for several pulsars at 327 MHz. The results from the work reported in this thesis have important implications on the question of using pulsars as probes for studying the electron density irregularities in the interstellar medium.

Statement No.(3) required under O.771

Proper references have been made where the work of other people is used or described in the thesis. The rest of the thesis can be claimed as original.

Statement No.(4) required under O.771

The observations were made in collaboration with Shri S. Krishnamohan. However, most of the analysis and interpretation described in this thesis were done by me.

LIST OF PUBLICATIONS

1. 'A Steerable Array of 968 Dipoles for Illuminating a Parabolic Cylindrical Antenna'
Kapahi, V.K., Damle, S.H. and Balasubramanian, V.
Proc. Symp. on Antennas, Radio and Telecom. Res.Committee, CSIR, New Delhi, 1968 (Supplement 3).

2. 'Period and Declination of Pulsar MP 0450'
Mohanty, D.K., Balasubramanian, V. and Swarup, G.
Indian Acad. of Sciences, 72, 246, 1970.

3. 'Large Steerable Radio Telescope at Ootacamund, India'
Swarup, G., Sarma, N.V.G., Joshi, M.N., Kapahi, V.K., Bagri, D.S., Damle, S.H., Ananthakrishnan, S., Balasubramanian, V. Bhave, S.S. and Sinha, R.P.
Nature Phys. Sci., 230, 185, 1971.

4. 'Search for Pulsed Radiation from Cyg X-1 at 327 MHz'
Mohanty, D.K., Balasubramanian, V. and Swarup, G.
Nature, Phys. Sci., 232, 191, 1971.

5. 'Two New Pulsars'
Mohanty, D.K., Balasubramanian, V. and Swarup, G.
IAU Circular No. 2356, 1971.

6. 'Parameters of Twelve Weak Pulsars at 327 MHz'
Krishnamohan, S., Balasubramanian, V. and Swarup, G.
Nature Phys. Sci., 234, 151, 1971.

7. 'Use of Aluminium in a Large Steerable Dipole Array'
Balasubramanian, V. and Ananthakrishnan, S.
Seminar on Use of Aluminium in Electrical Engineering, (The Inst. of Engrs., India), Madras, Dec. 14-16, 1973, P. 21-28.

8. 'An Electrically Steerable Array of 968 Dipoles for the Ooty Radio Telescope'
Kapahi, V.K., Damle, S.H., Balasubramanian, V. and Swarup, G.
J. Inst.Elec. Telecom. Engrs., 21, 117, 1975.

9. 'On the Large Duty Cycle of a New Pulsar'
Mohanty, D.K. and Balasubramanian, V.
Mon. Not. R. astr. Soc., 171, 10P, 1975.

10. 'Interstellar Scintillation of Pulsars'
Balasubramanian, V. and Krishnamohan, S.
Paper presented at the IV Meeting of ASI at Ootacamund, March 1978.

ACKNOWLEDGEMENTS

For guiding me through this thesis, with many valuable comments and criticisms, I am grateful to Prof. Govind Swarup. I deem it a great privilege to have been associated with him for the past thirteen years, in the construction as well as the operation of the Ooty Radio Telescope. His inexhaustible enthusiasm to undertake challenging tasks is infectious, owing to which he has instilled a sense of confidence in me. I wish to record my indebtedness to him for this beneficial influence.

I owe a great deal to my colleagues S. Krishnamohan and D.K. Mohanty for whatever knowledge I have gained on the subject of Pulsars. This thesis could not have been accomplished but for the benefit of the innumerable discussions I had with them and the help provided by them. In particular, the computer programs developed by S. Krishnamohan were used by me for data acquisition and analysis.

It is a pleasure to thank my colleagues Mr. N.V.G. Sarma, Dr. M.N. Joshi and Dr. V.R. Venugopal for providing me constant encouragement.

I thank Sankararaman Sr., Selvanayagam, Balu Jr. and Madhusudan for the construction of the twelve channel receivers.

The enthusiastic and able support of the young team of observers at Radio Astronomy Centre considerably speeded up the work of data handling. I am grateful to them all and in

particular to E.S. Krishnan who developed quite a few computer programs for my work.

I wish to acknowledge the cooperation provided by the team of engineers and technical staff responsible for the operation and maintenance of the OP the computer system and other facilities.

Many thanks are due to Mathews, Srinivasan, Premkumar, Siva Sr. and Jayaraman for the neat accomplishment of the jobs of typing, tracing and reprography, inspite of the heavy pressure of other routine work. The help from my wife Seetha colleague Balan in proof-reading is gratefully acknowledged.

I feel urged to acknowledge the sustained interest shown in my endeavours by my friend and colleague, Dr. S. Ananthakrishnan. In spite of his being away from the scene of my work, he had kept up his interest through frequent letters. Many a thanks are due to him for those letters which pushed up my sagging spirits.

TABLE OF CONTENTS

...2

LIST OF FIGURES

LIST OF TABLES

CHAPTER 1

INTRODUCTION

Observations of scintillation of a distant source is a powerful technique for investigating the properties of the intervening turbulent medium. The characteristic feature of scintillations is random fluctuations of amplitude and phase of the propagating signal. Studies of scintillations of radio galaxies, quasars and pulsars have provided valuable information on the nature of ionospheric, interplanetary and interstellar media. It may be noted that the observed features of the irregular fluctuations of intensity depend not only on the properties of the turbulent medium but also on the angular size of the observed source.

In this thesis we present a study of interstellar scintillations (ISS) of several pulsars, which are a new class of galactic radio sources discovered a decade ago. They are characterised by the very regular repetition rates of their radio pulse emission. More than 300 pulsars have been discovered so far. The periods of the pulse trains from the known pulsars are in the range of 0.033 sec to about 4 secs. In view of such short and accurate periodicities, pulsars are believed to be highly compact and magnetised, rotating neutron stars. Also, pulses are observed to arrive at higher radio frequencies earlier than at lower frequencies. This dispersion of the signal is the same as expected from the propagation of radio waves in an ionised interstellar gas. Hence

the rate of change of pulse arrival times with frequency of a pulsar is directly related to the value of the parameter called dispersion measure (DM) which is equal to the total electron content along the line of sight to the pulsar. Another notable feature of pulsar emission is the highly erratic fluctuations of their intensities. Both the characteristic time scales and the correlation bandwidths of these irregular intensity variations have been observed to encompass wide ranges in their respective domains. In our study of interstellar scintillations of pulsars, we are concerned with both of the above aspects.

1.1. INTENSITY FLUCTUATIONS OF PULSARS

The characteristic time scales of pulsar intensity variations are known to span a wide range, from fraction of a second to several weeks or longer (Lyne and Rickett 1968a,b; Rickett 1969; Mc Lean 1973). As discussed below, we cannot attribute all these fluctuations, with their varied time scales, to scintillations due to the interstellar medium. Those with short time scales, the pulse to pulse fluctuations, have been observed to be highly correlated over a frequency range of several hundred MHz (Lyne and Rickett 1968b). In contrast, the intensity fluctuations with time scales on the order of minutes are correlated only over a narrow range of frequencies, on the order of a few to several hundred kHz (Rickett 1969). It was shown by Scheuer (1968) that the pulse to pulse fluctuations are an intrinsic property of the

source, but the fluctuations with time scales on the order of a few to several minutes are likely to arise from scintillations caused by the interstellar medium (also Salpeter 1969). Dynamic spectra of several pulsars observed at different frequencies (Ewing et al. 1970) show narrow band features whose widths scale approximately as the fourth power of frequency. This is in agreement with the ISS hypothesis of intensity variations with time scales on the order of minutes. The most convincing evidence in favour of the ISS hypothesis came from the work of Rickett (1969; 1970) who showed a correlation between the observed dispersion measure and the characteristic bandwidth over which the intensity fluctuations are correlated. This result implies that the fluctuations in electron density are related to their mean value.

1.2. SCINTILLATIONS DUE TO THE INTERSTELLAR MEDIUM

The interstellar medium contains large regions of ionized gas at densities of $10^{-1\pm1}$ electrons cm^{-3}. The evidence for the existence of such a general distribution of free electrons comes not only from the observed dispersion of pulsar signals but also from the rotation measures of polarised extragalactic radio sources. As mentioned above, the observed deep fading of pulsar intensities, with time scales of a few or several minutes, indicates that the medium between us and the source has irregularities in electron density. Random fluctuations in electron density result in

corresponding fluctuations in the refractive index of the medium and consequently random phase changes are imposed on radio waves propagating through such an irregular plasma. Depending on the spatial distribution of the irregularities, different parts of an initially plane wavefront can undergo random phase deviations on traversing the medium and emerge as a distorted wavefront. Another equivalent statement of this propagation effect is that the electron density irregularities scatter the radio wave randomly. Interference effects arising due to the distorted wavefront give rise to a spatially random diffraction pattern. Owing to the relative velocity between the medium and the Earth, the random diffraction pattern is swept past the observer, resulting in random temporal fluctuations of intensity. Statistical properties of the fluctuations in intensity will depend on the statistical properties of the irregular medium.

It was predicted from the theory of scintillations of pulsars by Salpeter (1969) that the pulse shapes will be asymmetrically broadened at metre wavelengths, notably in the case of pulsars with large DM. This has been verified by observations (Lang 1971a; Staelin and Sutton 1970; Rankin et al. 1970; Ables et al. 1970; Lang 1971b; Lyne and Smith 1972; Davies et al. 1972). Under the framework of the theory of ISS of pulsars, the asymmetrical broadening of pulses - to be called scattering broadening - is inversely related to the intensity decorrelation bandwidth.

The fact that pulsar radiation exhibits interstellar scintillations shows that pulsars are compact sources with angular size less than about a microarc second. This is to be expected because pulsars are highly compact neutron stars. As in the case of interplanetary scintillation (IPS) which was used in the search for and determination of angular sizes of small diameter radio sources in the range of angular size 0".1-1".0 interstellar scintillations could also be used to search for radio sources smaller than about a microarc second. At the present time such tests have been negative on all sources except pulsars (Condon and Backer 1976; Armstrong et al.1977).

Another consequence of scattering of radio waves by the turbulent interstellar medium is that small diameter radio sources will suffer an apparent angular broadening as seen from the Earth. The angular broadening amounts to about 0.1 seconds of arc at metre wavelengths and its evidence is found from studies of IPS (Readhead and Hewish 1972).

1.3 PROPERTIES OF INTERSTELLAR MEDIUM INFERRED FROM STUDIES OF ISS OF PULSARS

It is possible, in principle, to deduce all the statistical properties of the IS medium using scintillation observations of pulsars. But a thorough investigation is difficult in practice as it requires long stretches of continuous data taken simultaneously at several frequences and also

at several stations on the Earth with large mutual separations. Added to it are difficulties in interpretation of such data because of the complex nature of pulsars as well as of the IS medium. Some of these problems are discussed in later sections of this chapter. Nevertheless, observational study of even limited aspects of ISS of pulsars can yield a wealth of details about the IS medium.

1.3.1. Estimates of Electron Density Fluctuations and Their Scale Sizes From Measurements of Decorrelation Bandwidths

Theoretical models of irregularities in IS medium impose restrictions on the permissible range of values of the standard deviation and characteristic scale size of the fluctuations in the electron density of the medium. Additional restrictions on these values can be derived by using the observationally determined value of the characteristic decorrelation bandwidth for intensity fluctuations, in conjunction with a theoretical model. This method is useful in estimating the magnitude and scale size of the electron density fluctuations in the IS medium. Observed values of scattering broadening are also usable for this purpose owing to its inverse relationship with decorrelation bandwidth.

1.3.2. Drift Velocities of Scintillation Pattern from Multistation Observations

Simultaneous observations of a pulsar at the same frequency with two or more radio telescopes which are separated

by distances on the order of a few thousand kilometres can yield estimates of the velocity of the drifting scintillation pattern (Lang and Rickett 1970; Galt and Lyne 1972; Rickett and Lang 1973; Slee et al. 1974). If the diffraction pattern due to the IS medium does not rapidly evolve temporarily as it drifts, then one expects the cross correlation of the intensity fluctuations at the two stations to go through a maximum value as the time lag between the two data is varied. The component of the drift velocity along the baseline joining the two stations is given by dividing their distance by the lag corresponding to the maximum value of the cross correlation. The drift velocity of the scintillation pattern depends also on the proper motion of the source, apart from the velocities of the medium and the Earth. Hence, multistation observations of several pulsars can yield evidence on whether pulsars are high velocity objects or not, which has implications on theories of formation of pulsars.

1.3.3. Nature of the Spectrum of Scale Sizes of Irregularities Inferred From Multifrequency Observations

The exact form of the functional relationship between an ISS parameter, say, decorrelation bandwidth, and the frequency of observation depends on the nature of the spectrum of sizes of the irregularities. Hence, simultaneous observations at different frequencies of ISS of pulsars are useful for understanding the nature of the irregularity spectra. Investigators have considered both Gaussian and power law spectra. Much

attention has been devoted to the Kolmogorov spectrum which is a special case of power law spectra, because natural turbulance results generally in a Kolmogorov spectrum. Attempts at deciphering the exact nature of the turbulance spectrum have been most successful in the case of the Crab and Vela pulsars and results have been in favour of a Kolmogorov spectrum (Mutel et al. 1974; Isaacman and Rankin 1977; Backer 1974; Lee and Jokipii 1976). But this conclusion cannot be extended easily to the general interstellar medium under the framework of the models which assume homogeneity of the medium (Rickett 1977). As discussed in Section 5.5 of this thesis, evidence for inhomogeneity of the general IS medium is indicated from the observed dependence of ISS parameters on dispersion measure.

1.4. ISS PARAMETERS AND DISPERSION MEASURE

The dispersion measure (DM) of a pulsar is given by the line integral of the electron density N_e along the line of sight from the Earth to the pulsar

$$DM = \int N_e \, dl \qquad (1.1)$$

From theoretical models of the IS medium which assume Gaussian or power law spectra for the irregularities, one can derive relationships between ISS parameters, such as decorrelation bandwidth B_h and decorrelation time τ_ν (Section 2.5) and the parameters of the medium like r.m.s. value of the electron density fluctuations $<\delta N_e^2>^{\frac{1}{2}}$, the typical scale sizes L of the irregularity spectrum and the distance z to the pulsar.

The dependence of ISS parameters on the observing frequency ν can also be derived. To arrive at a theoretically expected relationship between ISS parameters and dispersion measure one usually makes the assumption that the r.m.s. value of the electron density fluctuations is proportional to the mean electron density, i.e.

$$<\delta N_e^2>^{\frac{1}{2}} \propto <N_e> \qquad (1.2)$$

The above proportionality implies spatial homogeneity of the general IS medium. With this assumption one can arrive at the following relationships:

$$B_h \propto (DM)^{-\alpha/(\alpha-2)} \lambda^{2\alpha/(\alpha-2)} \qquad (1.3)$$

$$\rho_{c.s.} \propto (DM)^{-1/(\alpha-2)} \lambda^{-2/(\alpha-2)} \qquad (1.4)$$

where $\rho_{c.s}$ is the spatial correlation scale of the intensity fluctuations. It is directly related to both the temporal scale τ_ν and the transverse velocity v, as given by $\rho_{c.s} \propto v\tau_\nu$. In equations (1.3) and (1.4) α is the index of the spectral distribution of the irregularities. For a power law spectrum the value of the index lies in the range $2 < \alpha < 4$, and for the Kolmogorov spectrum $\alpha = 11/3$. For a Gaussian spectrum, the above equations are valid for α equal to 4. By observational determination of decorrelation bandwidths for several pulsars as a function of DM and/or λ, one can test the validity of the relation (1.3) which is based on the

assumption of homogeneity, for different types of spectra. Similarly one can check the validity of eqn.(1.4) by observational determination of τ_ν for several pulsars. To carry out this test, single station observations alone are not sufficient. One needs to know values of the transverse velocity v for different pulsars which require simultaneous multistation observations.

1.5. OBSERVATIONAL AND INTERPRETATIONAL DIFFICULTIES IN ISS OF PULSARS

1.5.1. Observational Difficulties

For observations at about one metre wavelength, the decorrelation bandwidth ranges from a few hundred kHz to only a few kHz for DM in the range 5-50 pc cm^{-3}. Therefore, for carrying out useful observations aimed at reliable determinations of the decorrelation bandwidths one needs to use detectors with bandwidths as narrow as possible, say 10 kHz to 100 kHz. Further, in order to achieve sufficient signal to noise ratio for weak pulsars, one requires a large overall bandwidth. resulting in large number of detectors. This increases the data handling problems. Since the time scale of scintillations are on the order of a few minutes, one needs to have continuous data stretches of at least several tens of minutes length, so as to reduce the statistical errors of the measured ISS parameters.

1.5.2 Finite Bandwidth Effects

Use of detectors whose bandwidths are comparable to or larger than the decorrelation bandwidth results in considerable smoothing of the intensity variations due to scintillations (Rickett 1969). This is in consonance with predictions of the theoretical models for the case of strong scattering (Little 1968; Lee 1976). Therefore it is important that observational determinations of ISS parameters incorporate suitable corrections for the finite bandwidth effects. Because of the use of a large number of detectors and the need to incorporate methods of corrections for finite bandwidth of the detectors, the amount of data reduction is considerably increased.

1.5.3 Interpretational Problems

a) Intrinsic intensity variations:

Although intensity variations of pulsars having characteristic time scales of a few minutes are generally ascribed to scintillations due to the IS medium, there has not been any investigation so far to check whether variations with similar time scales could also be intrinsic to the source. The results from two station observations by Slee et al.(1974) indicated the possible existence of such intrinsic variations. It may be noted that the decorrelation bandwidths of intrinsic variations is generally much larger than those for ISS. Hence by observing the correlation of intensity fluctuations over a large range of frequencies, one may be able to distinguish

between ISS and intrinsic variations even though their time scales are similar. If the two are not seperated adequately, the derived ISS parameters will not be reliable, e.g. the velocity of the scintillation pattern derived from two station observations will be overestimated.

b) Temporal evolution of scintillation pattern:

Results from two station observations have also shown that in the case of many pulsars the data do not yield definite velocities of the scintillation pattern. This could be due to temporal evolution of the diffraction pattern and/or intrinsic variations (Slee et al. 1974). Another interesting result from two station observations is that in the case of a few pulsars one notices reversal of the direction of the pattern velocity (Rickett and Lang 1973; Slee et al. 1974) in a short interval. Such observations are explainable using a multiscreen model of the IS medium or by postulating the presence of a velocity shear in the medium (Uscinski 1975). The results indicate that the properties ofthe IS medium are more complex than postulated in theoretical models which assume it to be statistically homogeneous and stationary.

1.6 THE PRESENT WORK

This thesis deals with single station observations of 33 pulsars at frequencies near 327 MHz using the large cylindrical radio telescope at Ootacamund, India. The dispersion

measures of these pulsars are in the range 5 - 231 pc.cm^{-3}. Most of the observations were carried out during 1976-78. Of the 157 pulsars known at that time 102 are in the declination range covered by the Ooty Radio Telescope. The 33 pulsars observed by us are among the brightest of these 102. Continuous stretches of data, each lasting a few to several hours, have been acquired with multichannel receivers on each of the 33 pulsars and detailed analyses made. Cross correlations of intensity fluctuations at different frequencies with good quality have been obtained for 15 pulsars. Such correlation data have been reported earlier in the literature by others for about 9 pulsars, but they were obtained from data stretches much smaller than those used in the present work which includes 8 of the 9 pulsars. For 23 pulsars we have obtained fluctuation power spectra with good signal to noise ratio. Earlier work by others has resulted in power spectra for about 25 pulsars, which are available in literature. Our work includes 14 of the 25 pulsars but the effective number of cycles of scintillation in our spectral data for each of the 14 pulsars is larger than that for the work reported in literature. The organisation of the thesis based on the above observations is given below.

A brief review of the theory of ISS of radio waves as developed by Lee and Jokipii, based on the Markov approximation using coherence function approach is presented in Chapter 2. On the basis of this theory we have formulated the effects of

finite bandwidth of the detectors on ISS parameters and also developed a method to detect the presence of intrinsic intensity fluctuations with time scales similar to those due to ISS. For observing the pulsars multichannel receivers were used. The instrumentation and observational procedures are described in Chapter 3. The details of the techniques adopted for data reduction including cross correlation and power spectral analysis are also given. Chapter 4 deals with the methods used for deriving the values of the ISS parameters of interest from the observed data. Procedures adopted for evaluating the possible statistical uncertainties on the estimates of these parameters are also described in this Chapter. Presentation and discussion of the results obtained from our observations form the main topics of Chapter 5. The results and discussions pertain to four aspects: (i) Estimates of ISS parameters and their comparison with theoretical models (ii) Evidence for the existence of intrinsic intensity fluctuations with time scales similar to those produced by ISS (iii) Inhomogeneity of the interstellar medium as inferred from the dependence on DM of observed ISS parameters (iv) Estimates of the characteristics of the IS medium and the clumpiness of the electron density distribution in it.

CHAPTER 2

REVIEW OF THEORY OF INTERSTELLAR SCINTILLATION OF PULSARS

2.1. INTRODUCTION

The phenomenon of scintillations of a distant radio source arises due to scattering of radio waves during their passage through a plasma with irregularities in electron density. The nature of the observed intensity fluctuations depends on the size distribution of the irregularities, and on φ_0 which is the root mean square (rms) phase fluctuation imposed by the medium on the incident wave front. In the case of ionospheric and interplanetary scintillations, the observed modulation index m of intensities is often small i.e. $m < 1$. This can be shown to arise due to the condition, $\varphi_0 \ll 1$, which is referred to as weak scattering (Salpeter 1967). In contrast to this, the observed interstellar scintillation (ISS) of pulsar radiation exhibits deep fading, i.e., $m \simeq 1$, which implies the condition of strong scattering i.e. $\varphi_0 \gg 1$.

2.2. THEORY OF INTERSTELLAR SCINTILLATION

Observed intensity fluctuations due to ionospheric or interplanetary or interstellar plasma are random. As such, one is interested only in statistical properties of scintillation which in turn can throw light on the statistical properties of the medium. The theoretical situation implies the solution of the equation of wave propagation in a medium with random fluctuations of refractive index. A complete analytic solution is

intractable owing to mathematical complexity. As such, solutions have been obtained using various simplifying assumptions. One of the approaches assumes that the medium could be replaced by a 'thin phase changing screen'. The thin screen approximation is justifiable in the case of ionospheric and interplanetary scintillations but is not valid for ISS. Nevertheless, thin screen model has been used (Scheuer 1968; Salpeter 1969) with a fair amount of success for obtaining order of magnitude estimates of the parameters of the medium causing ISS. Good accounts of thin screen, weak scattering models, as applicable to ionospheric and interplanetary scintillations are available in literature (Ratcliffe 1956; Salpeter 1967; Cohen 1969; Little 1976; Jokipii 1973).

For comparison of our observational results with theoretical predictions we have used a strong-scattering extended medium model. Thin screen models have not been used, but they are helpful in understanding the physics of scintillations produced by a random medium. Therefore, we firstly give a brief account of a simple thin screen model which is applicable to pulsar scintillations, in section (2.2.1). It is followed by a review of the theory of radio wave propagation in an extended random medium developed by Lee and Jokipii. In our brief review of this model we have restricted our attention to those aspects which are relevant to the present observations. Sections (2.3) and (2.4) deal with the propagation of nonmonochromatic waves in extended random media with

Gaussian or Kolmogorov spectra of irregularities. The assumption involved in extending the theory to investigation of intensity fluctuations is discussed in Section (2.5). This is followed by the predictions of the theory regarding the dependence of ISS parameters on dispersion measure. Section (2.7) describes the procedures derived by us from the theory to estimate finite bandwidth effects for receivers with any given bandshape. In the last section we discuss methods of dealing with difficulties encountered in determination of ISS parameters when intrinsic intensity variations are also present. A method is described by which the existence of intrinsic intensity fluctuations with time scales similar to those due to ISS can be detected.

2.2.1. The Thin Screen Model

The phase perturbation $\delta\varphi$ of the radio wave owing to its passage through an irregularity in electron density of magnitude δN_e and characteristic linear scale size L is given by

$$\delta\varphi = \delta N_e r_e \lambda L \qquad (2.1)$$

where r_e = classical electron radius and

λ = observing wavelength.

On passing through a depth z of such irregularities the rms phase deviation φ_0 becomes

$$\varphi_0 = (xL)^{\frac{1}{2}} \langle \delta N_e^2 \rangle^{\frac{1}{2}} r_e \lambda \qquad (2.2)$$

The above assumes a Gaussian spectral distribution for sizes of irregularities. Depending upon whether $\varphi_0 >> \pi$ radians or $\varphi_0 < \pi$ we distinguish two regimes of scattering, the former one being a case of strong scattering and the latter of weak scattering.

The modulation index m of intensity fluctuations is defined by

$$m^2 = \frac{\langle [\mathcal{I} - \langle \mathcal{I} \rangle]^2 \rangle}{\langle \mathcal{I} \rangle^2} = \frac{\langle I^2 \rangle}{\langle \mathcal{I} \rangle^2} \qquad (2.3)$$

where $\mathcal{I}$ is the total intensity, the mean-subtracted intensities being denoted by I . The angular brackets indicate averages. In the case of interplanetary scintillations (IPS) the modulation index is often small compared to unity, which implies that the scintillations are in the regime of weak scattering. Pulsar intensity fluctuations due to ISS, on the other hand, have modulation indices close to unity, which indicates that strong scattering is operative. i.e. for ISS,

$$\varphi_0 >> \pi \qquad (2.4)$$

Under the thin screen approximation we replace the IS medium by a thin screen placed near the middle of the depth z of the medium. The thin screen has the same scale size L and φ_0 as the actual medium.

There is enough experimental evidence from two-station observations of ISS of pulsars to show that $L >> \lambda$ for the IS

medium. Therefore one may use geometrical optics to calculate the rms scattering angle θ_s due to the irregularities. One obtains,

$$\theta_s = \lambda\varphi_o/(2\pi L) \qquad (2.5)$$

To have deep intensity variations it is necessary that several scattered rays reach the observer so that the interference amongst these scattered rays gives rise to deep scintillations. This requirement may be stated mathematically as,

$$z\theta_s > L \qquad (2.6)$$

2.2.1a Correlation of intensity fluctuations with frequency:

As has been mentioned earlier, it is observed in ISS of pulsars that the fluctuations in intensity are correlated over a narrow range of frequencies only. The scintillations will be similar at wavelengths λ and $\lambda+d\lambda$ if the phase differences between the various interfering beams are the same at $\lambda+d\lambda$ as at λ, to within say, π radians. The phase difference between any two interfering beams is composed of two parts (i) that due to differences between δN_o at the two physically separate regions on the screen traversed by the beams and (ii) that due to differences between the geometrical paths along which the rays have propagated. If we consider the direct ray and a scattered ray, the geometric path difference between them amounts to $\frac{1}{2}z\theta_s^2$ and this is much larger than the phase difference due to (i). Hence we may

neglect the phase delay due to (i). The time lag between direct and scattered rays is $z\theta_s^2/(2c)$ and hence the fluctuating intensities will be correlated over a bandwidth f_ν given by

$$f_\nu = 2c/(z\theta_s^2) \qquad (2.7)$$

It may be noted that owing to the time lag between direct and scattered rays an infinitely sharp pulse of radiation will be scattered into a pulse whose time profile will have an exponential decay with a characteristic decay time of f_ν^{-1} .

2.2.1b Time scale of scintillations:

The screen produces an irregular diffraction pattern in space. If the screen has a transverse velocity v with respect to the observer the diffraction pattern is swept past the observer with this velocity. The observed random intensity fluctuations are a manifestation of the swept diffraction pattern. The scale of the diffraction pattern at the Earth will be $c/(\nu\theta_s)$. If the characteristic time scale of the intensity variations is designated as τ_ν , then

$$v\tau_\nu = c/(\nu\theta_s) \qquad (2.8)$$

In the case of a radio source of considerable angular extent, different points on the source will generate diffraction patterns with relative shifts amongst peaks of the patterns and consequently the fluctuations due to the whole of the source will tend to smooth out. The critical angular size ψ_c

above which radio sources will not produce ISS is given by

$$\psi_c = c/(\pi\theta_s z) \qquad (2.9)$$

The conditions (2.4), (2.6) and (2.7) necessary for deep scintillations, restrict the range of allowable values of δN_e and L of the IS medium. For the thin screen model these conditions are shown graphically by Scheuer (1968) from which we note that deep scintillations necessarily imply a narrow bandwidth of correlation for intensity fluctuations.

2.3 RECENT DEVELOPMENTS IN THE THEORY OF WAVE PROPAGATION IN A RANDOM MEDIUM

Recent theoretical developments related to tackling the problem of scattering of light in the turbulent atmosphere of the Earth have resulted in fruitful approaches towards solution of the strong scattering problem (Tatarskii 1971; Brown 1972a, 1972b; Gurvich and Tatarskii 1975). In these approaches one tries to solve for the second and fourth order coherence functions of the random wave field, using plausible approximations, instead of solving the wave propagation equation. The coherence function approach gives solutions in the weak scattering regime also. The Rytov approximation to solve for the coherence functions, described by Tatarskii (1971) is applicable only in the weak scattering case. A more general approximation is the Markov approximation (Tatarskii 1971) which gives proper results for both strong and weak scattering conditions. The starting point of

these approaches is the quasi optical or parabolic equation of wave propagation (Tatarskii 1971; Lee and Jokipii 1975a). This equation is a scalar wave equation, neglecting polarization effects. The essence of parabolic approximation amounts to neglecting reflected waves. The range of validity of this assumption is discussed by Tatarskii (1971) and the satisfactory applicability of the parabolic and Markov approximations to ISS of pulsars is discussed by Lee and Jokipii (1975a). In the subsequent sections we briefly outline the coherence function approach using the parabolic and Markov approximations with more emphasis on the nonmonochromatic case. It was theoretically treated for the first time by Lee (1974).

2.3.1. Theory of ISS - Coherence Function Approach

We consider a plane monochromatic wave of frequency ν propagating along the +z direction and incident on a plasma of non-uniform electron density, filling the half space $z > 0$. The electron density $N_e(\bar{r})$ at any position $\bar{r} = (x,y,z)$ is such that the plasma frequency ν_p, at all $\bar{r}$, is much less than ν. The electron density N_e (and hence the refractive index $\varepsilon_\omega(\bar{r})$) is assumed to vary randomly. We consider ensemble averages of various quantities indicated by $\langle\ \rangle$.

$$\langle \omega_p^2 \rangle = \frac{4\pi \langle N_e \rangle e^2}{m} \qquad (2.10a)$$

$$\langle \varepsilon_\omega(\bar{r}) \rangle = 1 - \frac{\langle \omega_p^2 \rangle}{\omega^2} \qquad (2.10b)$$

$$N_e(\bar{r}) = \langle N_e(\bar{r}) \rangle + \delta N_e(r) \qquad (2.10c)$$

$$\beta(\bar{r}) = \frac{4\pi e^2 \, \delta N_e(\bar{r})}{mc^2} \qquad (2.10d)$$

$$k = \frac{\omega}{c} < \varepsilon_\omega(\bar{r}) >^{\frac{1}{2}} = \frac{\omega}{c}\left[1 - \frac{4\pi <N_e> e^2}{\omega^2 m}\right]^{\frac{1}{2}} \qquad (2.10e)$$

where $\omega = 2\pi\nu$

e = electronic charge

m = mass of an electron

δN_e = fluctuating component of electron density

c = velocity of light = 3×10^{10} cm/sec.

The following assumptions which are relevant in the case of the interstellar medium are made:

i) the fluctuations in refractive index are much less than one everywhere

ii) the scale of fluctuations in refractive index are much larger than the observing wavelength λ

iii) the total distance through the medium is much larger than the largest scale of refractive index fluctuations

iv) the medium is statistically homogeneous.

Under assumptions (i) and (ii) the wave propagation equation can be simplified to the 'parabolic equation',

$$2ik \frac{\partial u}{\partial z} + \nabla_\perp^2 u + k^2 \varepsilon u = 0 \qquad (2.11)$$

where $u = u(\bar{r})$ = complex Fourier component at angular frequency ω, of the electric field $\bar{E}(\bar{r},t)$ such that

$$\bar{E}(\bar{r},t) = \bar{E}_o e^{i(kz - \omega t)} \, . \qquad (2.12)$$

The operator $\nabla_\perp^2 = \frac{\partial^2}{\partial x^2} + \frac{\partial^2}{\partial y^2}$.

Let $\bar{\rho} = (x,y)$ be a transverse coordinate. The behaviour of the medium can be described by various coherence functions $\Gamma_{m,n}$ defined by

$$\Gamma_{m,n}(z,\bar{\rho}_1,\bar{\rho}_2,\ldots\bar{\rho}_m,\bar{k}_1,\bar{k}_2,\ldots\bar{k}_m,\bar{\rho}'_1,\bar{\rho}'_2,\ldots\bar{\rho}'_n,\bar{k}'_1,\bar{k}'_2,\ldots\bar{k}'_n)$$

$$=\langle u(z,\bar{\rho}_1,\bar{k}_1)\ u(z,\bar{\rho}_2,\bar{k}_2)\ \ldots\ldots\ u(z,\bar{\rho}_m,\bar{k}_m)\ u(z,\bar{\rho}'_1,\bar{k}'_1)$$

$$u(z,\bar{\rho}'_2,\bar{k}'_2)\ldots u(z,\bar{\rho}'_n,\bar{k}'_n)\rangle \qquad (2.13)$$

In particular $\Gamma_{1,1}$ describes angular spectrum and angular broadening, and $\Gamma_{2,2}$, intensity correlations.

Under the parabolic and Markov random process approximations, Lee (1974) has derived the following differential equation for $\Gamma_{m,n}$, for different transverse coordinates and different wave numbers

$$\frac{\partial \Gamma_{m,n}}{\partial z} = \frac{i}{2}\left[\frac{\nabla_1^2}{k_1} + \ldots + \frac{\nabla_m^2}{k_m} - \frac{\nabla_1'^2}{k'_1} - \ldots - \frac{\nabla_{n'}^2}{k_{n'}}\right]\Gamma_{m,n}$$

$$- \frac{1}{4}\left\{\sum_{i=1}^{m}\sum_{j=1}^{n}\frac{A(\bar{\rho}_i-\bar{\rho}_j)}{\bar{k}_i\bar{k}_j} - \sum_{i=1}^{m}\sum_{j=1}^{m}\frac{[A(\bar{\rho}_i-\bar{\rho}'_j)+A(\bar{\rho}'_j-\bar{\rho}_i)]}{k_i k'_j}\right.$$

$$\left. + \sum_{i=1}^{m}\sum_{j=1}^{n}\frac{A(\bar{\rho}'_i-\bar{\rho}'_j)}{\bar{k}'_i\bar{k}'_j}\right\}\Gamma_{m,n} \qquad (2.14)$$

where $\nabla_i^2 = \frac{\partial^2}{\partial x_i^2} + \frac{\partial^2}{\partial y_i^2}$

$$A(\bar{\rho} - \bar{\rho}') = \int_{-\infty}^{z} < \beta(z,\bar{\rho})\ \beta(z',\bar{\rho}') > dz \ .$$

Analytical solutions for the above transport equation for $\Gamma_{m,n}$ have not been found and numerical methods have been used for deriving results (Lee and Jokipii 1975b). The equation for $\Gamma_{1,1}$ is

$$\frac{\partial \Gamma_{1,1}}{\partial z} = \frac{i}{2}\left[\frac{\nabla_1^2}{k_1^2} - \frac{\nabla_2^2}{k_2^2}\right]\Gamma_{1,1} - \frac{1}{4}\left[\left(\frac{1}{k_1^2} + \frac{1}{k_2^2}\right) A(0) - \frac{2A(\bar{\rho}_1 - \bar{\rho}_2)}{k_1 k_2}\right]\Gamma_{1,1} \qquad (2.15)$$

For a statistically homogeneous medium $\Gamma_{1,1}$ depends on $\bar{\rho} = \bar{\rho}_1 - \bar{\rho}_2$ and not on $\bar{\rho}_1$ and $\bar{\rho}_2$. Also $\nabla_1^2 = \nabla_2^2 = \nabla_\rho^2$.

Define $$k_1 = k + \tfrac{1}{2}\Delta k \ ,$$

$$k_2 = k - \tfrac{1}{2}\Delta k \ .$$

Writing

$$\Gamma(z,\bar{\rho},\Delta k) = \Gamma_{1,1}(z,\bar{\rho},k_1,k_2)$$

and assuming $|\Delta k| \ll k$ eqn.(2.15) can be simplified to

$$\frac{\partial \Gamma}{\partial z}(z,\bar{\rho},\Delta k)+\frac{i}{2}\frac{\Delta k}{k^2}\nabla_\rho{}^2\Gamma+\frac{1}{2k^2}[A(0)-A(\bar{\rho})]\Gamma+\frac{\Delta k^2}{4}A(0)\Gamma=0. \qquad (2.16)$$

If the second term involving $\nabla_\rho{}^2$ is neglected and one solves for $\Gamma(z,\bar{\rho}=0,\Delta k)$ one obtains

$$\Gamma(z,\bar{\rho}=0,\Delta k) = \Gamma_R(z,\bar{\rho}=0,\Delta k) = \exp[-\frac{\Delta k^2}{4k^4}A(0)z] \qquad (2.17)$$

The above equation describes the effect of differing transit times of different rays due to the varying refractive index. Hence $\Gamma_R(z,\bar{\rho}=0,\Delta k)$ describes the 'pure refraction' effect. Obviously the effects dut to diffraction must be arising from the term proportional to $\nabla_\rho{}^2$, which is called the diffraction term. The diffraction effect is determined by defining a new $\Gamma_D(z,\bar{\rho},\Delta k)$ by

$$\Gamma(z,\bar{\rho},\Delta k) = \Gamma_D(z,\bar{\rho},\Delta k)\,\Gamma_R(z,\bar{\rho}=0,\Delta k). \qquad (2.18)$$

Then the equation for Γ_D becomes

$$\frac{\partial \Gamma_D}{\partial z}+\frac{i\Delta k}{2k^2}\nabla_\rho{}^2\Gamma_D+\frac{1}{2k^2}[A(0)-A(\bar{\rho})]\Gamma_D=0 \qquad (2.19)$$

It may be noted that the pure refraction effect is caused by variation of optical path along the line of sight and will not be observable during the course of observations lasting a few hours or a few days, as the position of the observer does not change appreciably with respect to the scattering medium during the observation. As such we will be

concerned only with Γ_D in discussing measurable ISS parameters, henceforth.

2.4 NATURE OF THE SPECTRUM OF IRREGULARITIES

Solutions for Γ_D obviously depend upon the functional form of $A(\bar{\rho})$ which in turn depends on the nature of the refractive index fluctuations in the medium. The spectrum $P_\varepsilon(\bar{q})$ of refractive index fluctuations is defined by

$$P_\varepsilon(\bar{q}) = \int < \varepsilon_k(\bar{r})\ \varepsilon_k(\bar{x}+\bar{r}) > \exp(i\bar{q}.\bar{r})\ d^3\bar{r} \qquad (2.20)$$

If one assumes the spectrum to be Gaussian,

$$P_\varepsilon(\bar{q}) = B_G \exp(-q^2/q_o^2) \qquad (2.21)$$

where $L_G = 1/q_o$ is the coherence scale of the fluctuations and

$$B_G = 128\pi^{7/2}(r_e^2/k^4)\ q_o^{-3} < \delta N_e^2 > \qquad (2.21a)$$

$r_e = e^2/mc^2$ = classical electron radius.

Alternatively one can assume a modified power law spectrum of the form

$$P_\varepsilon(\bar{q}) = \frac{B_p \exp(-q^2/q_1^2)}{(1+q^2/q_o^2)^{\alpha/2}} \qquad (2.22)$$

with $q_0 \ll q_1$. This spectrum is flat for $q < q_0$, is a power law with index $-\alpha$ for $q_0 < q < q_1$ and is cut off for $q > q_1$. $L_p = 1/q_0$ is referred to as the outer scale and $\ell = 1/q_1$, is the inner scale. Usually α has a range $2 < \alpha < 4$ and $\alpha = 11/3$ corresponds to the Kolmogorov spectrum. The justification for assuming a modified power law spectrum stems from the following two reasons: (i) natural turbulence is expected to result in a Kolmogorov spectrum of irregularity size distribution, (ii) IPS observations seem to indicate a power law spectrum for the inhomogeneities in the solar wind plasma (Jokipii 1973; Coles et al. 1974). The constant B_p is given by

$$B_p = 128\pi^{7/2} q_0^{-3} (r_e^2/k^4) < \delta N_e^2 > \Gamma_{(\alpha/2)} / \Gamma_{(\alpha/2-3/2)} \qquad (2.22a)$$

where $\Gamma_{(\alpha/2)}$ and $\Gamma_{(\alpha/2-3/2)}$ are gamma functions.

While finding solutions for eqn.(2.19) one is interested in solutions of $\Gamma_D(z, \bar{\rho} = 0, \Delta k \neq 0)$, apart from the solutions for the more general $\Gamma_D(z, \bar{\rho} \neq 0, \Delta k \neq 0)$. This is because one may arrive at theoretical predictions on pulse broadening due to interstellar scattering as well as the related effect of intensity decorrelation with observing frequency by using solutions of $\Gamma_D(z, \bar{\rho} = 0, \Delta k \neq 0)$ under certain assumptions regarding the relationships between $\Gamma_{1,1}$ and $\Gamma_{2,2}$ (Lee and Jokipii 1975; Lee 1976). As analytic solutions have not been found numerical methods have been used for solving eqn.(2.19) which are described by Lee and Jokipii (1975b). One finds that

the characteristic frequency scale ν_c of $\Gamma_D(z,\bar{\rho} = 0, \Delta k \neq 0)$ is given by

$$\nu_c = (c/2\pi)\beta_o^{-2/\mu} k^{2(\mu+2/\mu)} (z/2)^{-(\mu+2)/\mu} \qquad (2.23)$$

where $\beta_o = [A(0)-A(\bar{\rho})]/\rho^{-\mu}$

$\mu = \alpha - 2$ for power law spectra with $2 < \alpha < 4$

$= 2$ for Gaussian spectra.

The numerical solutions for Γ_D have been presented as graphical plots of $\Gamma_D(z,\bar{\rho} = 0, \Delta k \neq 0)$ as a function of $(\Delta\omega/\omega_c)^{\frac{1}{2}} = (\Delta\nu/\nu_c)^{\frac{1}{2}}$ by Lee and Jokipii (1975b). Two sets of solutions are available in their paper, one for Gaussian spectrum of refractive index fluctuations and the other for a Kolmogorov spectrum.

Solutions of Γ_D are useful in making quantitative predictions of the effect of finite receiver bandwidths on observable parameters of pulsar intensity scintillations, inspite of the fact that Γ_D describes only the correlation of electric fields due to the propagating electromagnetic wave. This is possible under certain assumptions as described in the next section.

2.5 INTENSITY FLUCTUATIONS

In order to discuss the fluctuations in intensity due to the medium one has to solve for $\Gamma_{2,2}$. This problem is also mathematically intractable. As such one proceeds by using known relations between second and fourth moments of the complex amplitude of the electric field i.e. relation between $\Gamma_{1,1}$ and $\Gamma_{2,2}$.

If the complex amplitudes are Gaussian random variates, then it can be shown (e.g. Hanbury Brown, pp 39, 1974) that

$$\Gamma_{2,2} = 1 + |\Gamma_{1,1}|^2 \qquad (2.24)$$

Lee and Jokipii (1975c) have shown that for monochromatic waves the above holds good even for non-Gaussian distribution of amplitudes if conditions of strong scintillation are satisfied. It is reasonable to assume that $\Gamma_{1,1}$ and $\Gamma_{2,2}$ are related in the same way even for different wavenumbers i.e. eqn. (2.24) holds good even for radiation in a finite bandwidth. With this assumption we can develop methods using solutions of Γ_D to correct the effects of finite bandwidths of receivers on observational measurements of parameters of decorrelation of pulsar intensities with radio frequency and time. These are discussed in Section (2.6).

2.6 DEPENDENCE OF PULSAR SCINTILLATION PARAMETERS ON DISPERSION MEASURE

To verify the validity of any theory of radio wave propagation in the IS medium a possible test is the comparison of the predictions of the theory with observational evidence regarding the dependence of various parameters of ISS of pulsars on dispersion measure as well as frequency. For example we may consider the dependence of f_ν on DM and ν, where f_ν is the characteristic frequency scale of correlation of the intensity fluctuations. Similarly one may investigate dependence of $\rho_{c.s.}$ on DM and ν, where $\rho_{c.s.}$ is the characteristic transverse spatial scale of intensity fluctuations. $\rho_{c.s.}$ is related to the decorrelation times of intensities as explained in Section (1.4). But there are two difficulties in deriving theoretically a relationship between any one of the ISS parameters and dispersion measure as described below.

Scintillation parameters depend on fluctuations in electron densities about their mean and not on the mean electron density itself. As such, without a knowledge of the relationship between $< N_e >$ and $< \delta N_e^2 >$, one cannot deduce theoretical relationships between ISS parameters and dispersion measure. To circumvent this difficulty one makes plausible assumptions regarding the dependence of $< \delta N_e^2 >$ on $< N_e >$ in the IS medium. The simplest of the assumptions could be of the form

$$< N_e >^2 \propto < \delta N_e^2 > \qquad (2.25)$$

Under the framework of the theory using the coherence function approach for the case of nonmonochromatic waves, described in the earlier sections, one cannot readily evaluate the relevant predictions quantitatively. The prime reason for this is the lack of analytic solutions for Γ_D in terms of $A(\rho)$, z, ν and ν' for the case of wide band radiation. On the other hand, if one considers monochromatic waves only - implying an infinitesimally narrow bandwidth of the detector - one can arrive at the necessary quantitative predictions involving f_ν (or $\rho_{c.s.}$) and ν, z and $\langle \delta N_e^2 \rangle$, for both Gaussian and power law spectra of irregularities.

For Gaussian spectra it turns out to be

$$f_\nu \propto \frac{\nu^4}{z^2 \langle \delta N_e^2 \rangle} \tag{2.26}$$

For a power law spectrum with index α we obtain

$$f_\nu \propto \frac{\nu^{2\alpha/(\alpha-2)}}{z^{\alpha/(\alpha-2)} \langle \delta N_e^2 \rangle^{2/(\alpha-2)}} \tag{2.27}$$

Specifically, in the case of the Kolmogorov spectrum with $\alpha = 11/3$ the relationship (2.27) becomes

$$f_\nu \propto \frac{\nu^{4.4}}{z^{2.2} \langle \delta N_e^2 \rangle^{1.2}} \tag{2.28}$$

The relationship between $\rho_{c.s.}$ and DM can be obtained from the asymptotic analytic solutions of $\Gamma_{2,2}$ (Lee and

Jokipii 1975c) for propagation of monochromatic waves under conditions of strong scattering. For the case of Gaussian spectrum of irregularities we obtain

$$\rho_{c.s.} \propto \frac{\nu}{z^{\frac{1}{2}} < \delta N_e^2 >^{\frac{1}{2}}} \tag{2.29}$$

For the case of power law spectra one has to consider two possible situations (i) $\ell < \rho_{c.s.} < L$ and (ii) $\rho_{c.s.} < \ell$. For $\ell < \rho_{c.s.} < L$ we get

$$\rho_{c.s.} \propto \frac{\nu^{2/(\alpha-2)}}{z^{1/(\alpha-2)} < \delta N_e^2 >^{1/(\alpha-2)}} \tag{2.30}$$

and for the case of $\rho_{c.s.} < \ell$ we obtain the same relationship as in (2.30). It may be noted that for $\ell > \rho_{c.s.}$ the relationship does not involve the spectral index α in so far as the dependences on ν, z and $< \delta N_e^2 >$ are concerned.

For Kolmogorov spectrum with $\alpha = 11/3$, for the case of $\ell < \rho_{c.s.} < L$ we get

$$\rho_{c.s.} \propto \frac{\nu^{1.2}}{z^{0.6} < \delta N_e^2 >^{0.6}} \quad . \tag{2.31}$$

By applying (2.25) we rewrite, eqn. (2.26) giving the predicted dependence on DM of f_ν and $\rho_{c.s.}$ for a Gaussian irregularity

spectrum, as below:

$$f_\nu \propto \frac{\nu^4}{(DM)^2} \tag{2.32}$$

$$\rho_{c.s.} \propto \frac{\nu}{(DM)^{\frac{1}{2}}} \quad . \tag{2.33}$$

For Kolmogorov spectrum of irregularities the corresponding relations are as follows:

$$f_\nu \propto \frac{\nu^{4.4}}{(DM)^{2.2} < N_e >^{0.2}} \tag{2.34}$$

$$\rho_{c.s.} \propto \frac{\nu^{1.2}}{(DM)^{0.6}} \quad \text{for } \ell < \rho_{c.s.} < L \tag{2.35}$$

$$\rho_{c.s.} \propto \frac{\nu}{(DM)^{0.5}} \quad \text{for } \rho_{c.s.} < \ell \tag{2.36}$$

2.7 BANDWIDTH EFFECTS ON FREQUENCY CROSS CORRELATION OF INTENSITIES DUE TO SCINTILLATION

2.7.1 Bandwidth Effects

The intensity of a Fourier component at frequency ν observed at position $(z, \bar{\rho})$ is given by

$$g_{(z,\bar{\rho},\nu)} = \left| u(z,\bar{\rho},\nu) \right|^2$$

The normalised cross correlation of intensities at two Fourier components, observed respectively at $(z,\bar{\rho}_i)$ and $(z,\bar{\rho}_j)$, is given by

$$P_I(z,\bar{\rho}_i,\nu_i,\bar{\rho}_j,\nu_j) = \frac{\langle \vartheta_i \vartheta_j \rangle}{\langle \vartheta_i \rangle \langle \vartheta_j \rangle} - 1 \qquad (2.37)$$

For $\nu_i = \nu_j$, P_I becomes the 'spatial intensity correlation function' which is related to the observed temporal intensity fluctuations through the relative velocity of the medium with respect to the observer. For $\nu_i \neq \nu_j$ and $\bar{\rho}_i = \bar{\rho}_j$, P_I becomes the 'frequency cross correlation' of intensity fluctuations.

P_I as defined above refers to detectors with zero bandwidth. For a detector with finite bandwidth and an intensity response $G_i(\nu)$ such that $\int G_i(\nu)d\nu=1$, the observed intensity is given by

$$\vartheta_i(z,\bar{\rho}) = \int \left|u(z,\bar{\rho},\nu)\right|^2 G_i(\nu)d\nu \qquad (2.38)$$

and the intensity correlation function Q_I becomes

$$Q_I(z,\bar{\rho}_i,\nu_i,\bar{\rho}_j,\nu_j) = \frac{\iint \langle u_i u_i^* u_j u_j^* \rangle G_i(\nu)G_j(\nu')d\nu d\nu'}{\left[\int \langle u_i u_i^* \rangle G_i(\nu)d\nu\right]\left[\int \langle u_j u_j^* \rangle G_j(\nu)d\nu\right]} - 1 \qquad (2.39)$$

If we invoke the assumption that the simple relationship between $\Gamma_{1,1}$ and $\Gamma_{2,2}$, given in eqn.(2.24) holds good even for nonmonochromatic waves then we can express Q_I as

follows:

$$Q_I(z,\bar{\rho}_i,\nu_i,\bar{\rho}_j,\nu_j) = \frac{\iint |\langle u_i u_j^* \rangle|^2 G_i(\nu) G_j(\nu') d\nu d\nu'}{[\int \langle \vartheta_i \rangle G_i(\nu) d\nu][\int \langle \vartheta_j \rangle G_j(\nu) d\nu]} \qquad (2.40)$$

Since $\langle u_i u_j^* \rangle = \Gamma_{1,1} = \Gamma_R \Gamma_D$ is known from the solution of the transport equation for $\Gamma_{1,1}$ (eqn.(2,15)), Q_I can be readily evaluated from eqn.(2.40). For reasons described in Section (2.3.1) one can neglect the contribution to $\Gamma_{1,1}$ by refraction effects so that $|\Gamma_{1,1}|^2$ can be substituted by $|\Gamma_D|^2$ in order to evaluate Q_I .

2.7.2. Nature of the spectrum of refractive index fluctuations in the medium and its effect on the observed intensity correlation functions.

The most interesting aspect of the theory of interstellar scintillation described above is that, comparison of the shape of observed intensity correlation functions with that predicted by eqn.(2.40) can throw light on the nature of the spectrum of refractive index fluctuations in the interstellar medium. One notes that (Lee 1976) the dependence of $|\Gamma_D|^2$ on $\bar{\rho}$ and $\Delta\nu$ for a Gaussian spectrum is slightly different from that for a Kolmogorov (power law) spectrum. This is seen from the graphical plots of $|\Gamma_D|^2$ vs $(\Delta\nu/\nu_c)$ (Fig.2.1) and P_I vs ρ/ρ_c (Fig.2.2). These plots are taken from the paper by Lee (1976). The differences appear marginal but become more accentuated in the case of the theoretically predicted

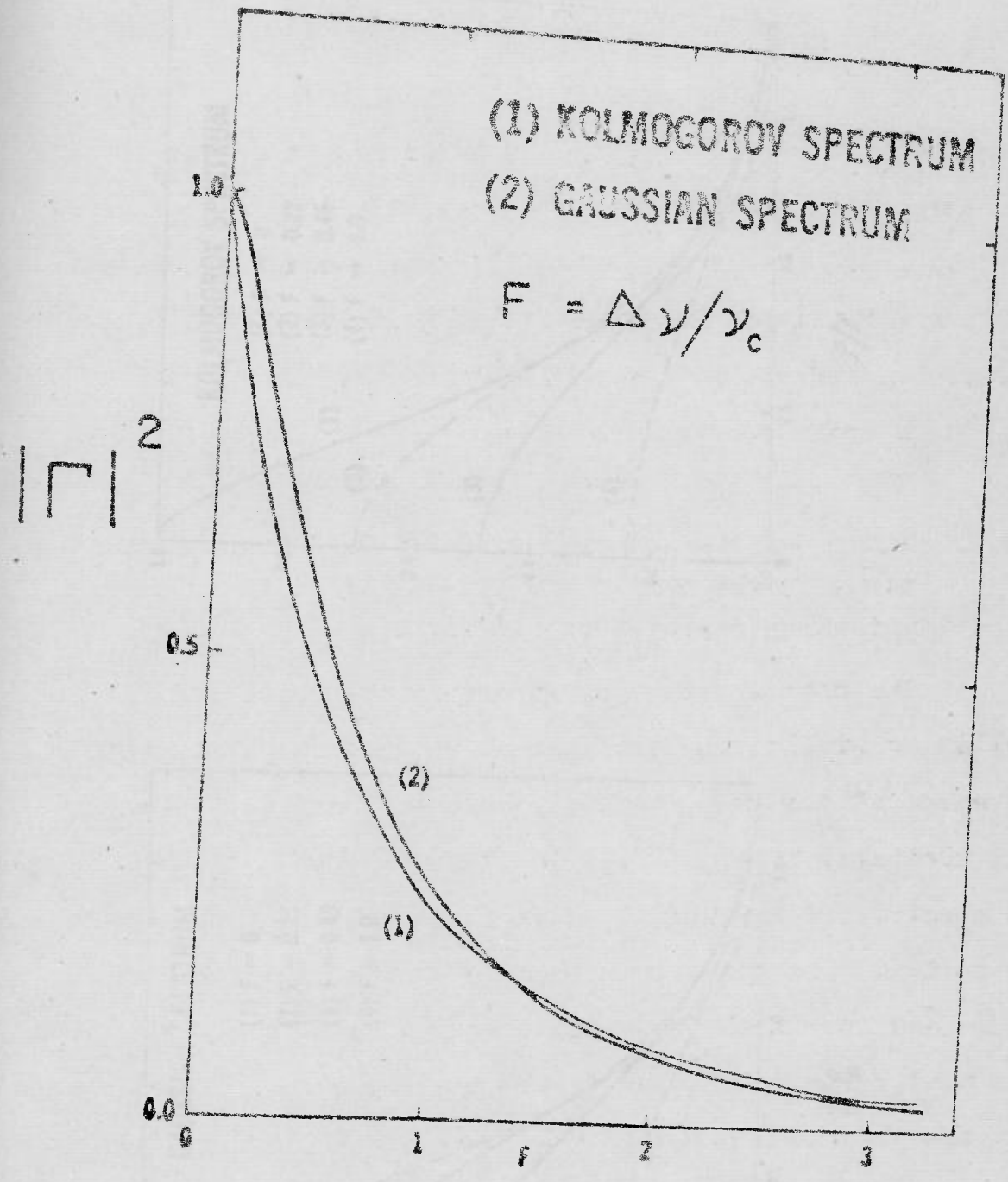

Fig. 2.1 FREQUENCY SPACE CORRELATION OF INTENSITY FLUCTUATIONS FOR RECEIVERS OF ZERO BANDWIDTH

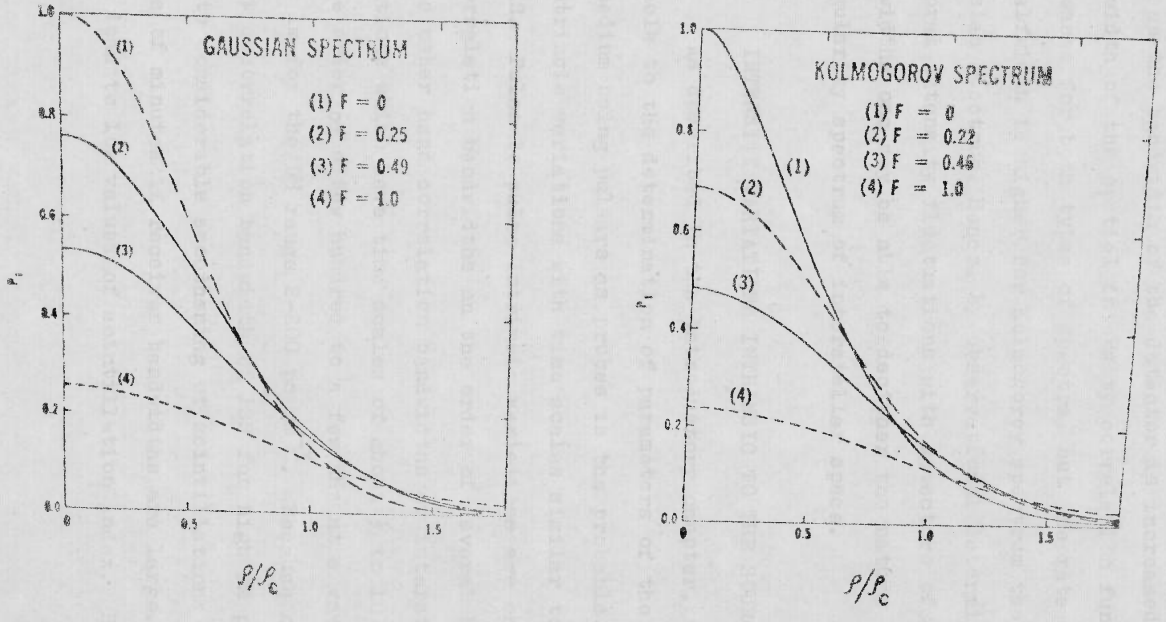

Fig.2.2 SPATIAL INTENSITY CORRELATION FOR RECEIVERS OF ZERO BANDWIDTH

bandwidth effect on spatial intensity correlation functions (Figs. 5,6 and 7 in Lee 1976) for the two spectra. One finds that as the bandwidth of the detector is increased, the halfwidth of the spatial intensity correlation function increases for both types of spectra, but the rate of increase of halfwidth is higher for Kolmogorov spectrum than for Gaussian spectrum. Hence, by observational determination of temporal intensity fluctuations with detectors of different bandwidths one may be able to decipher the nature of the irregularity spectrum of interstellar space.

2.8 INTENSITY VARIATIONS INTRINSIC TO THE SOURCE

As described in the introductory chapter, the major obstacle to the determination of parameters of the interstellar medium using pulsars as probes is the probable existence of intrinsic variations with time scales similar to those due to ISS. Pulse to pulse intrinsic variations are characterised by correlation bandwidths on the order of several hundred MHz. On the other hand correlation bandwidths of interstellar scintillations which have time scales of about $\frac{1}{2}$ to 10 minutes are on the order of a few hundred to a few kHz at a wavelength of about 1m for the DM range 2-200 pc cm^{-3}. Because of the narrow decorrelation bandwidth of ISS for high DM pulsars, one expects considerable smoothening of scintillations with time scales of minutes if receiver bandwidths are large. This would lead to low values of scintillation index. But, for

several pulsars of high DM observed with large bandwidths we find relatively high values of m which indicate possible presence of intrinsic variations of similar time scales as ISS (Chapter 5). If one assumes that irrespective of their time scales the intrinsic fluctuations are always characterised by much larger correlation bandwidths than those due to ISS, then one can estimate the degree of contamination of ISS fluctuations by intrinsic fluctuations. In the following sections we describe the methods we have adopted for this purpose.

2.8.1. Frequency Cross Correlations

Following Sutton (1971) we write

$$g(t) = x(t)\, y(t) \qquad (2.41)$$

where $x(t)$ is the intrinsic pulse intensity and $y(t)$ describes the scintillation superposed on intrinsic intensity by the medium. Writing $x(t) = \langle x\rangle + \varepsilon x(t)$ and $y(t) = \langle y\rangle + \varepsilon y(t)$, $I(t) = \langle x\rangle \varepsilon y(t) + \varepsilon x(t)\langle y\rangle + \varepsilon x(t)\varepsilon y(t)$ where angular brackets indicate time averages. The frequency cross correlation of intensities at ν_i and ν_j as defined as

$$\gamma_{ij} = \frac{\langle I_i(t)\, I_j(t)\rangle}{\sigma_i \sigma_j} = \Gamma_{OBS} \qquad (2.42)$$

where $\sigma_i = \langle I_i^2(t)\rangle^{\frac{1}{2}}$ = rms fluctuation of mean subtracted intensities. Assuming that intrinsic variations are correlated over a wide band, i.e. $x_i(t) = x_j(t)$, the observing time is

sufficiently long so that $\langle y_i \rangle = \langle y_j \rangle$, $\sigma_i = \sigma_j$ and also cross products of uncorrelated terms can be ignored, then

$$\gamma_{ij} = \frac{\langle \varepsilon y_i \varepsilon y_j \rangle + A}{\langle (\varepsilon y_i)^2 \rangle + A} \tag{2.43}$$

where

$$A = \frac{\langle (\varepsilon x)^2 \rangle \langle y \rangle^2}{\langle x \rangle^2 + \langle (\varepsilon x)^2 \rangle} \; . \tag{2.43a}$$

For large frequency separations the frequency cross correlation will be

$$\gamma_{ijp} = \frac{A}{\langle (\varepsilon y_i)^2 \rangle + A} = p \tag{2.44}$$

and refers to broad band intrinsic variations of a pulsar. Even in the presence of intrinsic variations, it can be shown from eqns.(2.43) and (2.44) that the frequency cross correlation due to ISS is given by

$$\Gamma_{ijm} = \frac{\langle \varepsilon y_i \; \varepsilon y_j \rangle}{\langle (\varepsilon y_i)^2 \rangle} = \frac{\gamma_{ij} - p}{1-p} \equiv \Gamma_{ij} = \Gamma_{SCINT} \tag{2.45}$$

Equation (2.43) shows that in the presence of intrinsic variations, the frequency cross correlation will decay to a nonzero base level equal to p when the frequency separations are much larger than f_ν, the characteristic decorrelation frequency of ISS. Alternatively, when the observed frequency

cross correlation shows a zero pedestal p , it indicates the presence of ISS only. When both ISS and intrinsic variations are present, we expect the observed frequency cross correlation as shown in Fig.(2.3). As was shown by Sutton (1971), the true f_ν due to ISS in such a case is given by the width of the function $\Gamma_{ijm}(j)$ which is given by eqn.(2.45).

The value of p can be related to the modulation index of the variations intrinsic to the pulsar, $\alpha' = \frac{RMS(\varepsilon x)}{\langle x \rangle}$. If the modulation index due to the interstellar medium alone is $\beta' = \frac{RMS(\varepsilon y)}{\langle y \rangle}$, the observed scintillation index m is given by

$$m^2 = \frac{\langle I^2 \rangle}{\langle I \rangle^2} = \frac{\langle x \rangle^2 \langle (\varepsilon y)^2 \rangle \langle (\varepsilon x)^2 \rangle \langle y \rangle^2 + \langle (\varepsilon x)^2 \rangle \langle (\varepsilon y)^2 \rangle}{\langle x \rangle^2 \langle y \rangle^2}$$

$$= \alpha'^2 + \beta'^2 + \alpha'^2 \beta'^2 \quad . \qquad (2.46)$$

One may also deduce by algebraic manipulation of eqns.(2.43) and (2.44) that

$$p = \alpha'^2 / m^2 \quad . \qquad (2.47)$$

If one observes pulsars with identical narrow bandpass receivers at several closely spaced frequencies and computes the frequency cross correlation of intensity fluctuations and the modulation indices m_j for each of the channels j, then by the use of equations (2.46) and (2.47) the values of α' and β' can be estimated. And hence one can get an idea of the significance of intrinsic causes as compared with ISS in producing the observed intensity fluctuations.

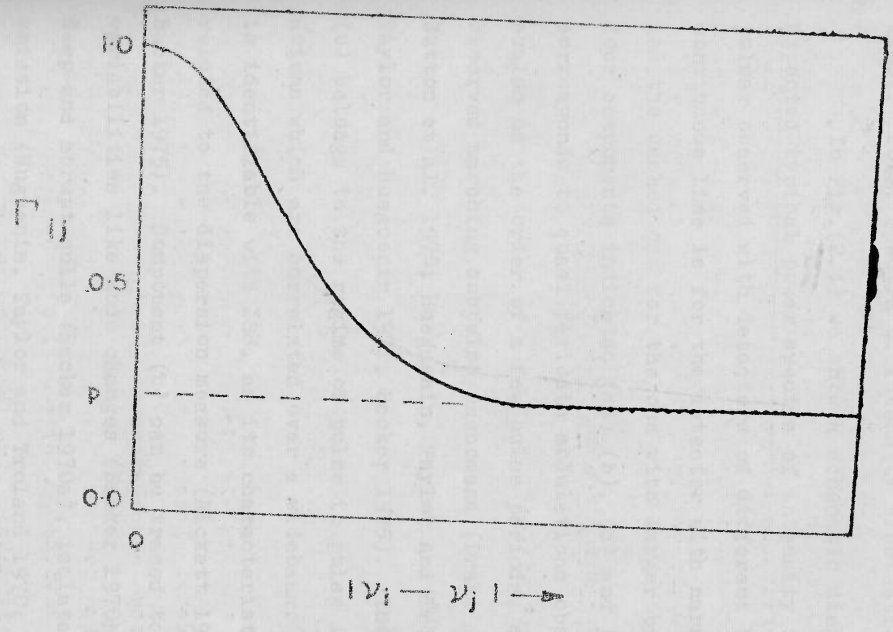

Fig.2.3 SCHEMATIC DIAGRAM OF FREQUENCY CROSS CORRELATION WHEN BOTH INTRINSIC DISCRIMINATIONS AND ISS ARE PRESENT

But it may be noted that this method does not give any insight into the possible time scales of the two types of fluctuations. For such purposes it is useful to study the power spectra of intensity fluctuations of pulsars.

2.8.2. Power Spectra of Intensity Fluctuations

In Fig.(2.4) we show a schematic diagram of the expected typical power spectra of intensity fluctuations of a pulsar observed with detectors of different bandwidths. The continuous line is for the detector with narrower bandwidth and the dashed one for the one with larger bandwidth. Of the four components indicated (a), (b), (c) and (d), component(d) corresponds to quasi periodic modulations observed with time scales on the order of a few pulse periods, such as the observed marching subpulse phenomena (Drake and Craft 1968; Sutton et al. 1970; Hueguenin, Taylor and Troland 1970; Taylor and Hueguenin 1971; Backer 1975). The 'white' level (c) belongs to the regime of pulse to pulse intrinsic fluctuations which are correlated over a wideband. Component (a) is identifiable with ISS, as its characteristic width is related to the dispersion measure (Rickett 1970; Lang 1971; Backer 1975). Component (b) can be traced to intrinsic variabilities like mode changes (Backer 1970b; Lyne 1971), deep and abrupt nulls (Backer 1970a), isolated bursts of emission (Huguenin, Taylor and Troland 1970; Backer et al. 1975) and any other modulations of similar period as ISS ($\frac{1}{2}$ to 10 min) (Lang 1969). Component (b) can mix up with the

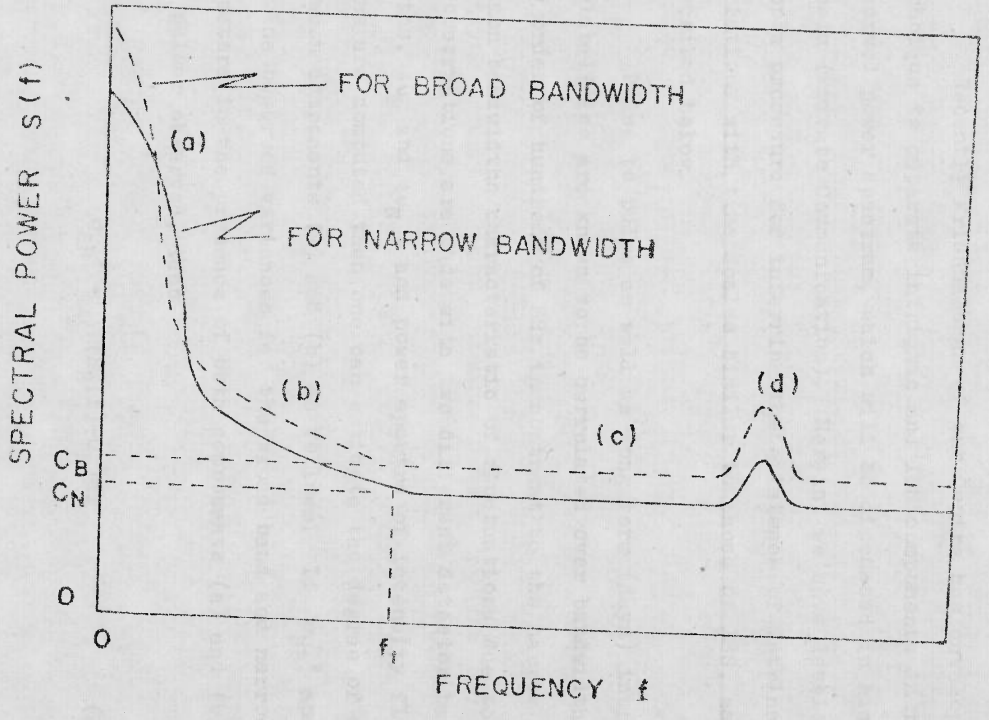

Fig. 2.4 SCHEMATIC DIAGRAM OF EXPECTED POWER SPECTRA OF PULSAR INTENSITY FLUCTUATIONS FOR RECEIVERS OF DIFFERENT BANDWIDTHS

ISS component (a) heavily and make the straight forward determination of the true ISS power spectral widths unreliable.

Recently Krishnamohan of our Centre has developed a technique to separate intrinsic and ISS components in the observed power spectrum, which will be discussed in his thesis (Private Communication). Herein, we have developed a simple procedure for inferring the existence of intrinsic variations with time scales similar to those of ISS, as described below.

Pulse to pulse as well as long term (days) intrinsic variabilities are known to be correlated over bandwidths on the order of hundreds of MHz in contrast to the narrow correlation bandwidths characteristic of fluctuations due to ISS. If observations are made with two different detector bandwidths, $\Delta\nu_B$ and $\Delta\nu_N$, and power spectra of intensity fluctuations are computed then one can estimate the degree of mix up between components (a) and (b) as follows. If σ_{SB}^2 and σ_{SN}^2 are the observed variances for the broad band and narrow band detectors in the presence of both components (a) and (b) for the pulsar observed, then

$$\sigma_{SB}^2 = \int_0^{f_t} (S_B(f)-C_B)df \qquad (2.48a)$$

and

$$\sigma_{SN}^2 = \int_0^{f_t} (S_N(f)-C_N)df \qquad (2.48b)$$

where f_t is the frequency at which (b) merges with the 'white' level (c) (Fig.(2.4)). When intrinsic fluctuations alone are present and the ISS component (a) is completely absent over the spectral range of interest, it can be shown that (Appendix A)

$$\left[\frac{\sigma_{SB}^2}{\sigma_{SN}^2}\right]_p = R_p = \frac{\iint_{\nu\nu'} G_B(\nu)G_B(\nu')d\nu d\nu'}{\iint_{\nu\nu'} G_N(\nu)G_N(\nu')d\nu d\nu'} \qquad (2.49)$$

where $G_B(\nu)$ and $G_N(\nu)$ are the intensity responses of the broad and narrow band channels and the integrations are over the pass bands of the channels. The above relationship is based on the fact that intrinsic fluctuations are correlated over bandwidths which are much larger than the receiver bandwidths $\Delta\nu_B$ and $\Delta\nu_N$.

On the other hand, the presence of only the ISS component results in a ratio of σ_{SB}^2 to σ_{SN}^2 given by (Appendix A)

$$\left[\frac{\sigma_{SB}^2}{\sigma_{SN}^2}\right]_{SCINT} = R_c = \frac{\iint_{\nu\nu'} G_B(\nu)G_B(\nu')\Gamma_D^2(\delta\nu/f_\nu)d\nu d\nu'}{\iint_{\nu\nu'} G_N(\nu)G_N(\nu')\Gamma_D^2(\delta\nu/f_\nu)d\nu d\nu'} \qquad (2.50)$$

where $\delta\nu = |\nu - \nu'|$. One notes that R_p and R_c represent two ideal extremes such that R_p is always greater than R_c. If

both ISS and intrinsic fluctuations with similar time scales are present the observed ratio R_0 of the variances is expected to be such that $R_c < R_0 < R_p$. As described in Chapter 5, the above procedure has been used by us for analysis of data on 23 pulsars for which good power spectra were obtained and it is seen that in many cases intrinsic variations with ISS-like time scales are present.

CHAPTER 3

OBSERVATIONS AND ANALYSIS

3.1 INTRODUCTION

In this chapter we firstly describe the procedures of observations and analysis for the 33 pulsars studied by us. The latter sections in this chapter describe the methods which were used for correcting the ISS parameters computed from the raw data for the effects of receiver noise and other instrumental characteristics.

3.2 OOTY RADIO TELESCOPE

The observations were carried out with the Ooty Radio Telescope (ORT) operating at 326.5 MHz (Swarup et al. 1971). The ORT has a coverage in declination of $\pm 35^{\circ}$ and can track a source continuously for $9\frac{1}{2}$ hours. The feed at the focal line of the parabolic cylindrical reflector of ORT consists of a collinear array of 968 half wavelength dipoles which are linearly polarized (Kapahi et al. 1975). The ORT has a multibeam facility which provides twelve simultaneous beams with separation between adjacent beams in the north-south direction of $3(\sec \delta)$ minutes of arc. Both total power and phase switched modes of operations are available. Each beam in the total power mode has a half-power beamwidth of 5.5 arcmin in declination and $2^{\circ}.2$ in RA. The normal pass band of

ORT is 4 MHz centred at 326.5 MHz. The block diagram of the receiver system is given in Fig.(3.1). The full description of the system is available in references (Swarup et al. 1971; Sarma et al. 1975 a; Sarma et al. 1975 b). Pulsar observations presented in this thesis were done with Beam No.8 in the total power mode and using a receiver with filter banks of narrow bandwidth, as described in the following sections.

3.3 12-CHANNEL FILTER BANKS

Most of the observations were made with a multichannel receiver with a bandwidth of 300 kHz for each of the channels. But in some cases, where the dispersion measures (DM) of the pulsars were large, say DM > 35 pc. cm^{-3}, a 50 kHz system was used.

3.3.1. The 12-channel 300 kHz system

This system consists of a set of 12 tuned amplifiers each of 300 kHz half power width (Fig.(3.2)). Their centre frequencies (f_o) are around 5 MHz and the difference (δf_o) between centre frequencies of adjacent channels is 300 kHz. The normalised intensity response of the channels are shown in Fig.(3.3). Inputs to these amplifiers at about 5 MHz were derived by using a wideband mixer at the output of the main 30 MHz intermediate frequency amplifier of the ORT. The local oscillator signal to this mixer is generated by a crystal oscillator followed by frequency multipliers and power

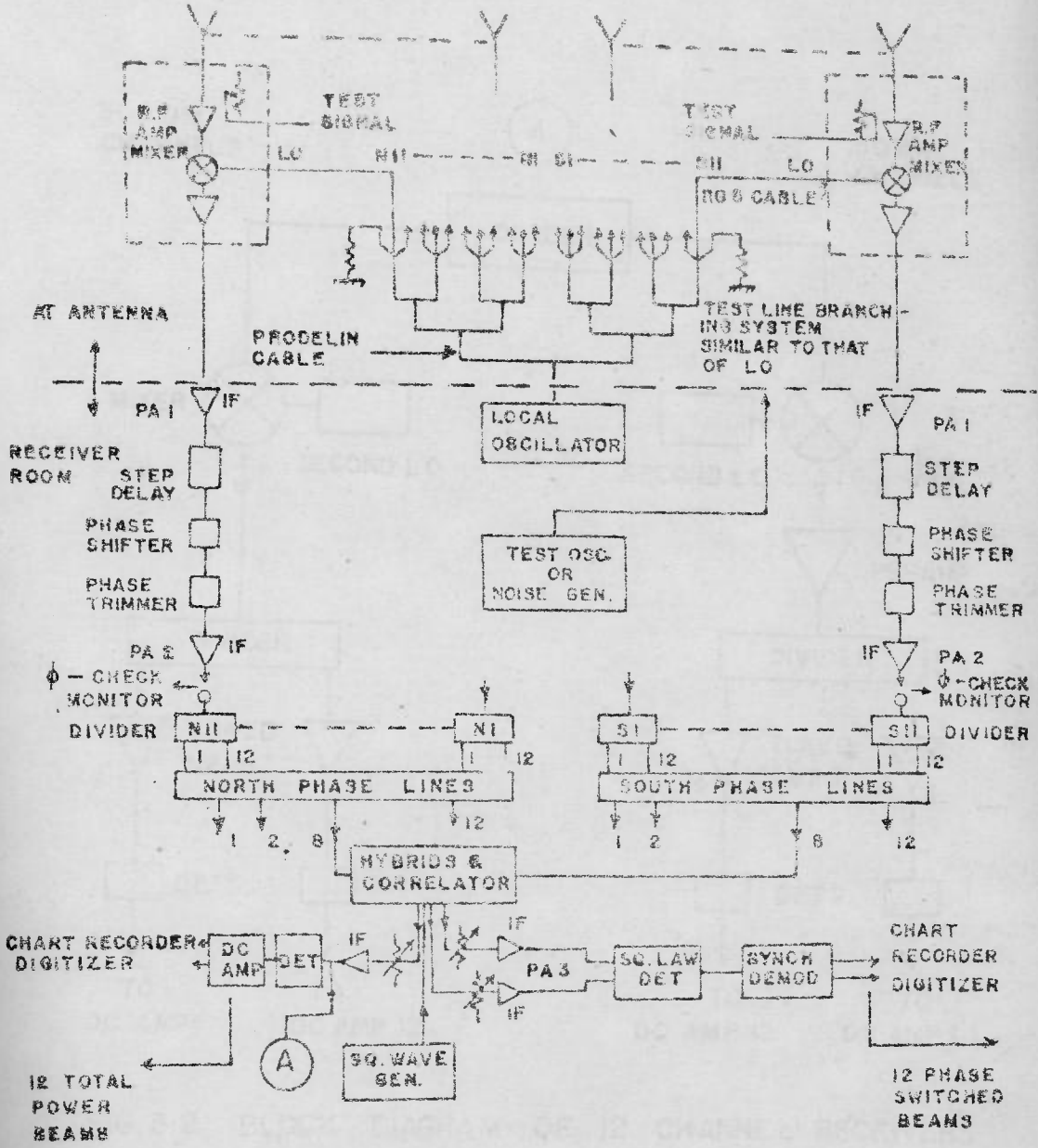

FIG. 3-1 BLOCK DIAGRAM OF RECEIVER SYSTEM OF THE OOTY RADIO TELESCOPE

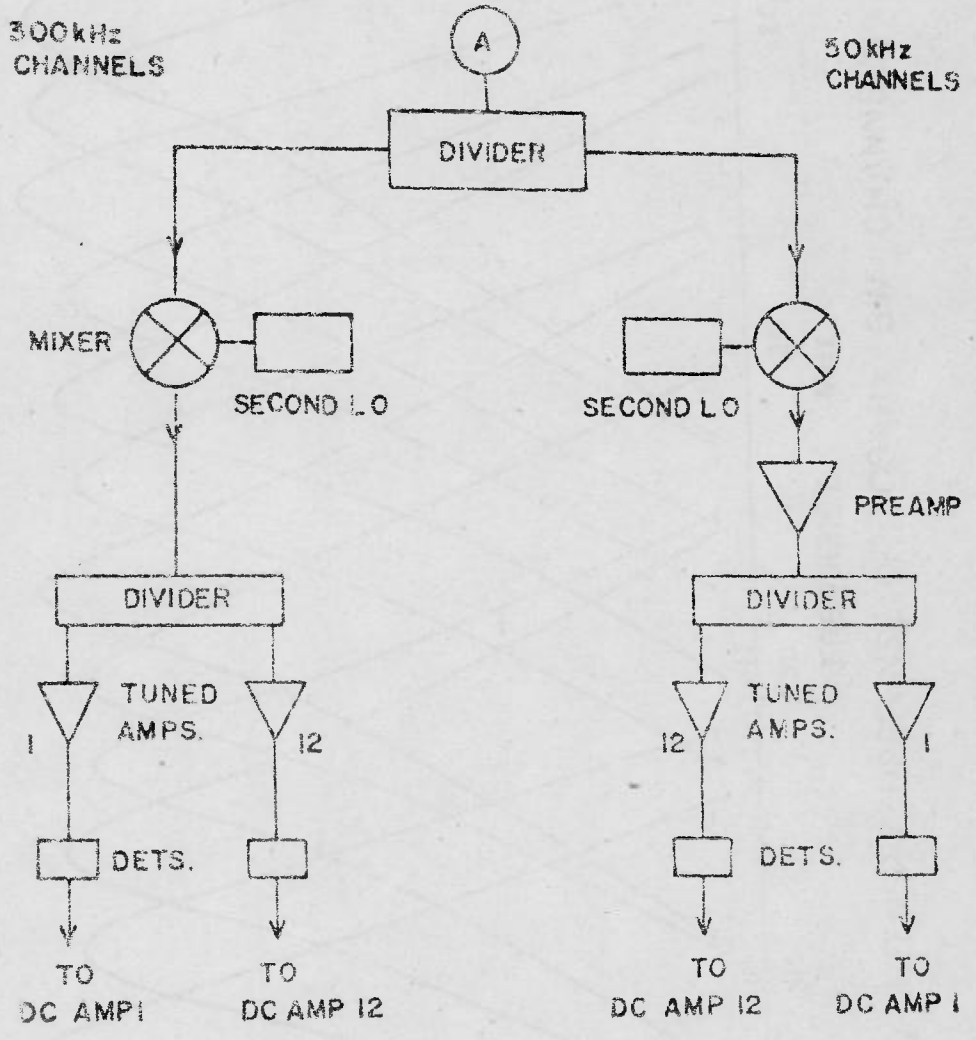

FIG. 3·2 BLOCK DIAGRAM OF 12 CHANNEL RECEIVERS

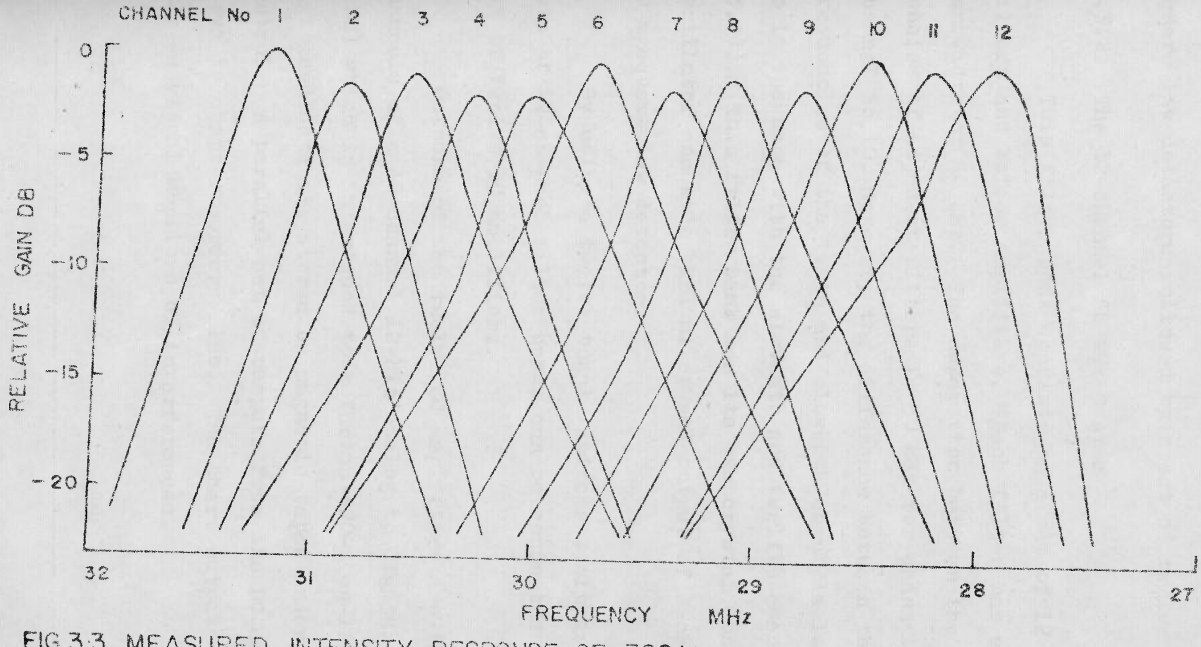

FIG. 3·3 MEASURED INTENSITY RESPONSE OF 300 kHz BW CHANNELS

amplifier. The output of the tuned amplifiers are fed to square law detectors followed by a set of twelve DC amplifiers.

3.3.2. The 12-channel 50 kHz System

This filter bank consists of a set of 12 passive filters and buffer amplifiers. Each filter has a half power bandwidth of 50 kHz. The separation between the centre frequencies of adjacent filters is 50 kHz for channel No.1 to channel No.10. However, the difference between the centre frequencies of the tenth and eleventh channels is 0.5 MHz and so is the case with the eleventh and twelfth channels (Fig. (3.4)). This filter bank has its own crystal controlled local oscillator and wide band mixer and output of each channel goes to a square law detector.

By using a twelve toggle switches, either of the two sets of 12-channel filter banks can be connected to the common set of twelve DC amplifiers.

Outputs of the twelve DC amplifiers are fed to twelve channels of a 48-channel 12-bit analog to digital converter (ADC) which is interfaced to a Varian 620-i on-line computer. Digitised data are stored on magnetic tapes under computer control. A parallel set of outputs from the DC amplifiers flows to chart recorders also. The chart outputs are used only as visual monitors of interferences.

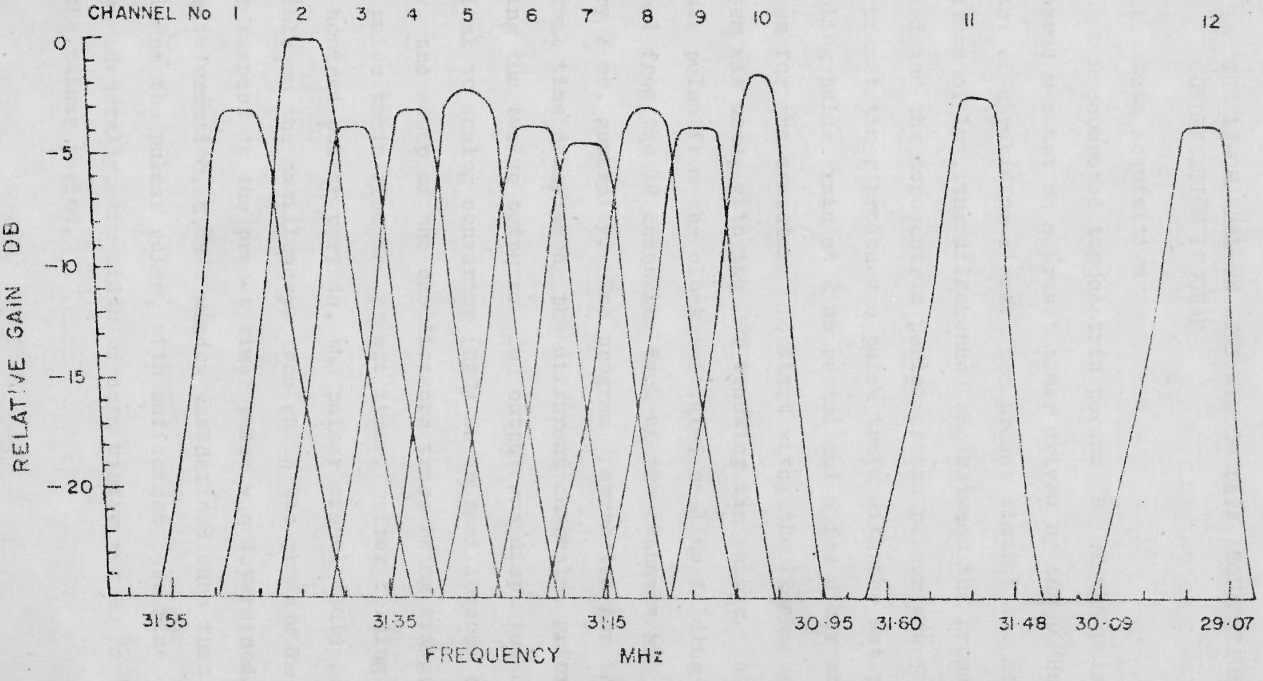

FIG. 3·4 MEASURED INTENSITY RESPONSE OF 50 kHz BW CHANNELS

3.4 THE 12-CHANNEL ON-LINE WINDOW DATA ACQUISITION AND CONDENSATION PROGRAM

3.4.1. Data Acquisition

Precomputed topocentric period P of the pulsar to be observed was set on a preset timer driven by the 1 MHz signal output of a rubidium clock. The preset timer being adjustable in steps of 1μs, the difference ΔP between the preset timer period and the topocentric period of the pulsar was $\leq 5 \times 10^{-7}$s. The preset timer produced a pulse train with the set period, a sampling pulse train at 2 ms period and a few other control pulses for the computer. To start with, the 12-channel 300 kHz system was used, with the ORT tracking the pulsar. A prescribed minute pulse from the clock initiated on-line folding of the signal from the 12 channels. Each of the channels was sampled every 2 ms, generally. The program corrected for the pulse arrival time delay among the different channels, prior to adding the twelve outputs. The output was displayed using a digital to analog converter (DAC) on an oscilloscope continually, the sweep of the oscilloscope trace being triggered by the pulse train from the preset timer. After folding for a few hundred pulsar periods, the pulsar signal would be clearly visible on the oscilloscope from which the phase of the pulssr pulse with respect to the preset timer pulse was determined. Using this information, a data window was defined such that it includes the pulsar pulse, with sufficient base line on either side. Generally, the width of data window was 20 % to 30 % of the pulsar period.

Once the data window was defined one could change over to the 50 kHz system or continue with the 300 kHz system itself. The former was preferred for pulsars of DM greater than 35 pc. cm.$^{-3}$, in order to resolve adequately intensity decorrelation with frequency and to reduce dispersion smearing within the bandwidth. (Pulse smearing due to dispersion across the bandpass at 327 MHz amounts to 0.012 ms. per pc. cm.$^{-3}$ for 50 kHz channels and 0.0715 ms. per pc. cm.$^{-3}$ for 300 kHz channels). The on-line folding was then terminated and the on-line acquisition of digitised data over the data window, from each channel at 2 ms. intervals, was started. An off-pulse base level for each channel was also acquired alongside the on-pulse window data by determining the mean over a few tens of milliseconds. This off-pulse base level was midway between the two consecutive on-line windows. The on-pulse samples and the off-pulse level for each channel were recorded digitally on magnetic tape. If $\Delta P \neq 0$, it resulted in a gradual drift of the pulsar pulse within the data window. The pulse position within the data window was monitored from time to time in the course of data acquisition to ensure that the pulses remained well within the window. The drift rate was computed during off-line analysis and corrected for.

3.4.2. Condensation

Data recorded in the above format has been used for two purposes: (a) scintillation studies presented here and

(b) detailed studies of pulse structure and subpulse variations, the results of which will be presented elsewhere. For studying the scintillation of pulsar signals due to the interstellar medium and possible intrinsic variations in pulsars with time scales similar to that of interstellar scintillations, such detailed data is not necessary. A pair of 'ONPULSE' and 'OFFPULSE' intensities for each pulse per channel is enough for ISS studies. To arrive at this simplified data format from the raw data a computer program named 'PULSCINT' was used. We will refer to the procedure of simplifying the data format as condensation of data. The 'PULSCINT' program developed by Krishnamohan is the one used for carrying out a major part of analysis of data, including condensation and computation of the frequency cross correlation function (CCF) and power spectra of pulsar intensities. The procedural details of condensation are described below.

The 'ONPULSE' intensity was computed from raw data and stored on magnetic tape as described below. A specified number k of adjacent 2 ms. samples over the pulse, from p_1th to p_{1+k}th, in the raw data were added. From this the corresponding off-pulse base level was subtracted to give the 'ONPULSE' intensity. k was chosen suitably so that 'ONPULSE' intensity was representative of the characteristic subpulse emission from the pulsar. Similarly an 'OFFPULSE' intensity was obtained by using ℓ adjacent samples, from n_1th to $n_{1+\ell}$th, from the raw data, such that these samples were

outside pulse duration. The data window used during acquisition of data was wide enough to permit this procedure. In general, k and ℓ need not be the same, in which case the 'OFFPULSE' power spectrum was corrected by a multiplicative correction factor 'a' in order to make quantitative comparison between 'ONPULSE' and 'OFFPULSE' power spectra possible. 'a' depends on k, ℓ and τ_R the receiver time constant (Appendix B). During condensation p_1 and n_1 were continually upgraded as consecutive pulses were condensed, by using the known drift rate of pulsar pulse within the data window, so that the condensed intensities were always from a fixed phase of pulsar period. The condensed data on magnetic tape consisted of 'ONPULSE' and corresponding 'OFFPULSE' value for each pulse, stored separately for each of the twelve narrow band channels. Consecutive N 'ONPULSE' values ('OFFPULSE' values) could be averaged to produce arrays consisting of intensity points constituting a time series. N could be varied as integral powers of 2 . The array length M was also variable. Generally, array lengths of 1024 or 2048 were used.

3.5 DATA ANALYSIS

In a study of the characteristics of fluctuations of pulsar signals one is interested in (a) correlation of intensities at different radio frequencies, (b) modulation index of the fluctuations and (c) power spectrum of the fluctuations.

We define below the parameters specifying the above three features of the observed fluctuations of pulsar emission.

3.5.1. The Cross Correlation Function (CCF), γ_{1j}

The CCF, γ_{1j}, between the intensities of first and jth channels of the multichannel receiver is defined by

$$\gamma_{1j} = \frac{< [\vartheta_1(t) - <\vartheta_1(t)>] [\vartheta_j(t) - <\vartheta_j(t)>] >}{\sigma_1 \sigma_j}$$

$$= \frac{<I_1(t) I_j(t) >}{\sigma_1 \sigma_j} \qquad (3.1)$$

where I_1, I_j are the mean subtracted intensities and σ_1^2, σ_j^2 are the variances of I_1, I_j given by

$$I_j(t) = \vartheta_j(t) - <\vartheta_j(t)> \qquad (3.2)$$

$$\sigma_j^2 = < [\vartheta_j(t) - <\vartheta_j(t)>]^2 > \qquad (3.3)$$

The angular brackets denote averages over time t.

3.5.2. Modulation Index m_j

The modulation index m_j for the intensities in the jth channel is defined by

$$m_j^2 = \frac{\sigma_j^2}{<\vartheta_j(t)>^2} \qquad (3.4)$$

3.5.3. Power Spectra

Acquisition of data on pulsar intensities with any channel for n consecutive pulses results in a time series (I(t),I(t+P), I(t+2P), ... , I(t+nP). This time series can be subjected to standard methods of power spectral analysis (Blackman and Tuckey 1959; Otnes and Enochson 1972) to yield power spectra which give the variance density S as a function of the fluctuation frequency f . In our analysis the power spectra of arrays of pulse intensities were computed by a subroutine of 'PULSCINT'. From 'PULSCINT' analysis we could obtain three kinds of spectra of mean subtracted intensities, namely, (a) $S_j(f)$ which is the spectrum for the jth channel (j = 1,2,3, ... 11, 12), (b) $\Sigma_{j=1}^{12} S_j(f)$ which we call as the Narrow Band All Channels Combined Spectrum (NBACCS) and (c) $S_B(f)$, the Broad Band Spectrum (BBS) which is derived from a time series of mean subtracted intensities with the intensities obtained by adding the corresponding pulse intensities from all the narrow band channels, prior to power spectral analysis.

3.5.4. Smoothing of Intensities of Consecutive N Pulses

As discussed in Section 1.1, the pulsar intensity fluctuations, in general, could be due to intrinsic causes as well as irregularities in IS medium. One of the most well-studied types of intrinsic fluctuations is the pulse to pulse variations which are correlated over a large range of radio

frequencies. This type of variations have time scales typically of a few or several periods in contrast to the time scales of ISS which are on the order of minutes. As such, the fluctuations due to pulse to pulse variations could be considerably smoothed out without appreciably affecting the fluctuations due to ISS, by averaging the intensities of consecutive 10 or 20 pulses. With 'PULSCINT' program we achieve this by assigning a suitable value, say 8 or 16 or 32, for the parameter N. γ_{1j}, m_j, $\langle g_j \rangle$, $S_j(f)$ and $S_B(f)$ were all computed from such arrays of smoothed intensities only.

3.6 CORRECTIONS TO γ_{1j}, σ_j^2, m_j^2 and $S_j(f)$ TO REMOVE EFFECTS DUE TO RECEIVER NOISE

The definitions as per the preceding sections, of quantities of interest relevant to ISS of pulsar signals - namely cross correlation function, variances of intensities, scintillation indices and power spectra of intensity fluctuations - are strictly valid only in the absence of receiver noise. In practice intensities recorded are always mixed up with receiver noise, resulting in uncertainties in determination of exact magnitudes of both intensities as well as their fluctuations due to ISS or intrinsic variations. Corrections to γ_{1j}, σ_j^2, m_j^2 and $S_j(f)$ computed from 'ONPULSE' intensities, using those computed from 'OFFPULSE' intensities, are necessary to remove these effects. Methods of correction for receiver noise are described below.

3.6.1. Corrections to γ_{1j} and σ_j^2

Let k and ℓ adjacent samples from raw data be added to produce 'ONPULSE' and 'OFFPULSE' intensities as described in an earlier section. Let σ_{jt}^2 and σ_{jn}^2 be the variances computed from the smoothed intensity arrays for 'ONPULSE' and 'OFFPULSE' respectively. σ_{jt}^2 includes contribution from both fluctuations of signals (due to both intrinsic variations and ISS) as well as receiver noise. Signal fluctuations being independent of noise fluctuations we can write

$$\sigma_{jt}^2 = \sigma_j^2 + a\sigma_{jn}^2 \qquad (3.5)$$

where σ_j^2 = variance due to signal fluctuations alone, 'a' is a correction factor due to the fact that the number of samples added to form 'ONPULSE' intensities and that for 'OFFPULSE' intensities are not equal i.e. $k \neq \ell$, and is given by (Appendix B)

$$a = \frac{k+2(k-1)e^{-t/\tau}+2(k-2)e^{-2t/\tau}+\ldots+2e^{-(k-1)t/\tau}}{\ell+2(\ell-1)e^{-t/\tau}+2(\ell-2)e^{-2t/\tau}+\ldots+2e^{-(\ell-1)t/\tau}} \qquad (3.6)$$

where t = sampling interval used in acquiring raw data

τ = RC time constant of the receiver channels.

From eqn. (3.5) σ_j^2 could be calculated.

The CCF is computed separately for both 'ONPULSE' and 'OFFPULSE' intensities. For 'ONPULSE' intensities one can write

$$\gamma_{1j\ ON} = \frac{\langle I_{1ON}\ I_{jON}\rangle}{\sigma_{1t}\sigma_{jt}} \qquad (3.7)$$

For the'OFFPULSE' case, i.e. for receiver noise alone, we write

$$\gamma_{1jOFF} = \frac{\langle I_{1OFF}\ I_{jOFF}\rangle}{\sigma_{1n}\sigma_{jn}} \qquad (3.8)$$

The 'true'frequency cross correlation function due to signal fluctuations γ_{1j} can be written as

$$\gamma_{1j} = \frac{\langle I_1\ I_j\rangle}{\sigma_1\sigma_j} = \Gamma_{OBS} \qquad (3.9)$$

From known values of γ_{1jON}, γ_{1jOFF}, σ_{jt}^2, σ_{jn}^2 and a, one can compute γ_{1j} using the relation

$$\gamma_{1j} = \left[\ \gamma_{1jON} - \gamma_{1jOFF}\ \frac{\sigma_{1n}\sigma_{jn}}{\sigma_{1t}\sigma_{jt}}\ \right] \frac{\sigma_{1t}\sigma_{jt}}{\sigma_1\sigma_j} = \Gamma_{OBS} \qquad (3.10)$$

The value of γ_{1jOFF} depends only on the intensity responses of the first and jth channels, which are invariant with respect to time. For each pulsar which was observed, γ_{1jOFF} were computed for different values of j(j=2,3,...11 and 12). From this set of values the mean value of γ_{1jOFF} corresponding

to each channel was obtained. These mean values were used in eqn.(3.10) to arrive at γ_{ij}. Mean values of γ_{1jOFF} are listed in Table (3.1) for both 300 kHz and 50 kHz systems.

3.6.2. Correction to m_j

The 'true' modulation index, m_j, that will be obtained in the absence of receiver noise is given by

$$m_j^2 = \frac{\sigma_j^2}{\langle \mathcal{I}_{jON} \rangle^2} \qquad (3.11)$$

as fluctuations due to receiver noise do not change the mean intensity $\langle \mathcal{I}_j \rangle$ when averaging time is much larger than the receiver's time constant so that $\langle \mathcal{I}_{jON} \rangle = \langle \mathcal{I}_j \rangle$. This applies to our data analysis where $\langle \mathcal{I}_{jON} \rangle$ is determined by averaging intensities over a few hours or more whereas the R-C time constant of the receiver is 3 ms.

The modulation index of the 'ONPULSE' intensities in the jth channel, computed by 'PULSCINT' can be expressed as

$$m_{jt}^2 = \frac{\sigma_{jt}^2}{\langle \mathcal{I}_{jON} \rangle^2} .$$

That is

$$m_j^2 = \frac{\sigma_j^2}{\langle \mathcal{I}_{jON} \rangle^2} = \frac{\sigma_{jt}^2}{\langle \mathcal{I}_{jON} \rangle^2} \cdot \frac{\sigma_j^2}{\sigma_{jt}^2}$$

$$= m_{jt}^2 \frac{\sigma_j^2}{\sigma_{jt}^2} .$$

TABLE 3.1

VALUES OF CORRELATION γ_{1jOFF} FOR OFF-PULSE NOISE

Ch.No.	Mean Value of γ_{1jOFF}	
	300 kHz System	50 kHz System
1	1.000	1.000
2	0.353	0.152
3	0.119	0.000
4	0.065	0.000
5	0·000	0.000
6	0.000	0.000
7	0.000	0.000
8	0.000	0.000
9	0.000	0.000
10	0.000	0.000
11	0.000	0.000
12	0.000	0.000

Hence we have,

$$m_j = \frac{m_{jt}\,\sigma_j}{\sigma_{jt}} \qquad (3.12)$$

'ONPULSE' modulation indices were corrected for receiver noise using eqn. (3.12).

3.6.3. Corrected Estimate of Variance of Intensity Fluctuations from Power Spectra

The variance σ^2 of fluctuations is related to the power spectrum of fluctuations by the integral relation

$$\sigma^2 = \int_0^{f_N} S(f)df \qquad (3.13)$$

where $S(f)$ = spectral power at frequency f and

f_N = Nyquist frequency.

If the variance σ_j^2 due to signal fluctuations alone were to be estimated from the 'ONPULSE' and 'OFFPULSE' spectra we have

$$\sigma_j^2 = \int_0^{f_N} S_{ON}(f)df - a\int_0^{f_N} S_{OFF}(f)df \qquad (3.14)$$

It may be mentioned here that for the parameters computed from broad band data similar methods were used for applying corrections due to receiver noise.

CHAPTER 4

METHODS OF COMPARISON BETWEEN OBSERVED AND THEORETICALLY ESTIMATED ISS PARAMETERS

4.1 ISS PARAMETERS OF INTEREST

Observation of pulsar intensity variations provide the following parameters related to the properties of the interstellar medium. These parameters are: (i) the decorrelation frequency f_ν , (ii) the scintillation index m due to ISS, (iii) the scintillation bandwidth f_o and (iv) the pulse broadening due to interstellar scattering Δt_s . We do not concern ourselves, in the work reported in this thesis, with the measurement of angular broadening θ_s due to interstellar scattering.

4.2 DECORRELATION FREQUENCY f_ν

The decorrelation frequency f_ν is defined as that value of frequency separation $\Delta\nu$ at which the normalised frequency correlation function, corrected for intrinsic fluctuations, decays to half its maximum value. This definition of decorrelation frequency is identical to that used by Lang (1971a). The parameter B_h , called the half visibility bandwidth, used by Rickett (1970) is directly related to f_ν as $B_h = 3.3 f_\nu$ (Sutton 1971). Ewing et al. (1970) had parameterized decorrelation of intensities with frequency by

measurement of half widths B of features on two dimensional contours of intensities against frequency and time. Though B is a function of f_ν it is difficult to establish a straightforward mathematical relation between f_ν and B, because of the very nature of the definition of B. Only an empirical relation $B = 10 f_\nu$ could be established (Sutton 1971).

As discussed in Section (2.7), the presence of intrinsic variations of intensities with time scale larger than the smoothing time N x P during which the consecutive pulse intensities are averaged, will be indicated by a steady non zero value p of Γ_{OBS} for large frequency separations. We did come across such situations for many pulsars. Hence the CCF was renormalised using the relation (Eqn.2.45)

$$\Gamma_{SCINT} = \frac{\Gamma_{OBS} - p}{1 - p} = \Gamma_{1j} \qquad (4.1)$$

The resulting curve of Γ_{1j} vs channel number j represents scintillation only and could be tested for predictions of the theory of scintillation outlined in Chapter 2.

4.3 SCINTILLATION INDEX m

The scintillation index m due to ISS is given by

$$m^2 = \frac{\sigma_m^2}{\langle S(t) \rangle^2} \qquad (4.2)$$

where σ_m^2 is the variance of fluctuations in intensity due to IS medium alone and $\langle I(t) \rangle$ is the mean intensity over which the fluctuations are observed. It is probable that intrinsic intensity fluctuations with similar time scales as those due to ISS exist. In such a case the observed modulation index m_j (eqn.3.4) cannot be a true representative of the scintillation index due to IS medium. As discussed in Section (2.7), if observations were done simultaneously with receivers of different bandwidths it is possible to estimate the true scintillation index. We postpone the description of the methods adopted by us to estimate scintillation indices from observations to a later section (Section 4.8).

4.4 SCINTILLATION BANDWIDTH f_e AND DECORRELATION TIME τ_ν

The scintillation bandwidth f_e is defined as the e^{-1} width of the ISS component in the power spectrum of intensity fluctuations and hence gives an idea of the typical time scales of ISS. An equivalent description of ISS time scales is given by the decorrelation time τ_ν which is defined as the e^{-1} width of the temporal intensity autocorrelation function (ACF) due to ISS. f_e and τ_ν are related to each other by $f_e = (2\pi\tau_\nu)^{-1}$, owing to the Fourier transform relationship between autocorrelation function and power spectrum. As in the case of determination of scintillation index, the existence of intrinsic variations with time scales similar to those of ISS complicates the problem of estimating

the true scintillation bandwidth from observed power spectra of intensity fluctuations. This has been discussed in Section 2.7 wherein we have referred to the method developed recently by Krishnamohan at our Centre to tackle this difficulty.

4.5 FINITE BANDWIDTH EFFECTS

From the theoretical discussion of intensity correlations as embodied in the evolution of $Q_I(z,\bar{\rho}_i,\bar{\rho}_j,\nu_i,\nu_j)$ in the second chapter, it is clear that $f_\nu, \tau_\nu, \Delta t_s$ and m are strongly dependent on the bandwidth of the detector used for the observations. It is preferable to remove the dependence of ISS parameters on detector bandwidths. In the measurements of f_ν by Lang (1971a) and f_e by Backer (1975) bandwidth effects were not eliminated or corrected for. Rickett (1970) had estimated B_h values incorporating corrections for bandwidth effects. His corrections were based on the theory of Uscinski (1968) which requires extremely strong scattering to be valid. We have adopted methods derived from the strong scintillation theory due to Lee and Jokipii which is based on Markov approximation, to estimate bandwidth effects on ISS parameters, as Markov approximation is valid for less restrictive conditions than those required for Uscinski's theory. The following sections describe the procedures used by us for estimating 'true' ISS parameters from observed CCF and power spectra.

4.6 COMPARISON OF OBSERVED CCF WITH THEORETICALLY PREDICTED CCF

4.6.1. Method for Estimating Decorrelation Frequency from Observations

Earlier investigators (e.g. Lang 1971, Sutton 1971) have determined the values of decorrelation frequency f_ν from observations by defining f_ν as the frequency separation at which the observed CCF (which is corrected for intrinsic intensity fluctuations) decays to half of its maximum value at zero frequency separation. Our method of estimating the value of f_ν from the observed CCF, $\gamma_{1j}(j)$, is somewhat different from this. Corrections for both intrinsic intensity fluctuations and finite bandwidth effects are incorporated in our method. A brief outline of our method is as follows:

(a) Firstly, from the observed frequency cross correlation function $\gamma_{1j}(j)$ we determine $\Gamma_{1j}(j)$ which is the CCF corrected for intrinsic intensity fluctuations, by using eqn.(2.45).

(b) Using the theory of ISS described in Chapter 2 and the known intensity response of the 12 channel receivers, we construct $\Gamma'_{1j}(j,f_\nu)$ which is the CCF expected from theory and f_ν is the decorrelation frequency for ideal, receivers of zero bandwidth. The function $\Gamma'_{1j}(j,f_\nu)$ is computed for all values of the channel number j and for several values of f_ν ranging between $f_{\nu min}$ and $f_{\nu max}$ at suitable discrete intervals Δf_ν. Two sets of

such curves $\Gamma'_{1j}(j,f_\nu)$ are constructed, one assuming Gaussian spectrum of irregularities and the other assuming Kolmogorov spectrum,

c) Finally, for the intrinsic-corrected CCF, $\Gamma_{1j}(j)$, we find the best-fitting model curve $\Gamma'_{1j}(j,f'_\nu)$ by the method of least squares. Now, the value of the decorrelation frequency for the observed CCF $\Gamma_{1j}(j)$ is given by f'_ν.

The details of the above method of determination of decorrelation frequencies from observations are given in the following sections.

4.6.2 Computation of the theoretically expected CCF, $\Gamma_{1j}(j,f_\nu)$

It may be recalled from Section (3.5) that we have defined the cross correlation of intensity fluctuations at two different channels by γ_{ij} which are normalised by the product of the rms values of the fluctuations in the two channels and not by the product of the mean values. If $G_i(\nu)$ and $G_j(\nu)$ are the intensity responses of the ith and jth channels respectively, then the theoretically expected CCF, Q'_I, which incorporates finite bandwidth effects due to the receivers, is given by (Appendix A),

$$Q'_{Iij} = Q'_{Iij}(z, G_i, G_j, \bar{\rho} = 0)$$

$$= \frac{\int_\nu \int_{\nu'} G_i(\nu) G_j(\nu') \Gamma_D^2 (|\delta\nu/f_\nu|) d\nu d\nu'}{\sigma'_i \sigma'_j} \qquad (4.1)$$

where $\delta\nu = \nu - \nu'$ and σ_i', σ_j' are the bandwidth affected rms values of the fluctuations in the ith and jth channels respectively. σ_i' and σ_j' are given by

$$\sigma_k' = \int_{\nu}\int_{\nu'} G_k(\nu) G_k(\nu') \Gamma_D^2(|\delta\nu/f_\nu|) d\nu d\nu' \qquad (4.1a)$$

for k = i or j. The integrations in eqn(4.1) are over the pass bands of the ith and jth channels. It may be noted that besides incorporating the ISS bandwidth effects, the formulation given by eqn.(4.1) includes any possible correlations of receiver noise in the two channels also which may arise due to overlap of the intensity responses of the channels.

The values of $\Gamma_D(|\delta\nu/f_\nu|)$ used for evaluating Q_{Iij}' were derived from the graphical plots of the solutions of Γ_D given by Lee and Jokipii for Gaussian and Kolmogorov spectra (Figs (1) and (3) of their paper.1975b). The solutions of Γ_D are given as functions of $(\Delta\omega/\omega_c) = (\delta\nu/\nu_c)$ where ν_c is the characteristic frequency scale of Γ_D which is the first order coherence function.[9] To arrive at Γ_D^2 as a function of f_ν which is the frequency scale of the second order coherence function we define f_ν as

$$f_\nu = b\nu_c \qquad (4.2)$$

where b is a constant nearly equal to 0.5. This definition is based on (i) the theoretically calculated CCF, P_I, for receivers of zero bandwidth decays to half of its peak value for values of frequency separations $0.52\nu_c$ and $0.44\nu_c$ in the cases of Gaussian and Kolmogorov spectra respectively, and

(ii) in the literature on ISS of pulsars f_ν is defined as the frequency separation at which the observed CCF decays to half of its peak value. As such the definition of f_ν as per eqn.(4.2) facilitates direct comparison of our measurements of decorrelation frequency with measurements by earlier workers.

The integrations in eqn.(4.1) were carried out numerically for i=1 and j=2,3,....,12, for both 300 kHz and 50 kHz receiver systems, and for Gaussian and Kolmogorov spectra. For the 300 kHz system $\Gamma'_{1j}(j,f_\nu)$ was evaluated for f_ν values which were integral multiples of 19.5 kHz in the Gaussian case; they were multiples of 16.5 kHz for Kolmogorov spectrum. The corresponding numbers for the case of the 50 kHz system were 3.125 kHz and 2.625 kHz, for Gaussian and Kolmogorov spectra respectively. For a few selected values of f_ν the computed CCF are shown in Figs (4.1), (4.2), (4.3) and (4.4). The relevant information on the receiver system, type of spectrum assumed and the value of f_ν for each curve are given in the respective figures. It may be noted that the curves for the 300 kHz system presented in Figs.(4.1) and (4.2) correspond to values of ν_c which are integral multiples of 150 kHz, for both the spectra. For example, the curve with f_ν value marked as 156 kHz in Fig.(4.1) and the one with f_ν value marked as 132 kHz in Fig.(4.2), have the same value of ν_c = 300 kHz. The differences in the values of f_ν assigned to them arise from the different values of the constant b

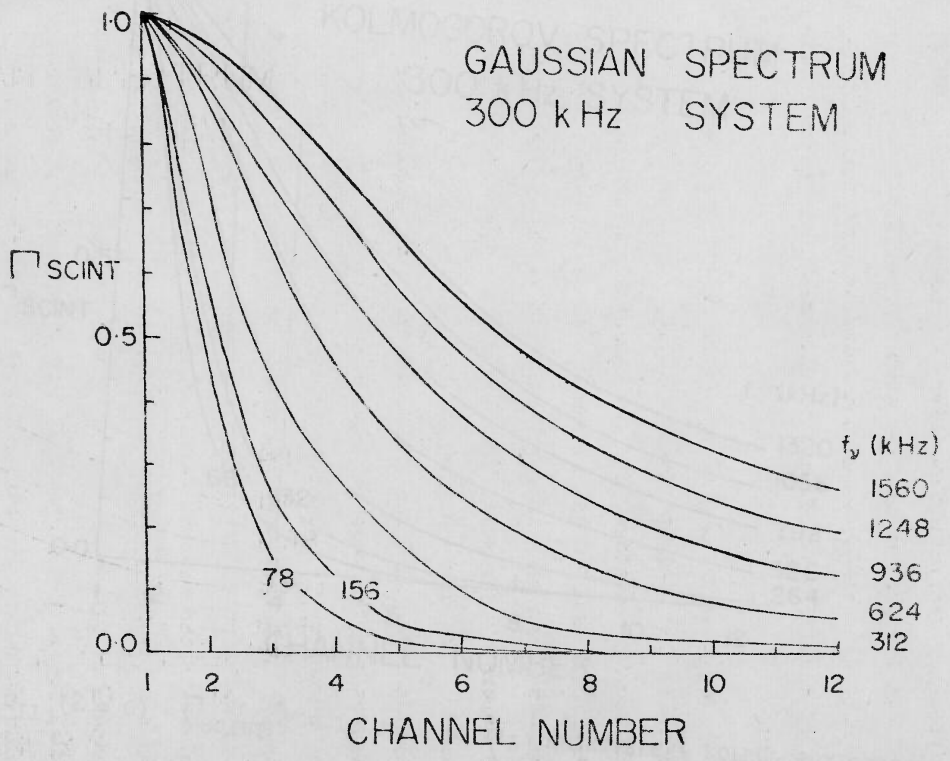

Fig.4.1 $Q'_{Ilj}(\bar{\rho} = 0) = \Gamma_{SCINT}$ for 120h.300 kHz RECEIVERS-GAUSSIAN SPECTRUM

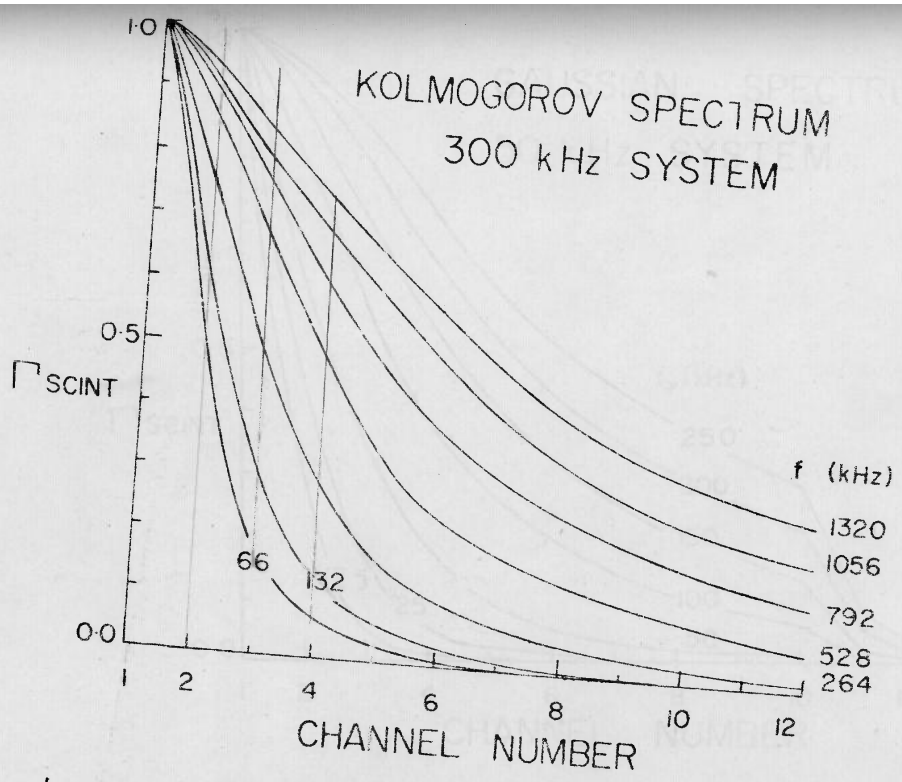

Fig.4.2 $Q'_{I1j}(\bar{\rho} = 0) = \Gamma_{SCINT}$ FOR 12 Ch. 300 kHz RECEIVERS - KOLMOGOROV SPECTRUM

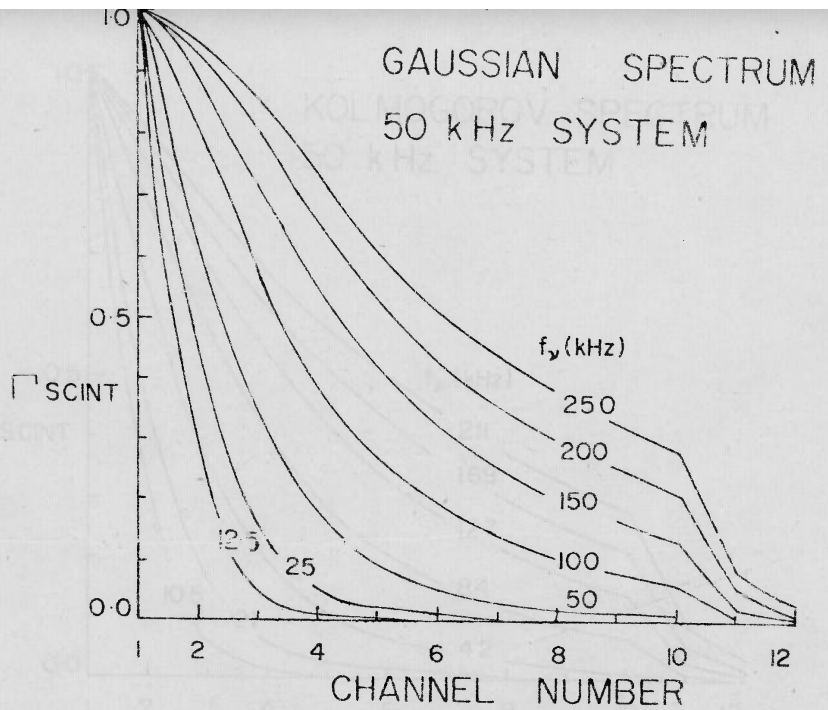

Fig.4.3 $Q'_{Ilj}(\bar{o} = 0) = \Gamma_{SCINT}$ for 12 Ch. 50 kHz RECEIVERS - GAUSSIAN SPECTRUM

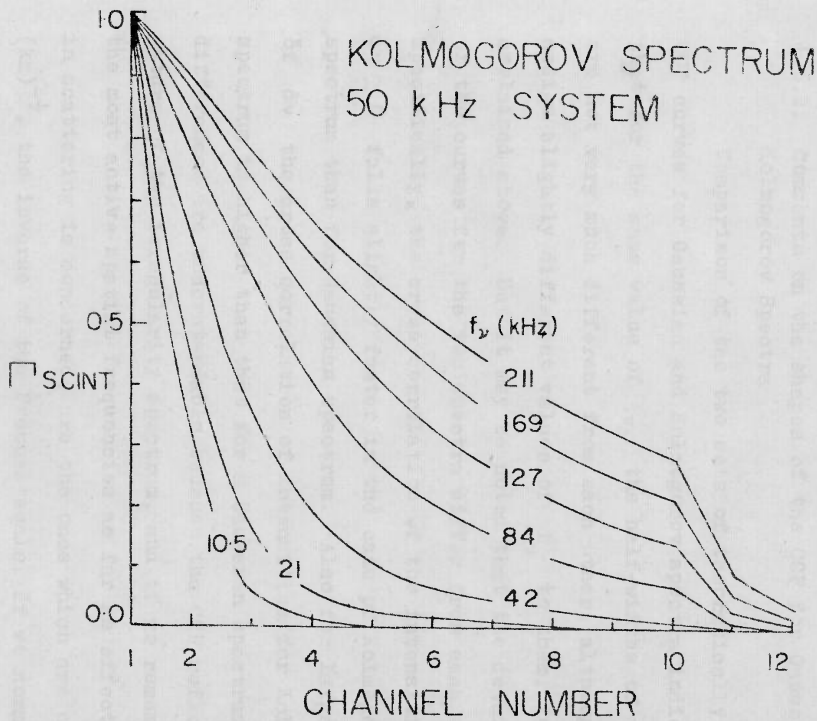

Fig.4.4 $Q'_{11j}(\bar{\rho} = 0) = \Gamma_{SCINT}$ FOR 12 Ch. 50 kHz RECEIVERS - KOLMOGOROV SPECTRUM

for the two spectra, in our definition of f_ν as per eqn. (4.2). Similarly the values of ν_c for the curves shown in Figs. (4.3) and (4.4), are integral multiples of 24 kHz.

4.6.2. Comments on the shapes of the CCF for Gaussian and Kolmogorov Spectra

Comparison of the two sets of theoretically expected CCF curves for Gaussian and Kolmogorov spectra indicates that for the same value of ν_c the half-widths of the curves are not very much different from each other, although we assign slightly different values of f_ν to them, for reasons explained above. But it may be noted that the detailed shape of the curves for the two spectra differ from each other. Specifically, the cross correlation of the intensities around $\delta\nu \simeq 0$ falls slightly faster in the case of Kolmogorov spectrum than for Gaussian spectrum. Also for larger values of $\delta\nu$ the cross correlation of intensities for Kolmogorov spectrum is higher than that for a Gaussian spectrum. These differences are understandable because the CCF reflects the nature of the irregularity spectrum, and if we remember that the most active spatial frequencies as far as effectiveness in scattering is concerned, are the ones which are close to $(kz)^{-\frac{1}{2}}$, the inverse of the Fresnel scale. If we normalize both the spectra with the peak power which occurs at the lowest spatial frequencies so that comparison of the relative distribution of power at different spatial frequencies for the two spectra is made easier, then we find that relative to

the Gaussian spectrum the Kolmogorov spectrum has proportionately larger power at frequencies around $(kz)^{-\frac{1}{2}}$. This is responsible for the faster decrease of CCF around $\delta\nu \simeq 0$ in the case of the Kolmogorov spectrum as compared with that for the Gaussian spectrum. Similarly for the Kolmogorov spectrum the presence at very low frequencies (i.e. very large scale sizes) of relatively more power than a Gaussian spectrum causes the slower decrease (than that for a Gaussian spectrum) of CCF at large frequency separations.

It is clear from the above, that the detailed shape of the observed curves of Γ_{ij} vs channel number may throw light on the nature of the spectrum of irregularities in interstellar space. But in the attempt to determine the nature of the spectrum from the shape of the observed CCF we are hampered by the fairly large statistical uncertainties on the observationally determined cross correlation of intensities at different radio frequencies. We adopted a least squares method to select a model curve of CCF that is best-fitting to the observed CCF. This method yielded a best estimate of the decorrelation frequency of the pulsar. The least squares method could also indicate which of the two spectral models yields a better fit. In the forthcoming sections we quantify the statistical uncertainties and describe the methods used in implementing the least squares fit.

4.6.3. Statistical Errors on Observed Cross Correlation Coefficient of Intensities

From the theory of the distribution of correlation coefficients one can show that variance due to statistical uncertainty on the observed correlation coefficient Γ_{ij} is given by (Johnson and Kotz 1970)

$$(\Delta\Gamma_{ij})^2 = \frac{[1-(\Gamma'_{ij})^2]^2}{n_c} = \frac{1}{w_j} \qquad (4.3)$$

where n_c = number of independent pairs of variables (I_i and I_j) between which correlation coefficient is estimated and Γ'_{ij} = population mean of the correlation coefficient. In our case n_c is the number of cycles of scintillation in the data corresponding to any one of the narrow band channels and is given by

$$n_c = f_e/\Delta f \qquad (4.4)$$

where f_e is the e^{-1} width of the scintillation part of the power spectrum of intensity fluctuations in a narrow band channel and Δf is the best resolution obtained from the spectrum given by the inverse of the total duration of the data; i.e. $\Delta f = (NxPxM)^{-1}$ where N is the number of consecutive pulses averaged, P is the period of the pulsar and M is the array length of the data (Chapter 3).

Γ'_{ij}, the population mean of correlation coefficients, is given by

$\Gamma'_{1j} = \Gamma^{(k)}_{1j}$ = theoretical expectation for Kolmogorov spectrum and

$\Gamma'_{1j} = \Gamma^{(G)}_{1j}$ = theoretical expectation for Gaussian spectrum.

4.6.4. The Method of Least Squares for Determining the Best-Fit Value of f_ν

From eqn.(4.3) it is clear that the rms errors on the observed cross correlation coefficients for different channels are different, being larger for larger separation of frequencies because Γ'_{1j} is smaller. As such the statistic χ^2 was defined as the sum of the squares of the deviations between observed and model-based cross correlation coefficients with each of the term in the sum of the squares weighted by the corresponding variance due to its statistical uncertainty, i.e.

$$\chi^2 = \sum_{j=2}^{12} (\Gamma'_{1j} - \Gamma_{1j})^2 \, W_j \qquad (4.5)$$

It may be noted that $\Gamma'_{1j} = \Gamma'_{1j}(f_\nu)$ so that $\chi^2 = \chi^2(f_\nu)$. Thus by comparison of the observed CCF with the set of model-based curves one can evaluate χ^2 as a function of f_ν and select the best-fitting model curve as the one that yields the minimum value of χ^2.

There is a serious difficulty inherent in this method owing to the very rapid change of the statistical weights W_j with Γ'_{1j}, when Γ'_{1j} changes from 0.8 to 1.0. This is shown

in Table (4.1) which lists W_j against Γ'_{1j} for $n_c = 1$. As a result, for $f_\nu < 750$ kHz in the case of the 300 kHz data and for $f_\nu < 120$ kHz in the case of the 50 kHz data, the minimum of $\chi^2(f_\nu)$ is almost entirely determined by the observed values of Γ_{12} and Γ_{13}; i.e. the observed cross correlation of intensities at channels 2 and 3 dominate and the values at other channels are given practically no weight in determining the best fitting model curve. Therefore, this procedure does not allow us to investigate details of the shape of the curve of Γ_{1j} vs channel number, for higher frequency separations.

In order to avoid this difficulty we have redefined $\chi^2(f_\nu)$ such that the statistical weight W_j is not more then $\frac{1}{2}\sum_{j+1}^{12} W_{j+1}$. If the weight W_j computed from eqn.(4.3) turns out to be greater than $\frac{1}{2}\sum_{j+1}^{12} W_{j+1}$, then W_j is set equal to $\frac{1}{2}\sum_{j+1}^{12} W_{j+1}$; otherwise W_j is left unchanged. In Tables (4.2) to (4.5) we present the statistical weights obtained by this method corresponding to Kolmogorov and Gaussian spectra for 50 kHz and 300 kHz channels for a few values of f_ν, as an example with n_c=1. These modified values of W_j were used in the least squares method. The above weighting procedure adopted by us is justified since the theoretical predictions differ mainly for large frequency separations. Therefore, we have given an increased weightage for correlation values at the higher frequency separations. It was noticed by us that the method using the modified weights tended to choose a best-fit

TABLE 4.1 VALUES OF UNMODIFIED STATISTICAL WEIGHTS W_j

$n_c = 1$

l_j'	W_j
0.0	1.000
0.1	1.020
0.2	1.085
0.3	1.208
0.4	1.417
0.5	1.778
0.6	2.441
0.7	3.845
0.8	7.716
0.85	12.986
0.9	27.701
0.92	42.386
0.94	73.806
0.96	162.693

TABLE 4.2

VALUES OF STATISTICAL WEIGHTS W_j

12Ch. 300 kHz receivers-Gaussian Spectrum - $n_c = 1$

f_ν (kHz) \ j	2	3	4	5	6	7	8	9	10	11	12
78	1.624	1.041	1.006	1.000	1.000	1.000	1.000	1.000	1.000	1.000	1.000
156	2.319	1.131	1.028	1.004	1.001	1.000	1.000	1.000	1.000	1.000	1.000
312	4.364	1.456	1.150	1.042	1.018	1.005	1.002	1.001	1.000	1.000	1.000
624	6.403 (12.674)	2.618	1.640	1.257	1.144	1.064	1.036	1.021	1.013	1.008	1.005
936	8.378 (30.533)	4.731	2.469	1.647	1.388	1.192	1.121	1.081	1.056	1.039	1.030
1248	11.612 (63.214)	7.462 (8.299)	3.824	2.217	1.741	1.394	1.265	1.183	1.131	1.095	1.076
1560	16.504 (113.909)	9.592 (13.822)	5.899	3.053	2.224	1.651	1.459	1.329	1.241	1.180	1.146

Note: Values in parentheses are unmodified weights obtained from eqn(4.3)

TABLE 4.3

VALUES OF STATISTICAL WEIGHTS W_j

12Ch. 300 kHz receivers-Kolmogorov Spectrum - $n_c = 1$

f_ν (kHz) \ j	2	3	4	5	6	7	8	9	10	11	12
66	1.664	1.045	1.007	1.000	1.000	1.000	1.000	1.000	1.000	1.000	1.000
132	2.414	1.148	1.034	1.005	1.001	1.000	1.000	1.000	1.000	1.000	1.000
264	4.555	1.505	1.170	1.051	1.022	1.007	1.003	1.001	1.001	1.000	1.000
528	6.481 (10.789)	2.649	1.684	1.286	1.163	1.078	1.043	1.026	1.016	1.010	1.007
792	8.118 (19.050)	4.137	2.432	1.676	1.409	1.208	1.137	1.092	1.064	1.045	1.035
1056	10.108 (29.348)	5.813	3.277	2.165	1.750	1.412	1.277	1.194	1.141	1.105	1.084
1320	12.453 (43.420)	7.855	4.186	2.682	2.143	1.655	1.462	1.333	1.247	1.188	1.154

Note: Values in parentheses are unmodified weights obtained from eqn.(4.3)

TABLE 4.4

VALUES OF STATISTICAL WEIGHTS W_j

12Ch. 50 kHz receivers - Gaussian Spectrum - n_c=1

f_ν (kHz) \ j	2	3	4	5	6	7	8	9	10	11	12
12.5	1.183	1.005	1.000	1.000	1.000	1.000	1.000	1.000	1.000	1.000	1.000
25	1.528	1.047	1.004	1.001	1.000	1.000	1.000	1.000	1.000	1.000	1.000
50	2.628	1.265	1.061	1.018	1.005	1.002	1.001	1.000	1.000	1.000	1.000
100	5.938 (7.385)	2.179	1.376	1.161	1.075	1.043	1.022	1.013	1.007	1.000	1.000
150	7.492 (18.201)	4.020	1.957	1.451	1.232	1.143	1.085	1.057	1.037	1.001	1.000
200	10.172 (37.742)	6.511 (7.322)	2.919	1.879	1.480	1.313	1.197	1.137	1.092	1.005	1.000
250	14.249 (67.152)	8.062 (12.374)	4.444	2.527	1.807	1.541	1.356	1.256	1.177	1.014	1.001

Note: Values in parentheses are unmodified weights obtained from eqn.(4.3)

TABLE 4.5

VALUES OF STATISTICAL WEIGHTS W_j

12Ch. 50 kHz receivers - Kolmogorov Spectrum - $n_c=1$

f_ν (kHz) \ j	2	3	4	5	6	7	8	9	10	11	12
10.5	1.203	1.006	1.000	1.000	1.000	1.000	1.000	1.000	1.000	1.000	1.000
21	1.676	1.056	1.006	1.001	1.000	1.000	1.000	1.000	1.000	1.000	1.000
42	2.715	1.299	1.073	1.054	1.007	1.003	1.001	1.001	1.000	1.000	1.000
84	5.968 (5.989)	2.172	1.401	1.177	1.085	1.049	1.026	1.015	1.009	1.000	1.000
127	7.121 (10.223)	3.261	1.928	1.459	1.241	1.153	1.093	1.063	1.042	1.001	1.000
169	8.554 (15.775)	4.527	2.507	1.842	1.474	1.311	1.200	1.143	1.097	1.006	1.001
211	10.286 (23.136)	6.126	3.125	2.247	1.764	1.521	1.345	1.250	1.176	1.016	1.002

Note: Values in parentheses are unmodified weights obtained from eqn.(4.3)

model curve with larger value of f'_ν than the one using unmodified weights. The two best-fit values of f'_ν were found to differ by about 20 % at large values of f'_ν and at low values, they could differ by a factor of 2 or 3.

Assuming a Gaussian spectrum, $\chi^2(f_\nu)$ was evaluated using eqn.(4.5), setting $\Gamma_{1j}' = \Gamma_{1j}^{(G)}$. The best-fit was chosen as that particular model curve with $f_\nu = f'_\nu$ such that $\chi^2(f'_\nu)$ was a minimum, and thus yielding the best estimate of the decorrelation frequency for the pulsar under consideration as f'_ν. This method of estimation of decorrelation frequency was applied to the model curve based on Kolmogorov spectrum of irregularities in IS medium, also.

4.6.5. Estimate of errors on f'_ν

To estimate the uncertainty σ_ν on f'_ν one may use the criterion (Bevington 1969, pp 242-243) that as f_ν changes from f'_ν to $(f'_\nu \pm \sigma_\nu)$ the minimum value of $\chi^2(f_\nu)$ changes by unity. But this criterion is valid only if the statistical uncertainties on Γ_{1j} are uncorrelated with those for $\Gamma_{1k}(j \neq k)$, i.e.

$$< \Delta\Gamma_{1j} \Delta\Gamma_{1k} > = 0 \text{ for } j \neq k \qquad (4.6)$$

where $\Delta\Gamma_{1j}$ and $\Delta\Gamma_{1k}$ are the statistical uncertainties on Γ_{1j} and Γ_{1k} respectively. For the condition implied by eqn.(4.6) to hold good irrespective of the actual decorrelation

frequency for the pulsar, each of the correlation coefficients $\Gamma_{12}, \Gamma_{13}, \Gamma_{14}, \ldots, \Gamma_{112}$ should have been measured using data on pulsar intensities spanning different intervals of time, with the temporal separation between the stretches of data, on the order of a decorrelation time τ_ν or more. This is not the case with our observations. From data spanning the same length of time we are computing Γ_{1j} for $j = 2,3,4, \ldots, 12$. In such a case Γ_{1j} and Γ_{1k} will be statistically independent only if the separation of centre frequencies, $|\nu_j - \nu_k|$ between the jth and kth channels is larger than f_D which is the e^{-1} frequency width of the CCF. This is not true for some of the pulsars observed. In those cases one cannot justifiably use the criterion

$$\chi^2_{min+1} = \chi^2(f'_\nu \pm \sigma_\nu) \qquad (4.7)$$

to estimate the uncertainty σ_ν.

4.6.6. Modified Criterion for Estimate of σ_ν

Owing to the above reasons we have used a slightly different criterion for estimating σ_ν from the variation of $\chi^2(f_\nu)$ with f_ν. This criterion is obtained from the following arguments. If the χ^2 were obtained from L number of independent measurements and if the model curve is a good approximation to the observed curve of Γ_{1j} vs j, then the expected χ^2 is given by $\chi^2 \simeq$ L-n where n is the number of parameters determined from the data (Bevington 1969). Also in such a case a change in f'_ν by an amount $\pm\sigma_\nu$ increases

χ^2 to χ^2_{min+1} . If only n_i of the L measurements were statistically independent, the degrees of freedom would be only n_i rather than (L-n). Hence, we infer that a change of $\pm\sigma_\nu$ is likely to increase χ^2 not by unity but $(L-n)/n_i$. i.e.

$$\chi^2(f'_\nu \pm \sigma_\nu) = \chi^2(f'_\nu) + \frac{L-n}{n_i} \qquad (4.8)$$

We have used the criterion specified by eqn.(4.8) to estimate the uncertainties σ_ν on f'_ν . In our case $n = 1$, because only one parameter, namely p , is obtained from the data. n_i can be estimated for our observations as follows: For the best fitting model curve let f'_D be the frequency separation at which Γ'_{1j} decays to e^{-1} . The effective number n_i of statistically independent measurements of cross correlation coefficients is given by

$$n_i = \frac{|\nu_1 - \nu_{12}|}{f'_D} \qquad (4.9)$$

where ν_1 and ν_{12} are the centre frequencies of the first and the twelfth channels.

In the case of some pulsars, mostly of high DM, the ISS frequency structure in the CCF was not resolved. In such instances we could estimate only the upper limits on decorrelation frequency. This was due to the fact that although $\chi^2(f_\nu)$ decreased continually with f_ν it seemed to approach the minimum value at unreliably small values of f_ν

which were much less than 5 % of the bandwidth of the narrow band receivers used for acquiring the data. In such cases, instead of computing χ^2_{min}, we estimated the upper limit on decorrelation frequency as 5 % of the bandwidth of the narrow band receiver. The approximate confidence level of the values of the upper limits was also calculated from the rate of change of $\chi^2(f_\nu)$ with f_ν, using arguments similar to those given in Sections (4.6.5) and (4.6.6). In all the cases of upper limits encountered in our data we could infer from the rate of change of $\chi^2(f_\nu)$ that the approximately calculated confidence level would be an under-estimate, indicating that the estimated upper limits are very reliable.

4.6.7. Kolmogorov vs Gaussian Spectrum

In the preceding sections we have described the methods used for estimating the decorrelation frequency for an observed pulsar from the observed CCF. These methods are such that effects of finite bandwidth of detectors are accounted for while estimating the decorrelation frequency for a pulsar from observations.

It is possible, in principle, to distinguish between Gaussian and Kolmogorov spectra of irregularities in the IS medium, using the above methods. Between the two model curves based on Gaussian and Kolmogorov spectrum the one that yields a lower value of χ^2_{min} is a more realistic model. But in practice this criterion cannot be implemented successfully

with ease and confidence. Comparison of the model curves of CCF for the two spectra show that the differences between $\Gamma_{1j}^{(G)}$ and $_{1j}^{(k)}$ are very marginal, on the order of 3 % or less, though the shape of one model curve is different from the other. From eqns (4.3) and (4.4) it is seen that if the data length has n_c number of scintillation cycles the statistical uncertainty is proportional to $(n_c)^{-\frac{1}{2}}$. Hence to achieve a statistical stability of a few per cent for Γ_{1j} data lengths containing several hundred scintillation cycles will be required. For pulsars with dispersion measure in the range 5-30 pc. cm^{-3}. the decorrelation times at metre wavelengths are on the order of 10 minutes for detector bandwidths of about a few hundred kilohertz. Consequently one would need 60 to 100 hours of observations to clearly establish the nature of the spectrum of irregularities in the IS medium by techniques using correlation of intensity fluctuations at different radio frequencies.

One may improve the statistical stability of the CCF of intensity fluctuations due to scintillation of a pulsar by combining the CCF obtained as a result of observations on different days providing that the observations were done with the same multichannel receiver. If $\Gamma_{1j}^{(1)}$, $\Gamma_{1j}^{(2)}$, $\Gamma_{1j}^{(3)}$, ..., $\Gamma_{1j}^{(K)}$ are the cross correlation coefficients between first and jth channel on K different days of observing and if $n_c^{(1)}$, $n_c^{(2)}$, ... , $n_c^{(K)}$ are the number of scintillation cycles in the data on the first, second, ... Kth day

respectively, then the resultant cross correlation coefficient $\Gamma_{1j}^{(C)}$ obtainable by combining all the

$$\Gamma_{1j}^{(C)} = \frac{n_c^{(1)}\Gamma_{1j}^{(1)} + n_c^{(2)}\Gamma_{1j}^{(2)} + \ldots + n_c^{(K)}\Gamma_{ij}^{(K)}}{n_c^{(1)} + n_c^{(2)} + \ldots + n_c^{(K)}} \qquad (4.10)$$

and the resultant number of scintillation cycles $n_c^{(C)}$ is given by

$$n_c^{(C)} = n_c^{(1)} + n_c^{(2)} + n_c^{(3)} + \ldots + n_c^{(K)} \qquad (4.11)$$

Two pulsars, namely PSR 0301+19 and PSR 1919+21 were observed by us on more than one occasion and we have combined the data as per eqns. (4.10) and (4.11). The CCF obtained by combining several observations was then subjected to least squares fit to estimate the decorrelation frequency of the pulsar. We postpone the presentation and discussion of results obtained to the next chapter.

4.7 SCINTILLATION INDICES

The scintillation index m_j' due to ISS for the jth channel incorporating the effects due to finite bandwidth of the channel is given by (Appendix A)

$$(m_j')^2 = \frac{\int_{\nu}\int_{\nu'} G_j(\nu)G_j(\nu')\Gamma_D^2(|\delta\nu/f_\nu|)\,d\nu\,d\nu'}{\int_{\nu}\int_{\nu'} G_j(\nu)G_j(\nu')\,d\nu\,d\nu'} \qquad (4.12)$$

$m_j'^2$ was computed by numerical integration for different values of f_ν for all channels for both Gaussian and Kolmogorov spectra. Owing to slight differences in gain and bandshape among the twelve channels there were slight variations in the computed values of m_j' for any given f_ν, from channel to channel. These differences amounted to a maximum scatter in the values of m_j' for any particular value of f_ν and for different channels, of not greater than 0.05. The mean curve of m_m' vs f_ν obtained from the set of values for the 12 channels, is shown in Figs.(4.5) and (4.6). Fig.(4.5) is for the 300 kHz system and shows the variation of scintillation index m_m' with f_ν for both Gaussian and Kolmogorov spectra. Fig.(4.6) is a similar curve for the 50 kHz system. It is seen that the model assuming a Kolmogorov spectrum yields scintillation indices which are less than those for Gaussian spectral model.

The intensity response $G_B(\nu)$ of the channel corresponding to the broad and spectrum (BBS) of intensity fluctuations given by

$$G_B(\nu) = \sum_{j=1}^{12} G_j(\nu) \qquad (4.13)$$

The scintillation index m_M' due to ISS for the broad band is given by (Appendix A)

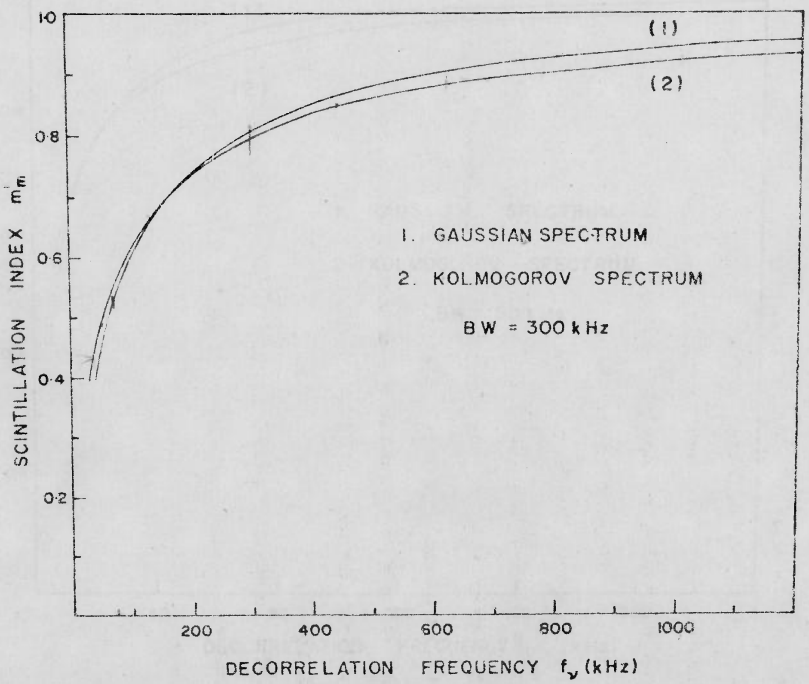

Fig.4.5 FINITE BANDWIDTH EFFECT ON SCINTILLATION INDEX FOR 300 kHz RECEIVER CHANNEL

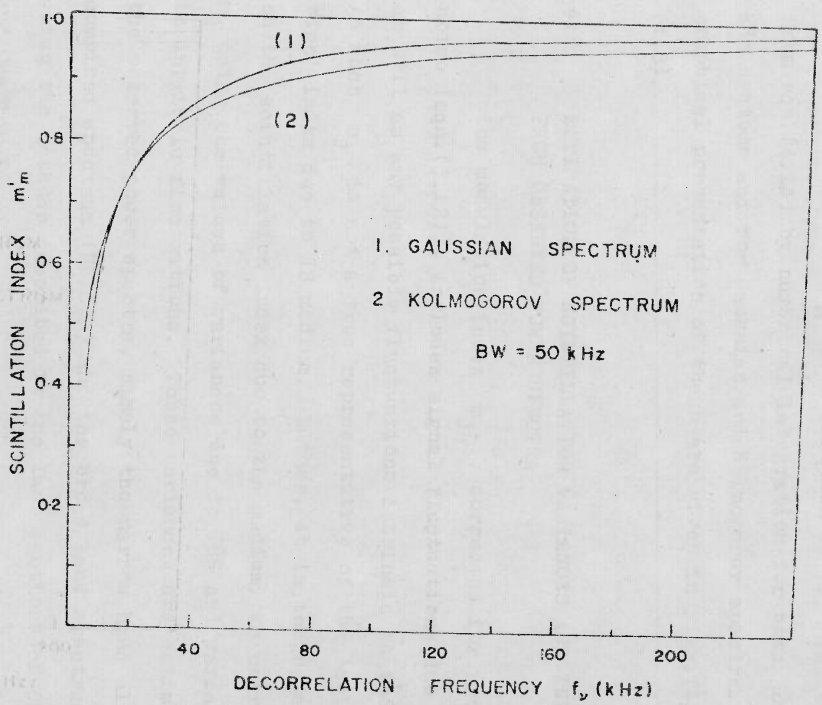

Fig.4.6 FINITE BANDWIDTH EFFECT ON SCINTILLATION INDEX FOR 50 kHz RECEIVER CHANNEL

$$(m'_M)^2 = \frac{\sum_{i=1}^{12}\sum_{j=1}^{12}\left[\int_{\nu}\int_{\nu'} G_i(\nu)G_j(\nu')\Gamma_D^2(|\delta\nu/f_\nu|)d\nu d\nu'\right]}{\sum_{i=1}^{12}\sum_{j=1}^{12}\left[\int_{\nu}\int_{\nu'} G_i(\nu)G_j(\nu')d\nu d\nu'\right]} \qquad (4.14)$$

The model curve for m'_M as a function of f_ν was evaluated from eqn.(4.14) by numerical integration for both 300 and 50 kHz systems and for Gaussian and Kolmogorov spectra. The graphical presentation of these are given in Figs.(4.7) and (4.8).

4.8 ESTIMATION OF SCINTILLATION VARIANCES AND INDICES FROM OBSERVED POWER SPECTRA

The modulation index m_j, corrected for receiver noise (eqn.(3.12)), includes signal fluctuations due to ISS as well as any possible fluctuations intrinsic to the source. As such m_j is not a true representative of the 'scintillation' index due to IS medium. Rather, it is the upper limit on the scintillation index due to the medium. We correct the m_j using the values of variances due to ISS and variances due to intrinsic fluctuations. These variances are estimated from the observed power spectra, namely the narrow band all channels combined spectrum (NBACCS) and the broad band spectrum (BBS) using the methods described in the last sections of Chapter 2 and Chapter 3.

Fig.(4.9) shows a schematic representation of the observed power spectra. Curve (1) marked S_{ON} is the 'ONPULSE' spectrum and curve (2) marked S_{OFF} is the 'OFFPULSE' spectrum.

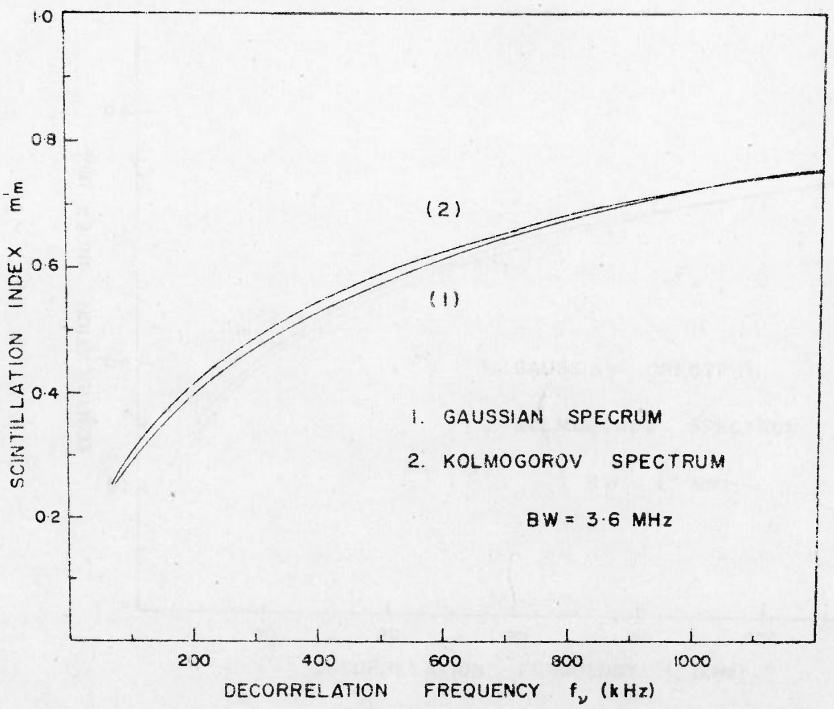

Fig.4.7 FINITE BANDWIDTH EFFECT ON SCINTILLATION INDEX FOR BROAD BAND DATA OBTAINED FROM 12 Ch. 300 kHz SYSTEM

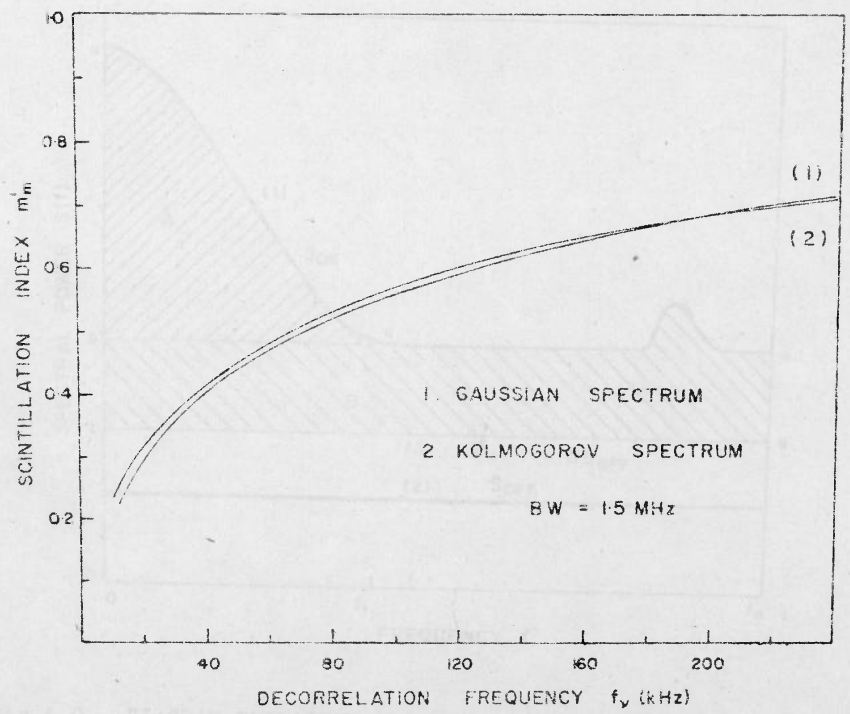

Fig.4.8 FINITE BANDWIDTH EFFECT ON SCINTILLATION INDEX FOR BROAD BAND DATA OBTAINED FROM 12 Ch. 50 kHz SYSTEM

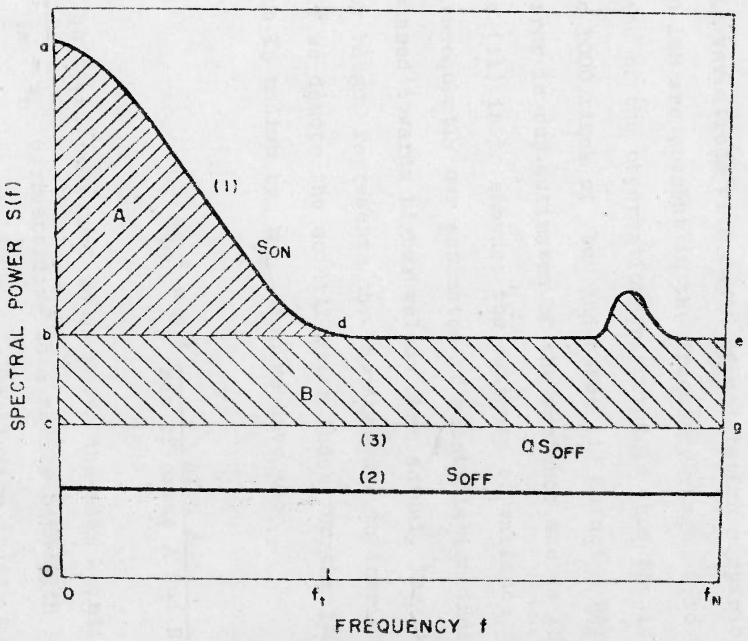

Fig.4.9 DIAGRAM EXPLAINING ESTIMATION OF VARIANCES OF INTENSITY FLUCTUATIONS FROM 'ONPULSE' AND 'OFFPULSE' POWER SPECTRA

The curve which is marked (3) is the OFFPULSE spectrum corrected for the differences in sampling widths of 'ONPULSE' and 'OFFPULSE' intensities, by multiplying by the factor 'a' (Section (3.6.1)). The area A bounded by (a), (b), (d) and curve (1) represents the variance due to ISS. This is not quite correct if (i) bc is comparable to ab and (ii) intrinsic variations with depth of modulation comparable to that due to ISS are present in the frequency range 0 to f_t. In the case of the observations reported in this thesis, ab is 80 to 1000 times of bc and hence (i) is not a serious source of error in our estimates of the variance due to ISS. The effect of (ii) is to enhance the estimate of variance due to ISS and consequently our estimates of scintillation indices could be biased towards higher values than actual. The area B bounded by bdegc represents the variance due to intrinsic fluctuations. If we denote the scintillation index for the jth channel, due to IS medium by m_{jm} then we have

$$m_{jm}^2 = m_j^2 \frac{\text{Area A}}{\text{Sum of areas A and B}} \qquad (4.15)$$

Eqn.(4.15) was used to estimate the mean scintillation index $\overline{m_{jm}} = m_m$ corresponding to a narrow bandwidth of 300 kHz (or 50 kHz). Similarly the scintillation index m_M corresponding to the broad band spectrum was also computed.

The estimates of the area A, representing the scintillation variance, obtained from the observed NBACCS and BBS enable us to determine the observed ratio R_0 of

scintillation variances for the two different bandwidths, for different pulsars. For calculating the theoretical value of this ratio, we firstly estimate the decorrelation frequency f_ν' of the pulsar from its CCF using the methods described in Section (4.6). This value of f_ν' is used in eqn.(2.50) to compute the variance ratio $R_c(f_\nu')$ expected from the theoretical model of the spectrum of irregularities in the IS medium. The theoretical and observed ratios, $R_c(f_\nu')$ and R_0 respectively, are compared with each other, to reveal the existence of intrinsic variations with modulation depth and time scales comparable to those due to ISS. Discussion of the results from this comparison is postponed to the next chapter.

4.9 BANDWIDTH EFFECTS ON POWER SPECTRA

On the basis of the theory of ISS based on Markov approximation, developed by Lee and Jokipii it is possible to model a power spectrum (or auto correlation function) of intensity fluctuations due to ISS, incorporating the effects due to the finite bandwidth of the detector. But we have not attempted this model computation owing to the following reasons: (i) The shape of the power spectrum depends heavily on the nature and time scales of intensity fluctuations intrinsic to pulsars. And it was seen from the analysis of our data that in several pulsars intrinsic intensity variations with timescales and modulation depths comparable to those due to ISS do exist. As such the shape of the observed power spectra cannot be attributed with confidence, to arise solely from ISS, thus invalidating the grounds for their comparison with model predictions,

(ii) The results of Lee (1976, Figs. (5) and (6)) indicate that the effect of finite bandwidth of detectors on the e^{-1} widths of ACF (or power spectra) of intensity fluctuations due to ISS is not appreciably large, so as to be easily detectable by observations.

As has been mentioned in Section (2.8) by using an algorithm developed by Krishnamohan (private communication) it is possible to effect a separation of the intrinsic and ISS components of spectra, from the observed NBACCS and BBS, in which case one can compare the ISS component of the spectra with the predictions of the model, by assuming the transverse velocity of the 'frozen' pattern of the scintillations.

CHAPTER 5

OBSERVATIONS, RESULTS AND INTERPRETATION

5.1 INTRODUCTION

In this chapter we present observations and results for 33 pulsars studied by us. We also discuss in detail our main results on intrinsic intensity variations of pulsars and the nature of the interstellar medium.

Most of the observations were carried out during the period from March 1976 to March 1978. Till the end of this observing period 157 pulsars were known, of which 102 pulsars are in the declination range of $\pm 32^{\circ}$, accessible to the Ooty Radio Telescope. Of these we chose 33 pulsars for our studies, based on the criterion that the expected average signal to noise per pulse for a narrow band receiver of either 300 kHz or 50 kHz bandwidth and time constant of 3 ms should be at least 0.25; we used 300 kHz bandwidth for pulsars with DM $\lesssim$ 35 pc. cm^{-3} and 50 kHz for pulsars with DM > 35 pc. cm^{-3}. The aim in using the narrower bandwidth for larger DM was to ensure that scintillations are not smoothed out considerably due to the receiver bandwidth being much larger than the decorrelation bandwidth. On this basis, about 40 pulsars were earmarked for observations. But we could obtain useful observational data only on 33 pulsars out of the 40. The data on the rest had very poor signal to noise ratio and hence not usable for meaningful analysis. This is most likely due to variabilities

of pulsar luminosities. It may be mentioned here that out of the 155 new pulsars discovered recently at Molonglo and the 17 at NRAO (Manchester et al. 1978 Damashek, Taylor and Hulse 1978); we can probably observe in future about 25 more pulsars with the ORT for the purpose of the type of studies discussed in this thesis.

Basic observational data on all the 33 pulsars are presented in Section (5.2). For 22 of these pulsars power spectra of intensity fluctuations, obtained with good signal to noise ratio, are also presented. We then present in Section (5.3), frequency cross correlation functions derived for 25 pulsars. For 15 out of these pulsars, definite values of decorrelation frequency could be determined and for the rest, only upper limits could be obtained, as described in Section (5.4). Evidence on intrinsic intensity variations with ISS-like time scales is given in Section (5.5).

The topic of discussion in Section (5.6) is the observed dependence of decorrelation frequency on dispersion measure and its implications on the nature of the IS medium. This is followed by a discussion of the observed dependence of power spectral widths on dispersion measure. In the last section we present estimates of the rms electron density deviations and their scale sizes, deduced from the measured values of decorrelation frequency. The inferences on the nature of the electron density distribution in the IS medium, based on the above estimates, are also presented.

5.2 Power Spectra of Intensity Fluctuations

As explained in Section (3.5.3) we have obtained power spectra of intensity fluctuations for narrow and broad bandwidths simultaneously using either a 12-channel 300 kHz system over 3.6 MHz or a 12-channel 50 kHz system over 1.5 MHz. Fig. (5.1a) to (5.1ℓ) show these spectra for 25 pulsars, presented in the order of increasing DM. The data of observation and the bandwidth used are indicated in each figure. Only the low frequency part of the spectrum is shown in each figure and not the entire spectrum over the whole span of frequencies from 0 to f_N, the Nyquist frequency. The Y-axis shows the relative spectral power in decibels, normalised by the peak power. In most cases both broadband and narrow band spectra are shown in the figures. But in the case of a few high DM pulsars, only the narrow band spectrum is shown. In these cases the low frequency ISS component of the spectrum is not recognisable, which should be due to the smoothing of scintillations by the finite bandwidth of the receiver. The narrow band power spectra for 22 pulsars showed easily recognisable low frequency components, out of the 33 pulsars which were observed.

The results are summarised in Table (5.1) in which columns 1 to 6 give the pulsar names (PSR), dispersion measures (DM), bandwidth of the receiver (BW), lengths of recordings in periods (NxM where N is the number of consecutive pulses averaged and M is the array length), e^{-1} widths of the narrow band scintillation spectra (f_o) and transition

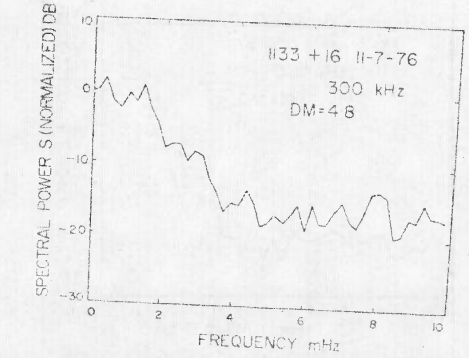

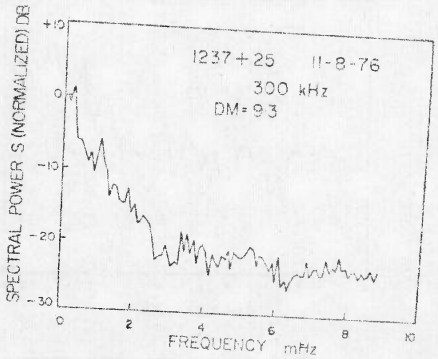

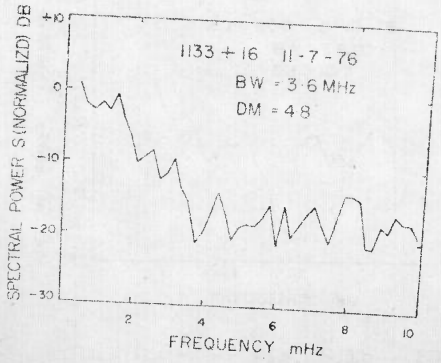

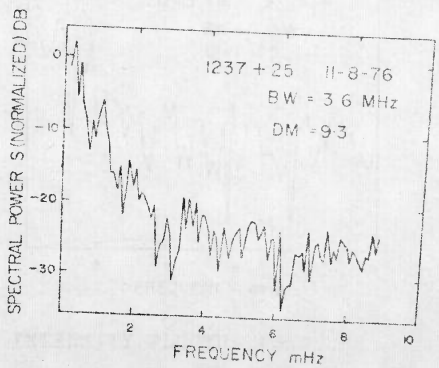

5.1 a POWER SPECTRA OF INTENSITY FLUCTUATIONS

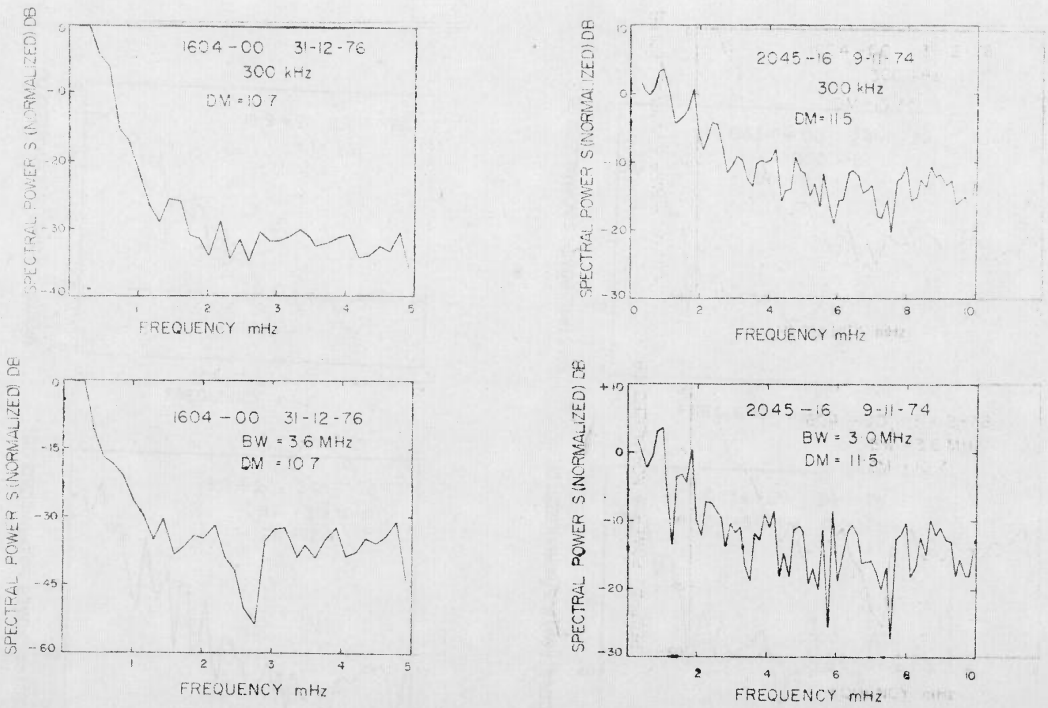

Fig. 5.1b POWER SPECTRA OF INTENSITY FLUCTUATIONS

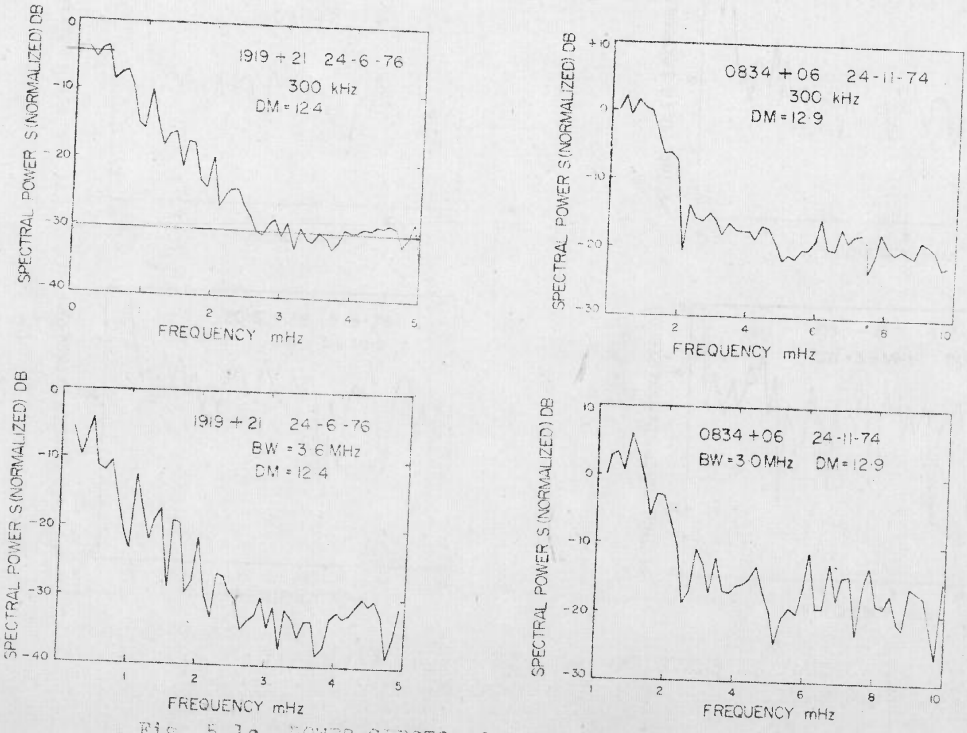

Fig. 5.1c POWER SPECTRA OF INTENSITY FLUCTUATIONS

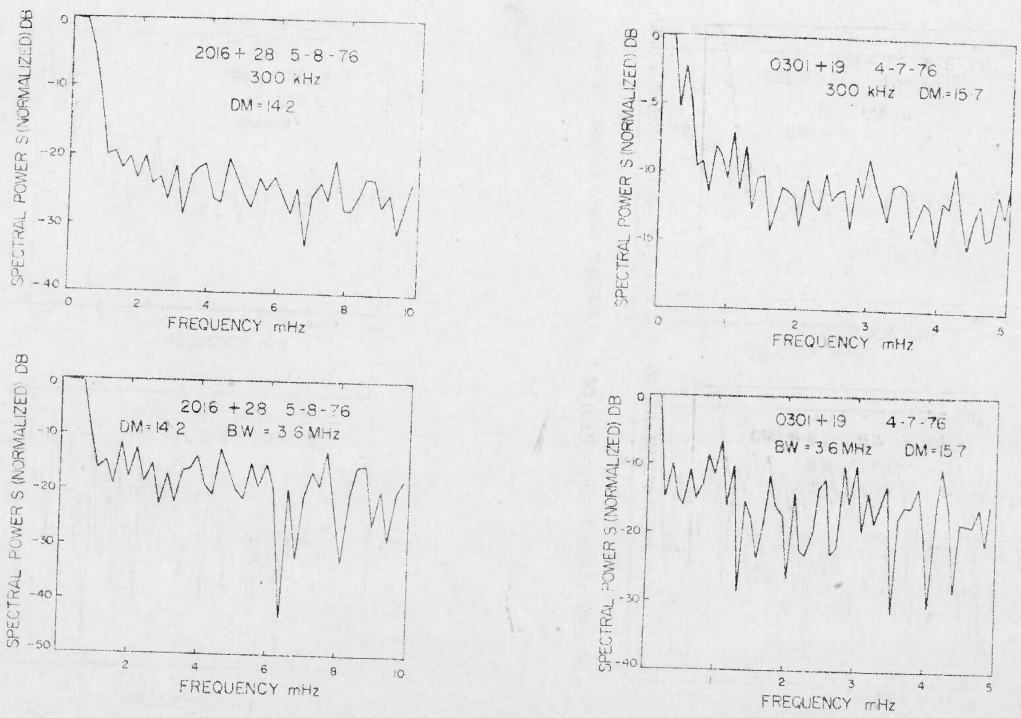

Fig. 5.1d POWER SPECTRA OF INTENSITY FLUCTUATIONS

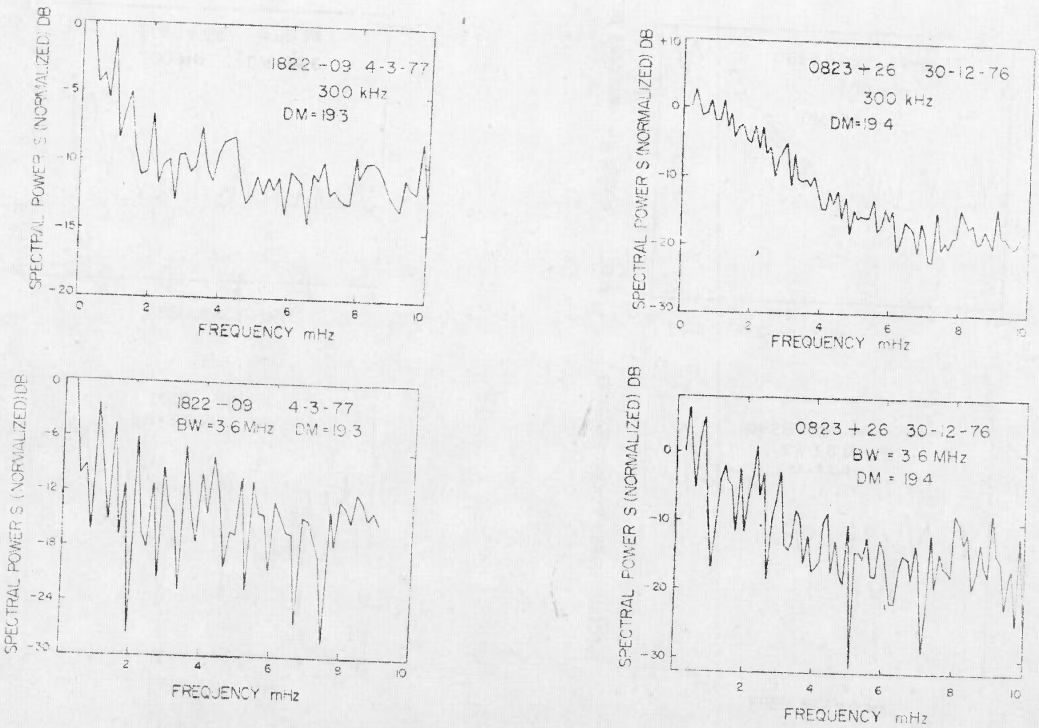

Fig. 5.1e POWER SPECTRA OF INTENSITY FLUCTUATIONS

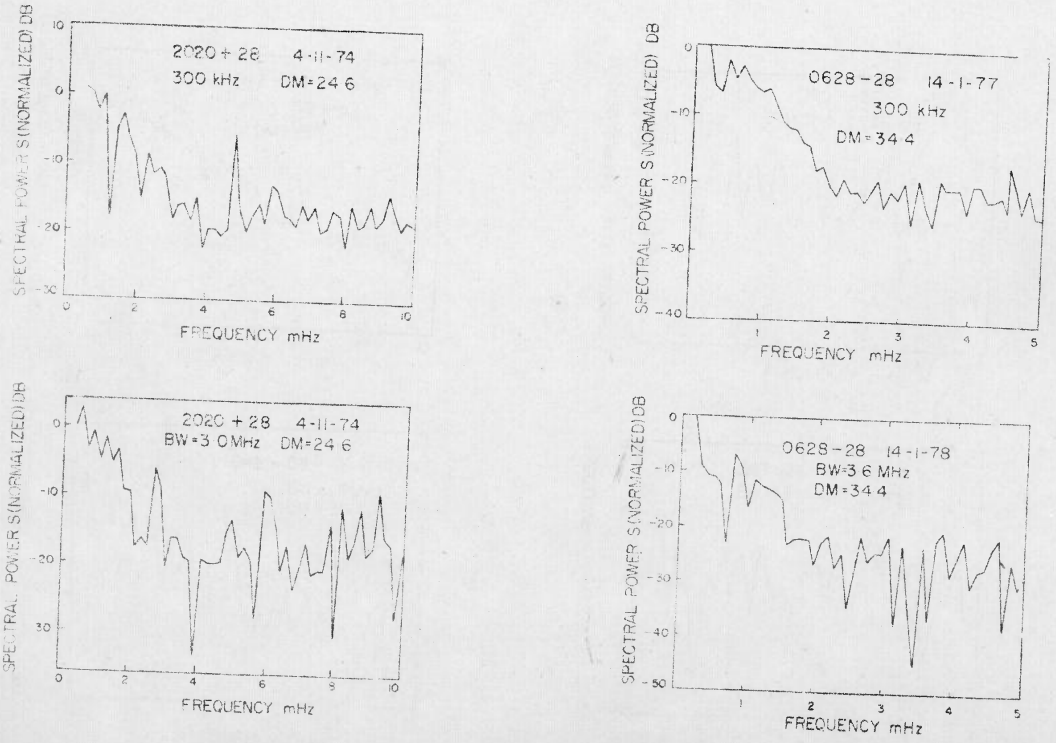

Fig. 5.1f POWER SPECTRA OF INTENSITY FLUCTUATIONS

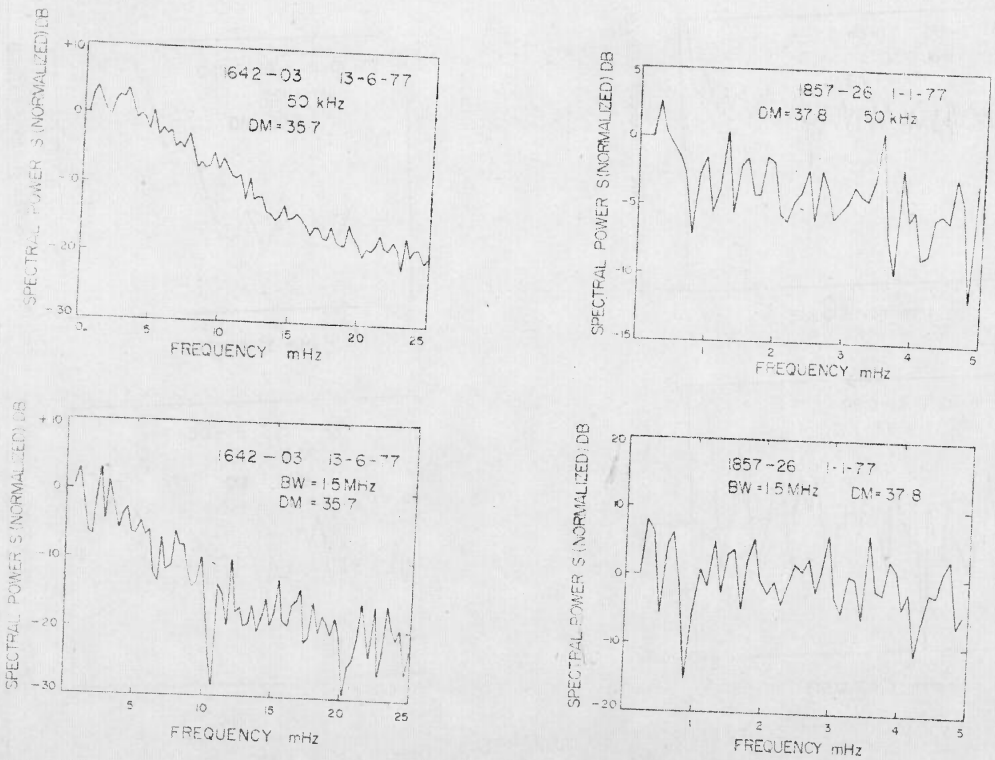

Fig. 5.1g POWER SPECTRA OF INTENSITY FLUCTUATIONS

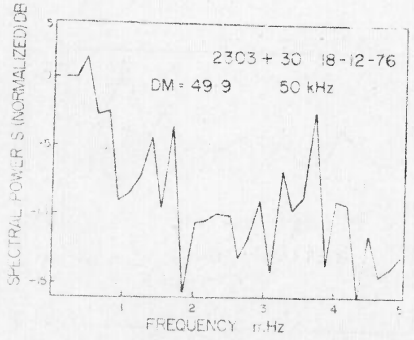

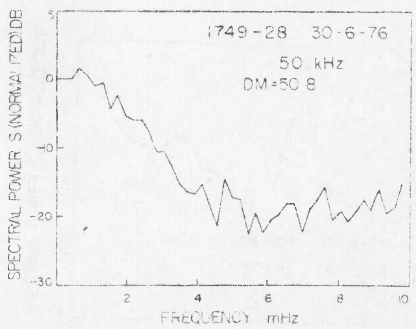

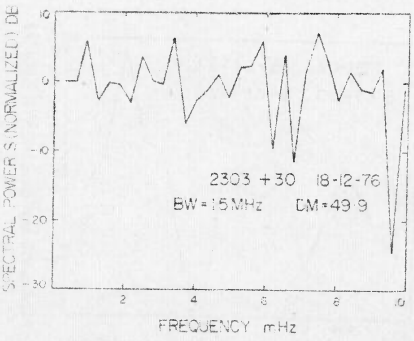

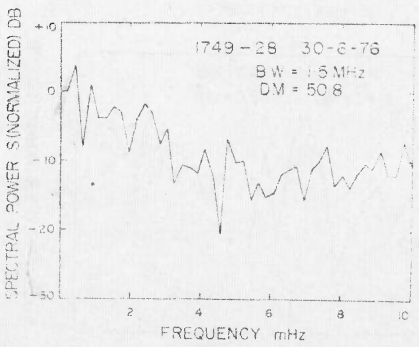

Fig. 5.1.1. POWER SPECTRA OF INTENSITY FLUCTUATIONS

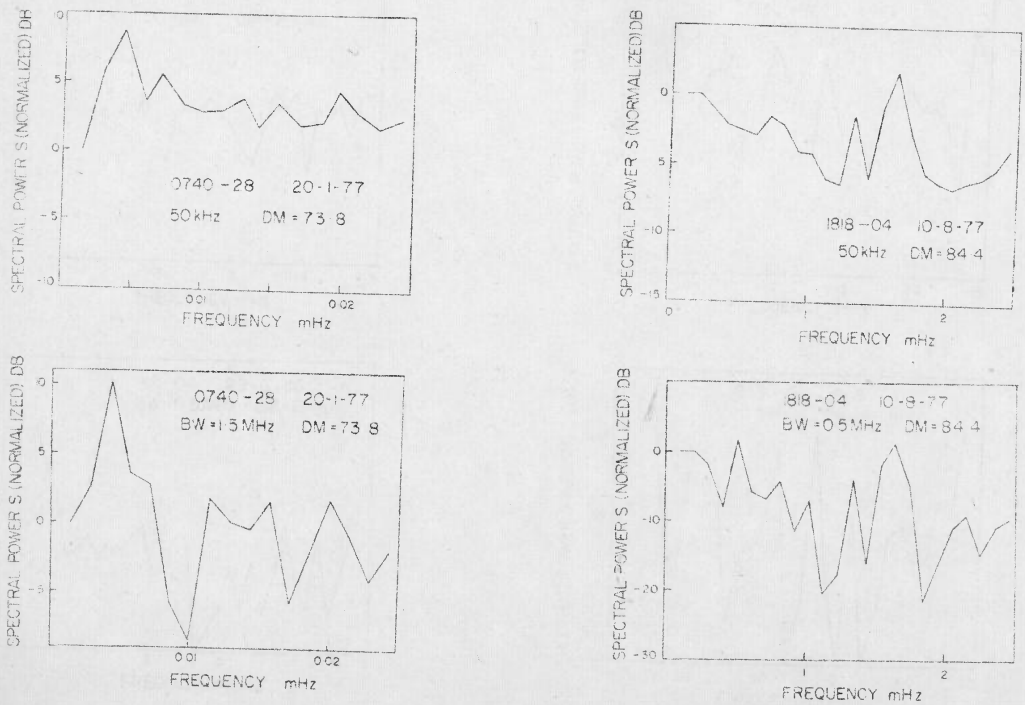

Fig.5.1.3. POWER SPECTRA OF INTENSITY FLUCTUATIONS

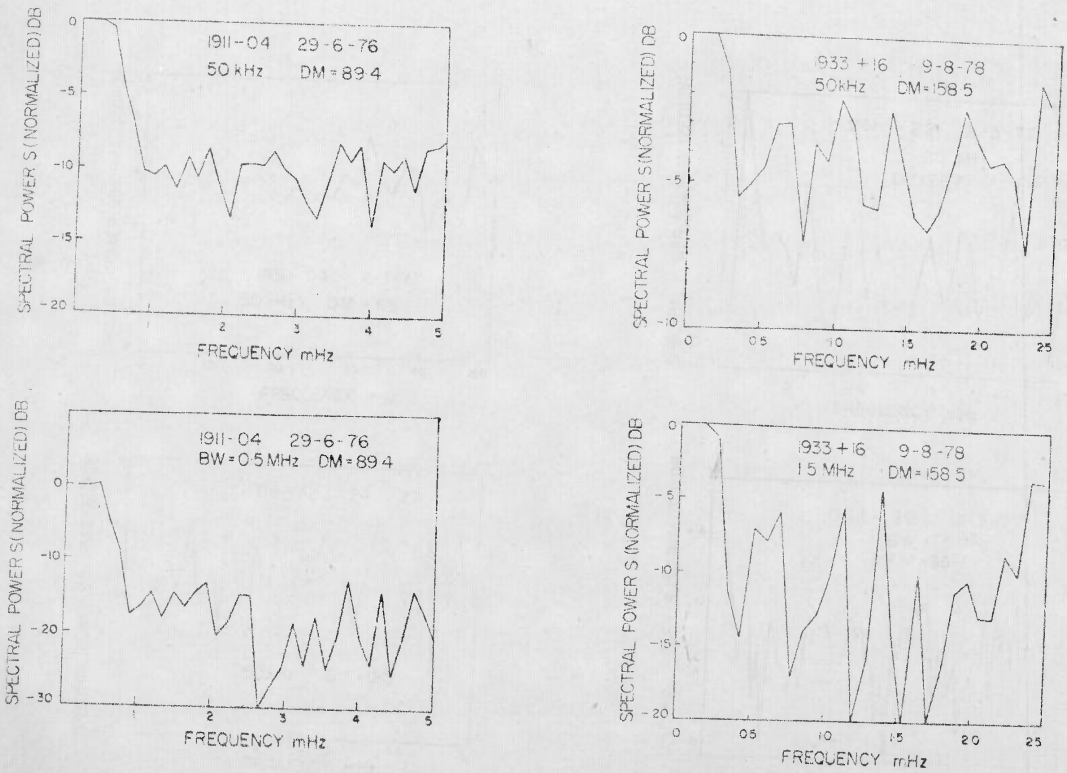

Fig. 5.11 POWER SPECTRA OF INTENSITY FLUCTUATIONS

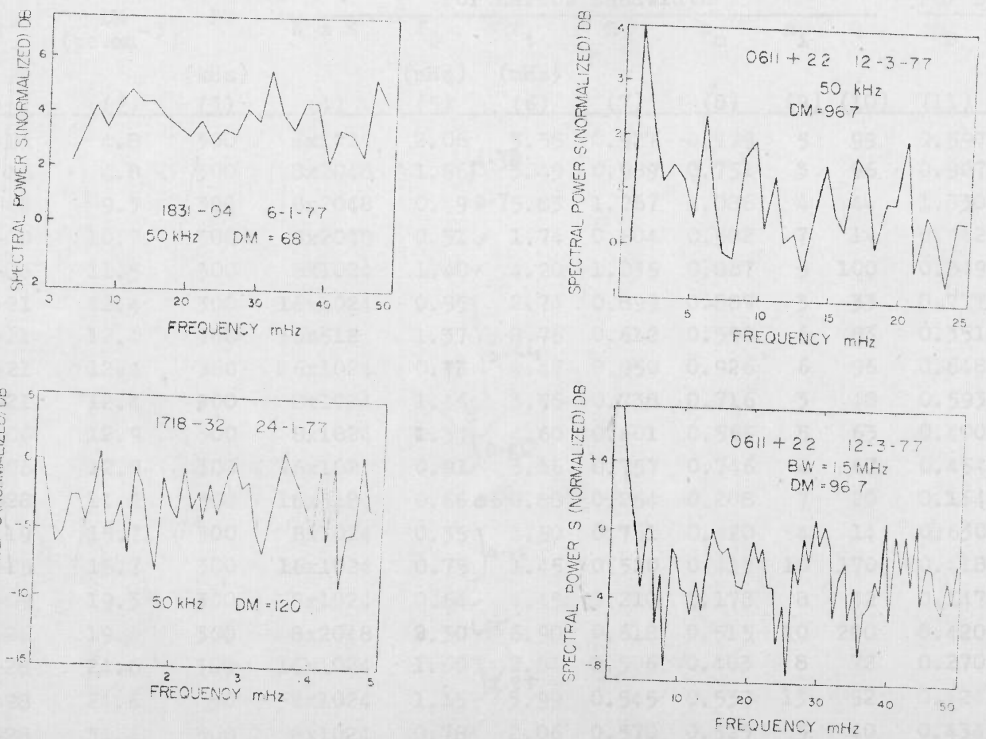

Fig. 5.11. POWER SPECTRA OF INTENSITY FLUCTUATIONS

TABLE 5.1 : MEASURED ISS PARAMETERS FOR 33 PULSARS (in pencil, from Backer)

Sr. No.	PSR	DM ($pc.cm^{-3}$)	B (kHz)	For narrow Bandwidth N x M	f_e (mHz)	f_t (mHz)	$\bar{m}_j$	m_m	n_i	Q	For Broad Bandwidth m_B	m_M	f'_e (mHz)
	(1)	(2)	(3)	(4)	(5)	(6)	(7)	(8)	(9)	(10)	(11)	(12)	(13)
1.a	1133+16	4.8	300	8x1024	2.06	5.55	0.927	0.779	5	95	0.597	0.460	0.82
b	1133+16	4.8	300	8x2048	1.56	3.49	0.989	0.751	3	96	0.907	0.665	1.44
2.	1237+25	9.3	300	8x2048	0.49	5.83	1.267	1.086	4	44	1.030	0.927	0.44
3.	1604-00	10.7	300	8x2048	0.51	1.74	0.604	0.582	7	14	0.462	0.436	0.14
4.	2045-16	11.5	300	8x1024	1.40	4.20	1.035	0.887	5	100	0.849	0.700	1.26
5.a	1919+21	12.4	300	16x1024	0.55	2.74	0.899	0.889	3	33	0.777	0.767	0.18
b	1919+21	12.4	300	16x512	1.37	8.76	0.612	0.598	6	83	0.351	0.346	1.28
c	1919+21	12.4	300	16x1024	0.78	4.47	0.950	0.926	6	96	0.648	0.648	0.64
d	1919+21	12.4	300	8x1024	1.46	3.56	0.738	0.716	3	48	0.593	0.584	0.91
6.a	0834+06	12.9	300	8x1024	1.34	4.60	0.601	0.565	5	63	0.400	0.359	1.53
b	0834+06	12.9	300	16x1024	0.91	3.16	0.757	0.746	4	67	0.454	0.446	0.62
7.	2016+28	14.2	300	16x512	0.66	0.88	0.254	0.208	7	20	0.164	0.094	0.44
8.a	0301+19	15.7	300	8x1024	0.35	1.50	0.751	0.420	4	14	0.630	0.259	0.09
b	0301+19	15.7	300	16x1024	0.75	1.45	0.520	0.417	10	170	0.418	0.261	1.41
9.	1822-09	19.3	300	8x1024	0.64	4.45	0.210	0.178	8	32	0.147	0.104	1.03
10.	0823+26	19.4	300	8x2048	2.30	6.90	0.618	0.515	10	200	0.420	0.278	1.61
11a	2020+28	24.6	300	16x1024	1.60	2.84	0.506	0.403	8	72	0.270	0.177	0.89
b	2020+28	24.6	50	32x1024	1.15	3.99	0.545	0.533	13	52	0.424	0.384	0.71
12.	0628-28	34.4	300	8x1024	0.78	2.06	0.570	0.523	5	40	0.434	0.343	0.20

..2

	(1)	(2)	(3)	(4)	(5)	(6)	(7)	(8)	(9)	(10)	(11)	(12)	(13)
13a	1642-03	35.7	300	8x2048	4.25	15.43	0.284	0.242	10	270	0.180	0.145	4.41
b	1642-03	35.7	50	8x2048	5.35	22.98	0.765	0.745	10	340	0.315	0.292	4.09
14.	1857-26	37.8	50	16x1024	0.60	2.99	0.278	0.108	10	60	0.235	0.079	0.60
15.	0450-18	39.9	50	8x1024	1.33	2.00	0.706	0.550	7	42	0.554	0.398	0.89
16a	0818-13	41.0	300	8x1024	2.46	7.10	0.187	0.173	10	100	0.159	0.133	1.58
b	0818-13	41.0	50	8x1024	2.86	7.79	0.397	0.249	10	290	0.219	0.121	1.58
17	2303+30	49.9	50	2x1024	1.55	1.55	0.708	0.477	7	49	0.549	-	-
18	1749-28	50.8	50	8x2048	1.84	4.12	0.408	0.350	9	153	0.254	0.146	1.84
19	1831-04	68	50	4x1024	-	-	0.756	-	10	-	-	-	-
20	0740-28	73.8	50	16x1024	4.03	4.76	0.214	0.062	10	110	0.142	0.049	4.03
21	1818-04	84.4	50	16x1024	0.71	1.73	0.164	0.080	8	40	0.136	0.065	0.71
22	1917+00	85	50	8x1024	-	-	0.499	-	10	-	-	-	-
23	1911-04	89.4	50	8x1024	0.59	0.89	0.199	0.164	8	32	0.146	0.130	0.59
24	0611+22	96.7	50	16x1024	2.87	4.00	0.231	0.158	10	160	0.190	0.142	2.87
25	1907+00	111	50	8x1024	-	-	0.402	-	10	-	-	-	-
26a	1700-32	113	300	8x1024	-	-	0.366	-	10	-	-	-	-
b	1700-32	113	50	4x1024	-	-	0.565	-	10	-	-	-	-
27	1718-32	120	50	8x1024	-	-	0.553	-	10	-	-	-	-
28	1845-04	141.9	50	4x1024	-	-	0.741	-	10	-	-	-	-
29	1933+16	158.5	300	32x1024	0.26	0.26	0.099	0.009	10	30	0.067	0.010	0.26
30	1845-01	163	50	4x1024	-	-	0.697	-	10	-	-	-	-
31	1907+02	190	50	8x2048	-	-	0.385	-	10	-	-	-	-
32	1900+01	228	50	2x1024	-	-	0.898	-	10	-	-	-	-
33	1831-03	231	50	8x1024	-	-	0.371	-	10	-	-	-	-

frequencies (f_t) at which the power level of the low frequency component (due to ISS) decays to the 'white' level due to pulse to pulse fluctuations and receiver noise. Column 9 gives n_i, the number of channels which are statistically independent, as estimated from eqn.(4.9). Q is the quality factor of the measurements and gives the number of degrees of freedom for the narrow band all channels combined spectrum. $Q = f_e x T x n_i = f_e x N x M x P x n_i$. Values of Q are listed in column 10. Columns 7 and 8 give the modulation indices $\bar{m}_j$ and scintillation indices M_m computed using eqn.(4.15) for the narrow band data; values of the corresponding two parameters, m_B and m_M, for the broad band data are listed in Columns 11 and 12 in the Table. The last column of the table gives the e^{-1} widths, f'_e , of the low frequency (ISS) components in the broad band spectra. In the case of many pulsars we could not derive values of f'_e because the low frequency component was not detected in their broad band spectra, although the corresponding NBACCS had a low frequency (ISS) component. As such we infer that in these cases the ISS fluctuations have been considerably smoothed out by the large receiver bandwidth corresponding to the broad band spectra. Also, for 9 out of the 33 pulsars even the narrow band spectrum did not show a detectable low frequency component. Hence we infer that the values of decorrelation frequency for these pulsars are much smaller than the bandwidth of 50 kHz which was used for observing them. For this group of pulsars, marked 'x' in the

table the DM is greater than 68 pc. cm^{-3}. An additional difficulty in observations of these pulsars was that quite a few of them were weak pulsars. Modulation index was the only parameter of their intensity fluctuations which could be measured. The possible statistical uncertainties on the estimated modulation indices are also fairly large owing to the fact that for these pulsars $\sigma_j/\sigma_{jn} < 0.3$.

5.3 OBSERVED FREQUENCY CROSS CORRELATION FUNCTIONS (CCF)

5.3.1. Case I - Resolved Frequency Structures of Scintillations at low DM

The observed cross correlation functions Γ_{1j} of intensities (CCF) for 15 out of the 33 pulsars observed, are shown in Fig.(5.2a,b...n). Only for these 15 cases, the frequency structure due to scintillation was well-resolved, showing gradual decrease in correlation of intensity fluctuations with frequency. The DM of these pulsars are in the range 4.9-50.9 pc.cm^{-3}. In the case of 6 pulsars (1133+16, 1919+21, 0834+06, 0301+19, 1642-03 and 0818-13) which were observed on more than one occasion, the CCF obtained on different occasions are presented individually. Two of these 6 pulsars, namely 1919+21 and 0301+19, were observed more than once with identifical configurations of the 12-channel receivers. For these two pulsars, the resultant CCF obtained by combining the observations on different occasions, using the method described in Section(4.6.6), are also presented. Such combined CCF are indicated by (R) in the graphical plots.

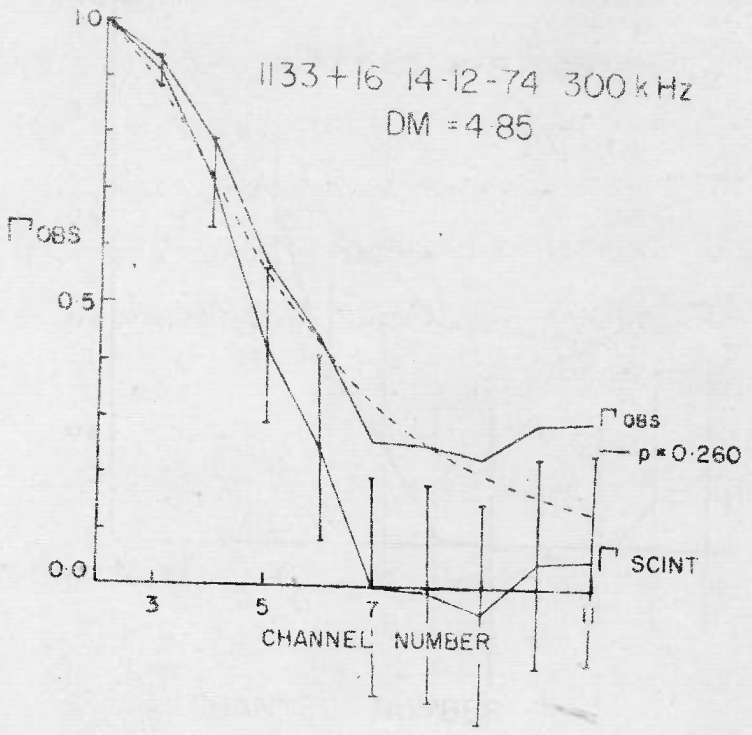

Ajp Pedestal problem i.e. I suspect I've got too much of pedestal in subtracted.

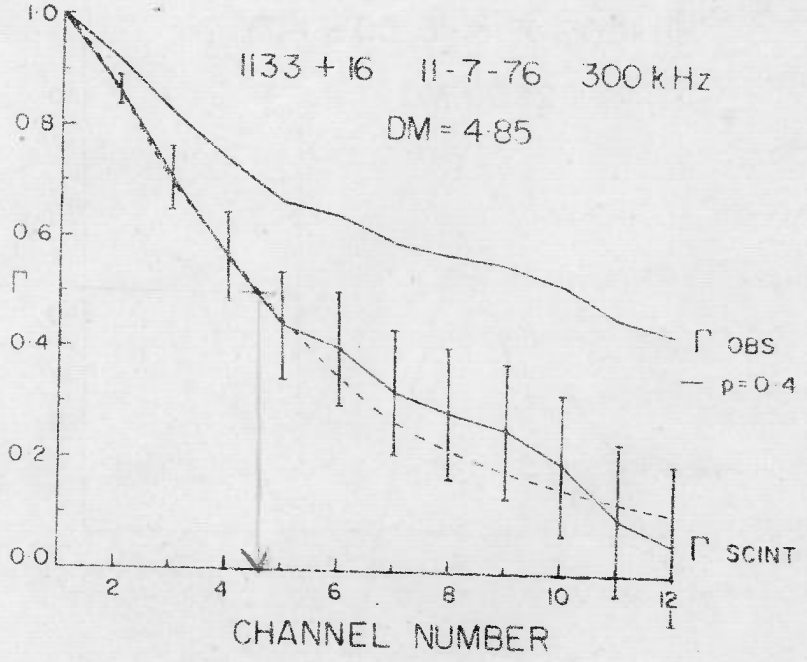

O.K.

Fig. 5.2a FREQUENCY CROSS CORRELATION FUNCTIONS Γ_{1j}

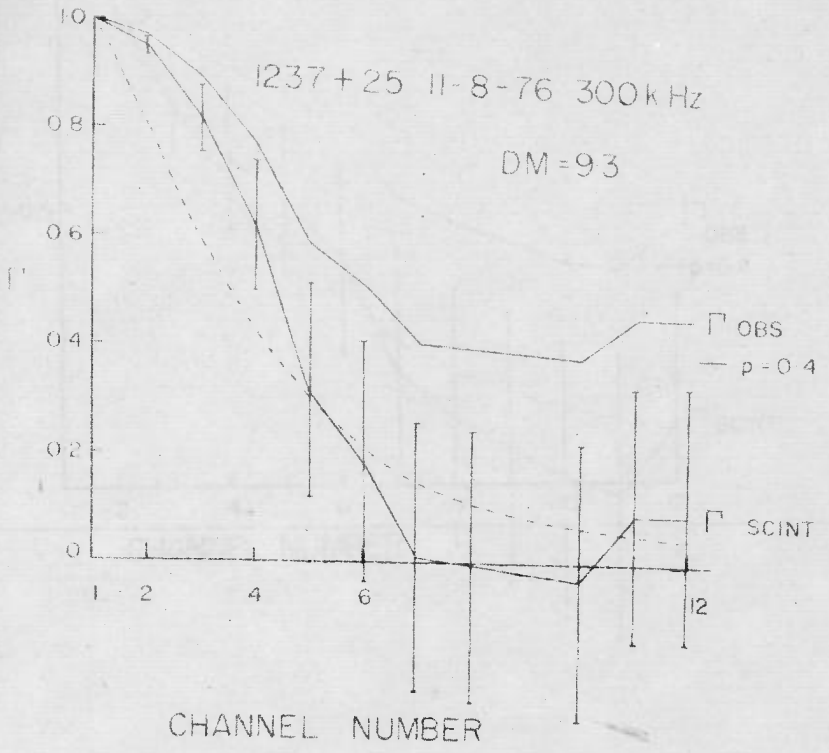

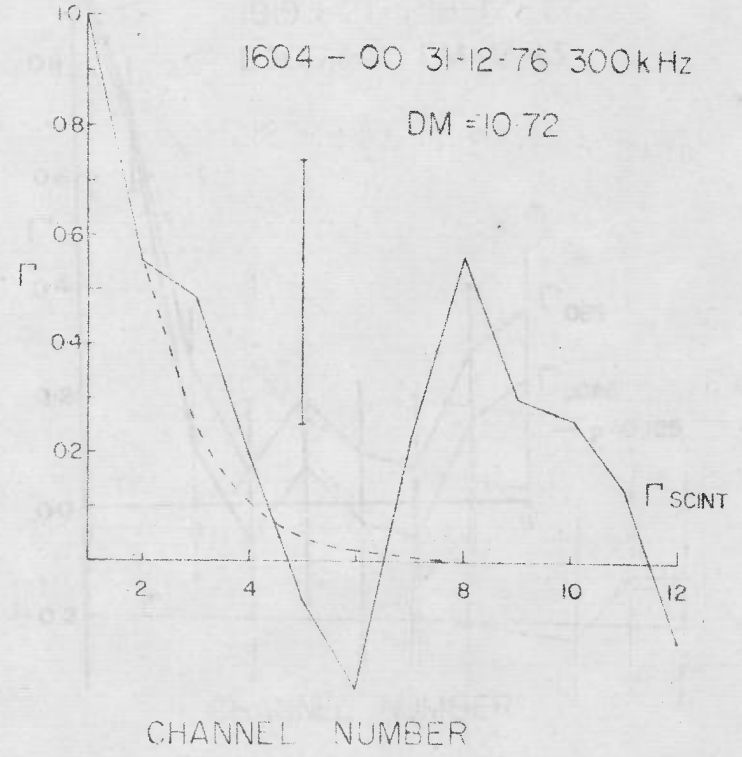

Fig.5.2b FREQUENCY CROSS CORRELATION FUNCTIONS Γ_{ij}

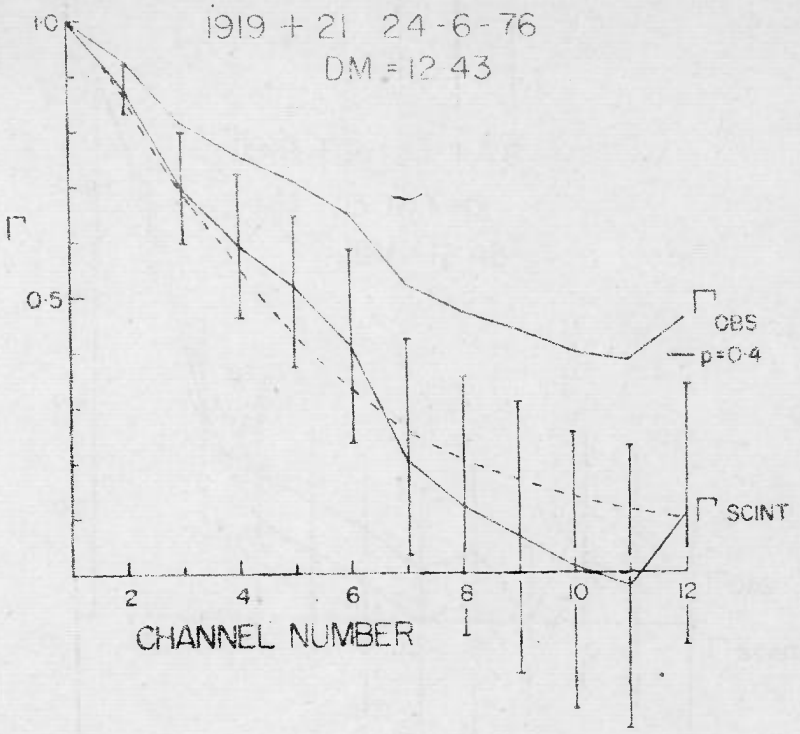

D.K.

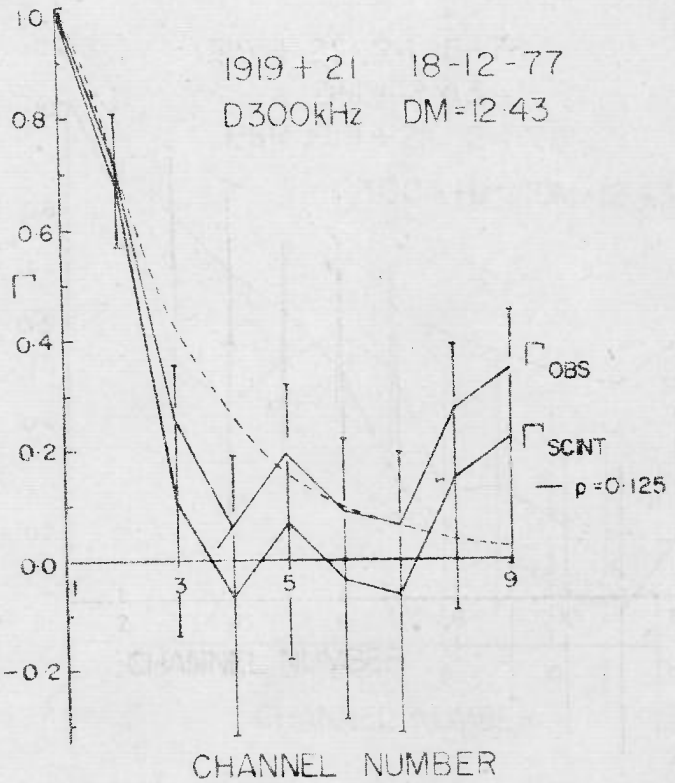

Fig. 5.2c FREQUENCY CORRELATION FUNCTIONS $\Gamma_{1\,j}$

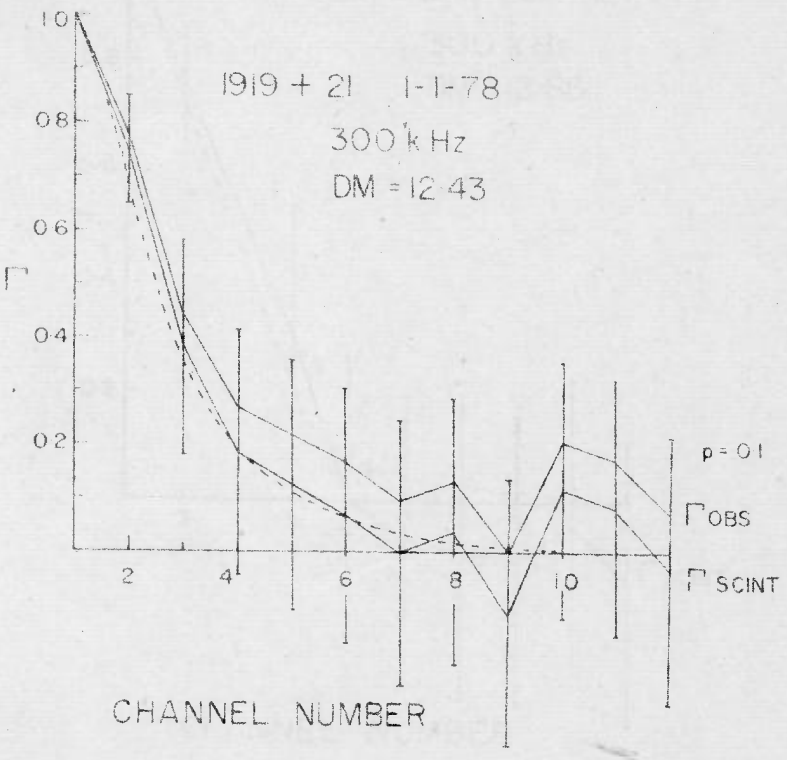

O.K.

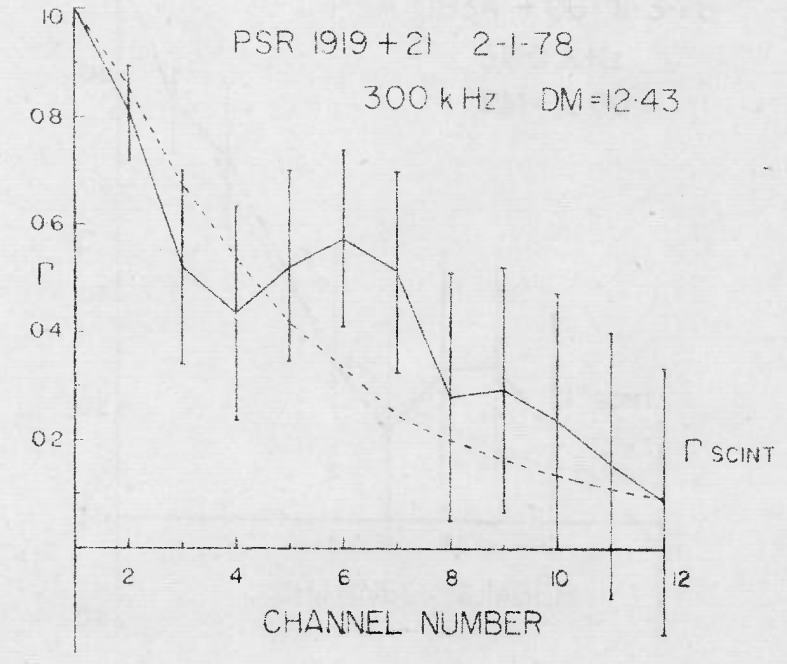

O.K.

5.2a FREQUENCY CROSS CORRELATION FUNCTIONS Γ_{1j}

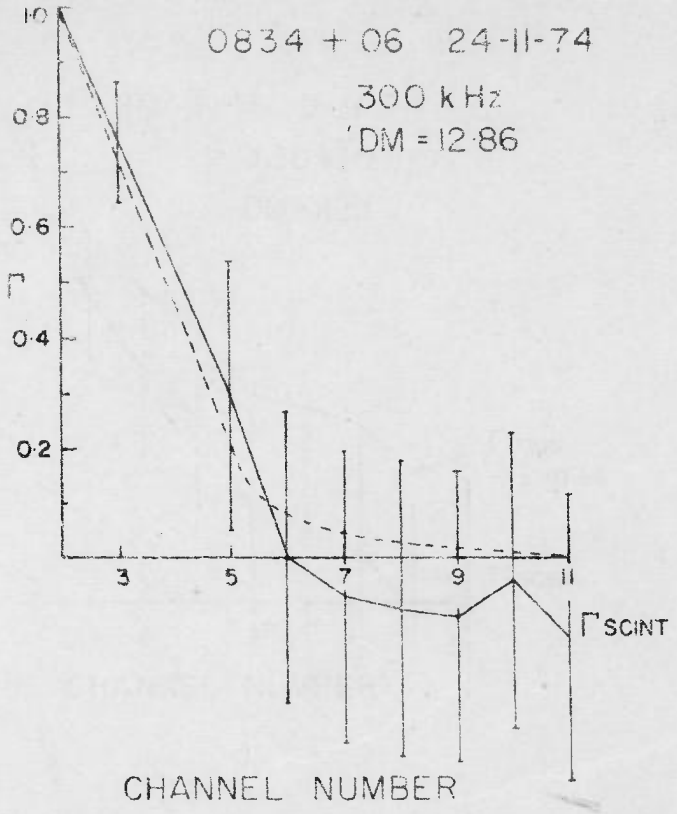

o.k.

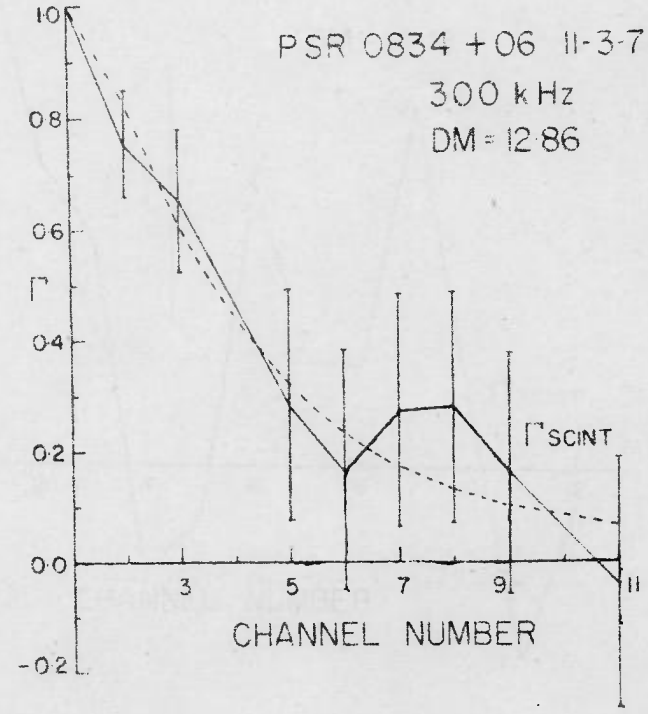

o.k.

Fig.5.2e FREQUENCY CROSS CORRELATION FUNCTIONS Γ_{ij}

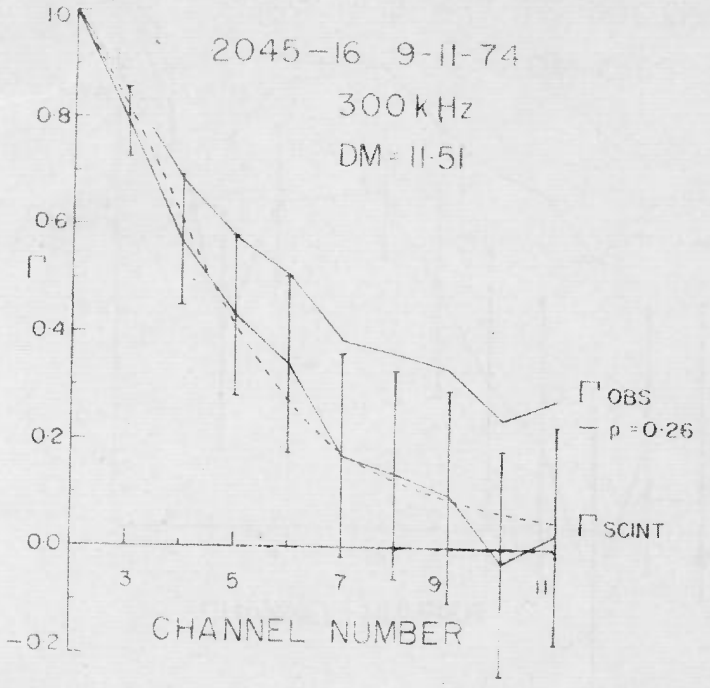

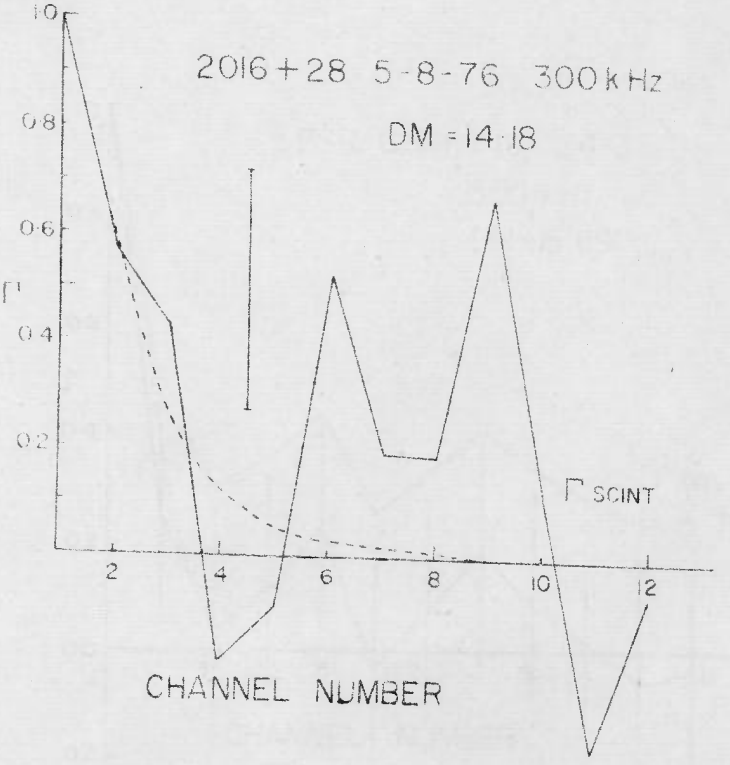

Fig. 5.2f FREQUENCY CROSS CORRELATION FUNCTIONS Γ_{1j}

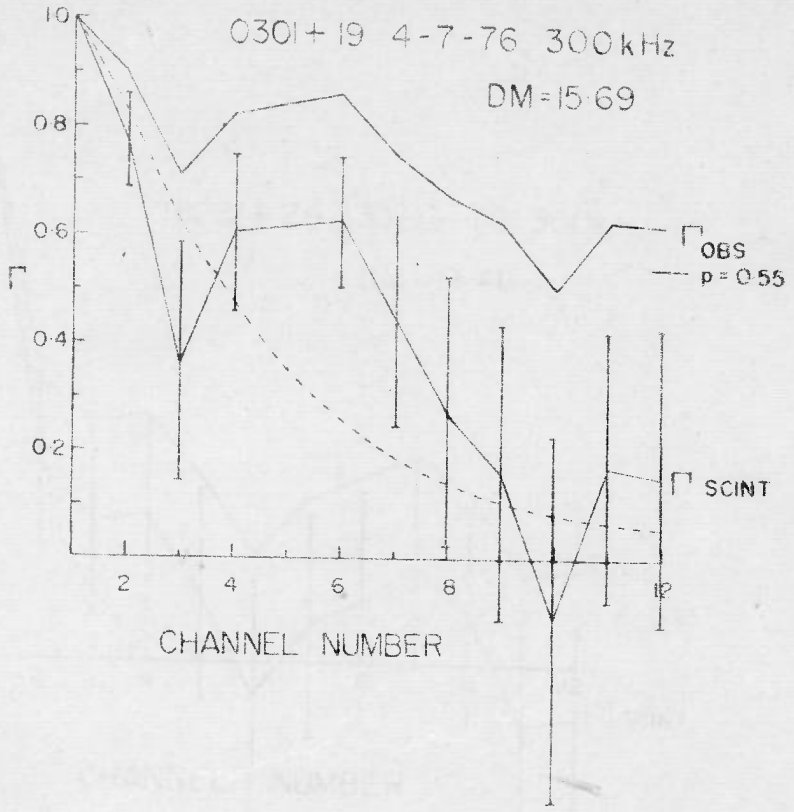

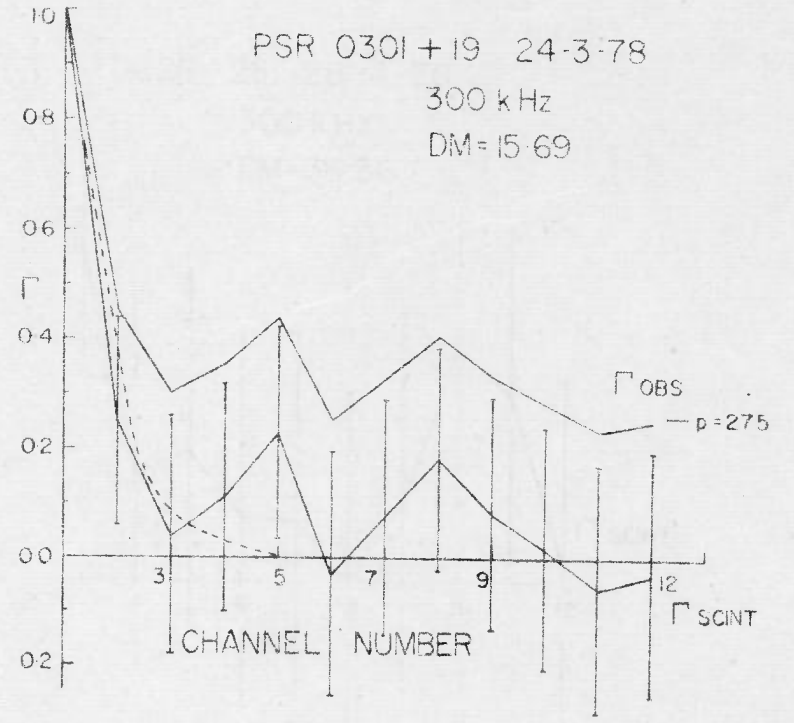

Fig. 5.2e FREQUENCY CROSS CORRELATION FUNCTIONS Γ_{ij}

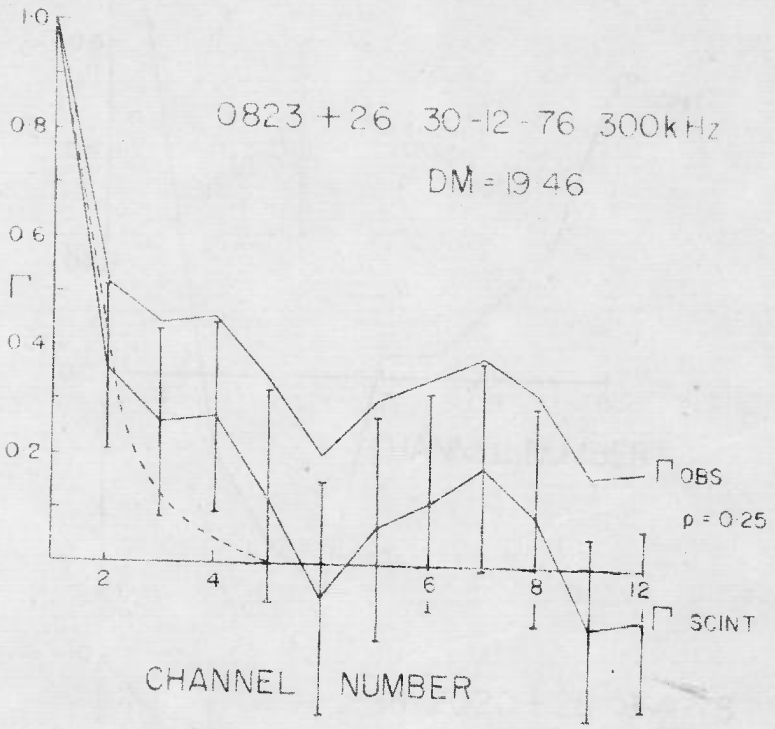

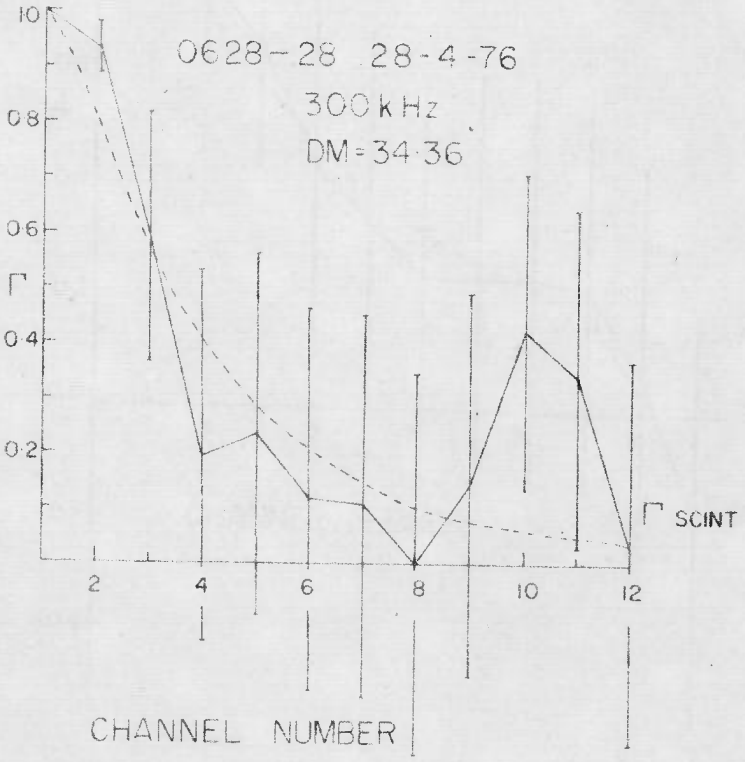

Fig.5.2h FREQUENCY CROSS CORRELATION FUNCTIONS Γ_{ij}

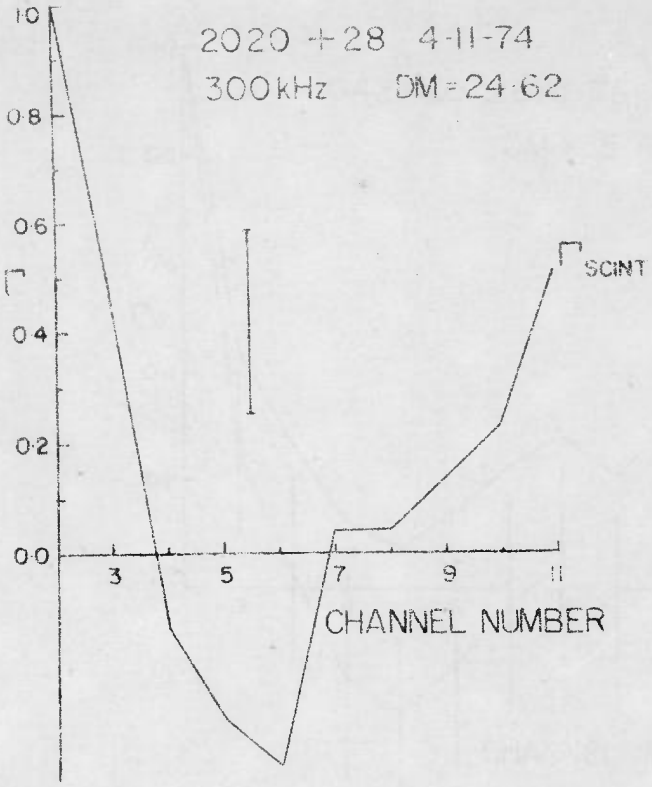

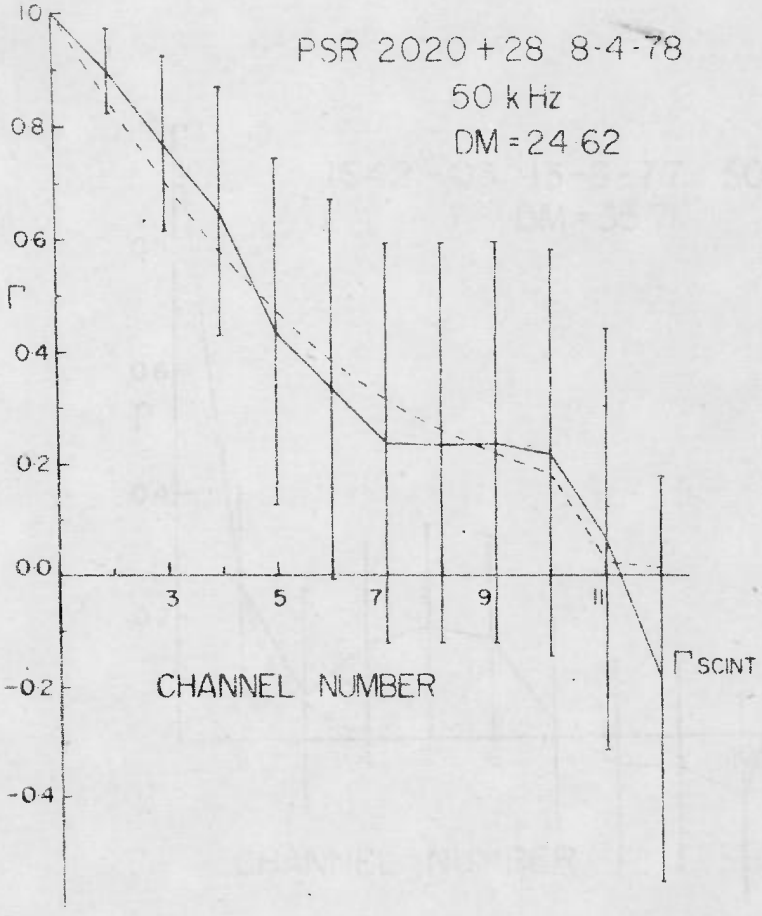

o.k. ✓

Fig. 5.2i FREQUENCY CROSS CORRELATION FUNCTIONS Γ_{1j}

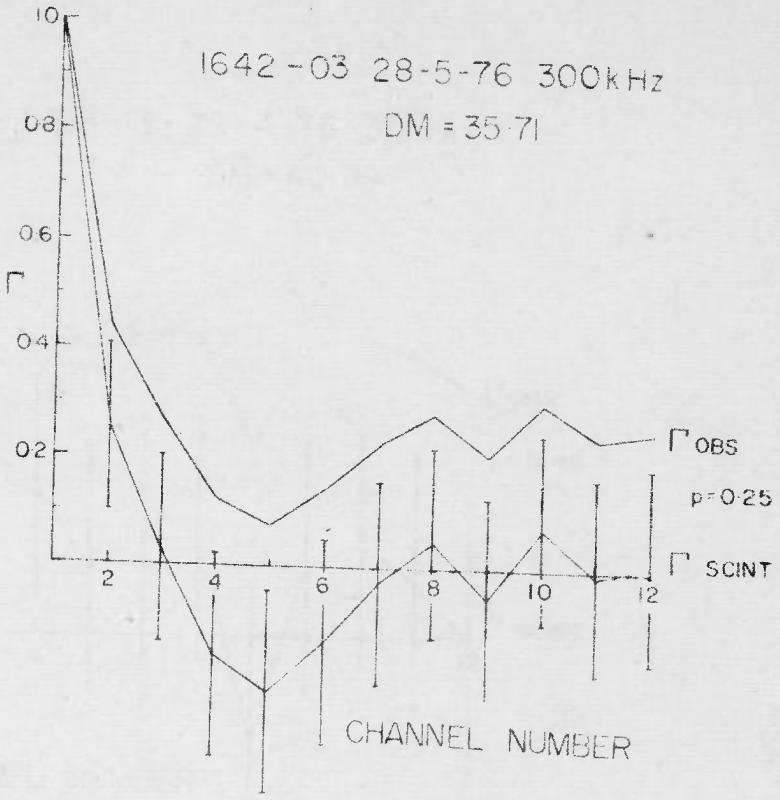

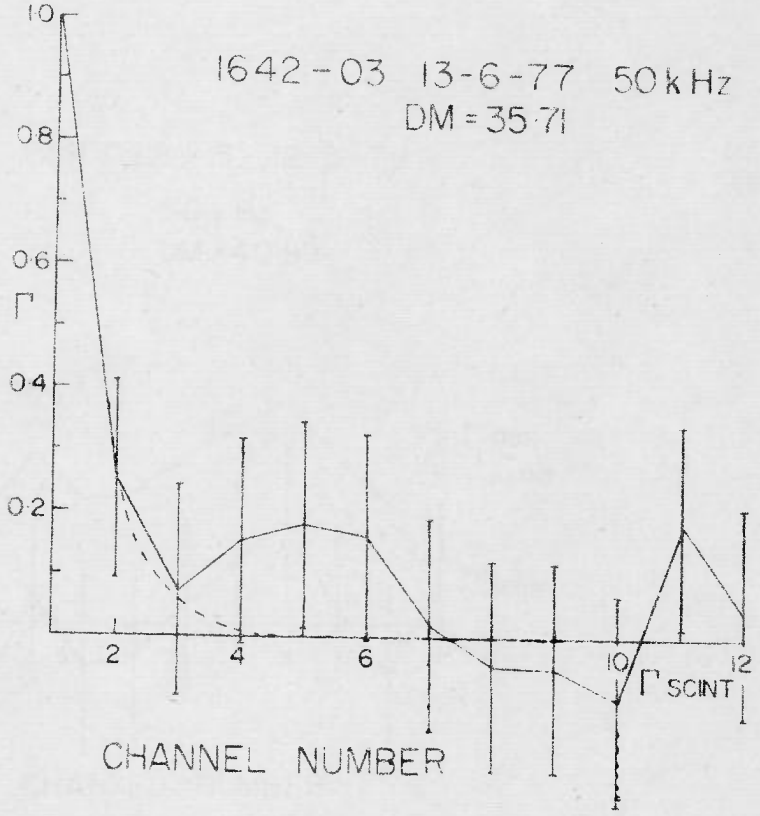

Fig.5.2j FREQUENCY CROSS CORRELATION FUNCTIONS $\Gamma_{1,j}$

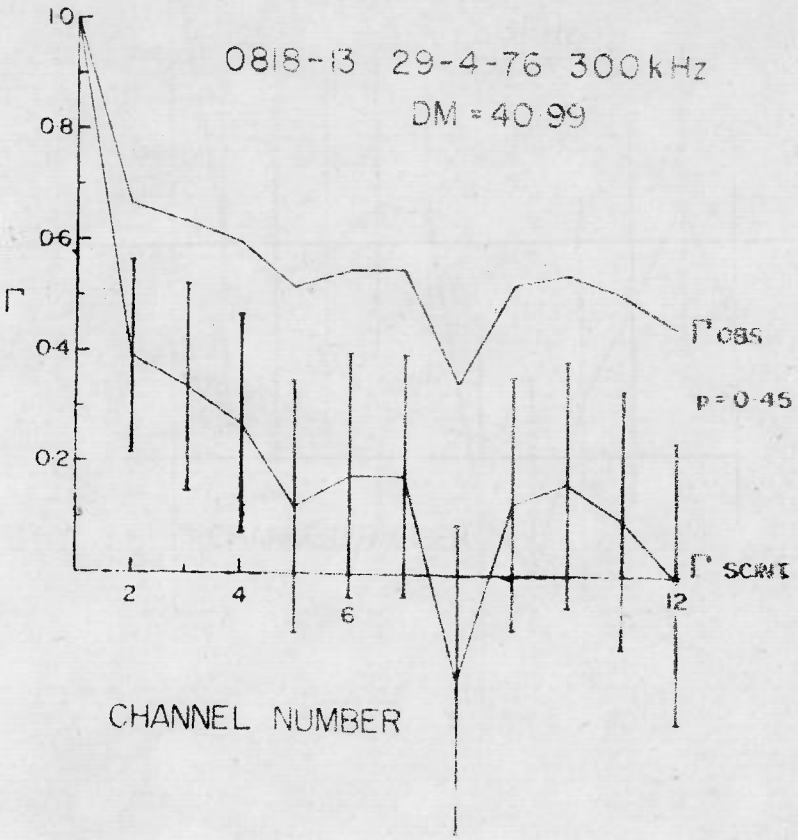

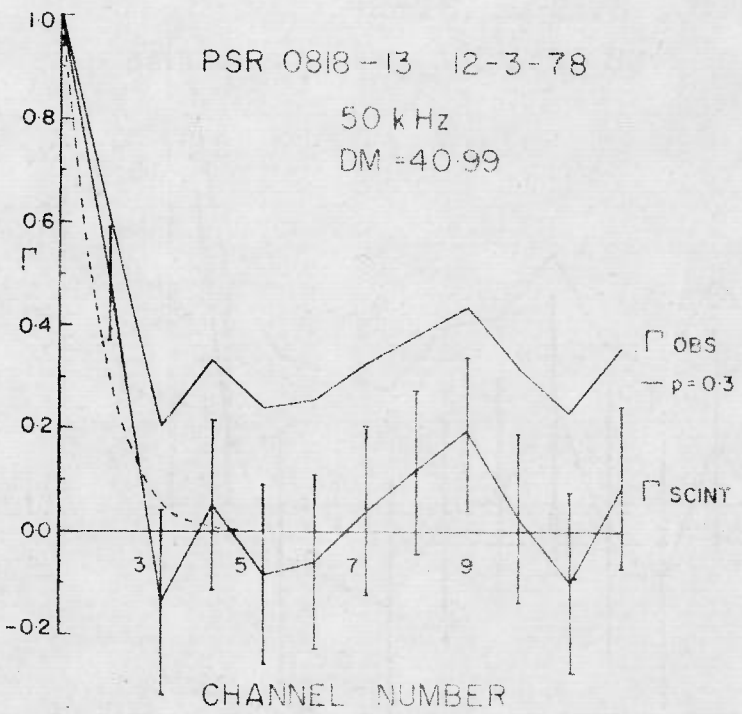

Fig.5.2k FREQUENCY CROSS CORRELATION FUNCTIONS Γ_{ij}

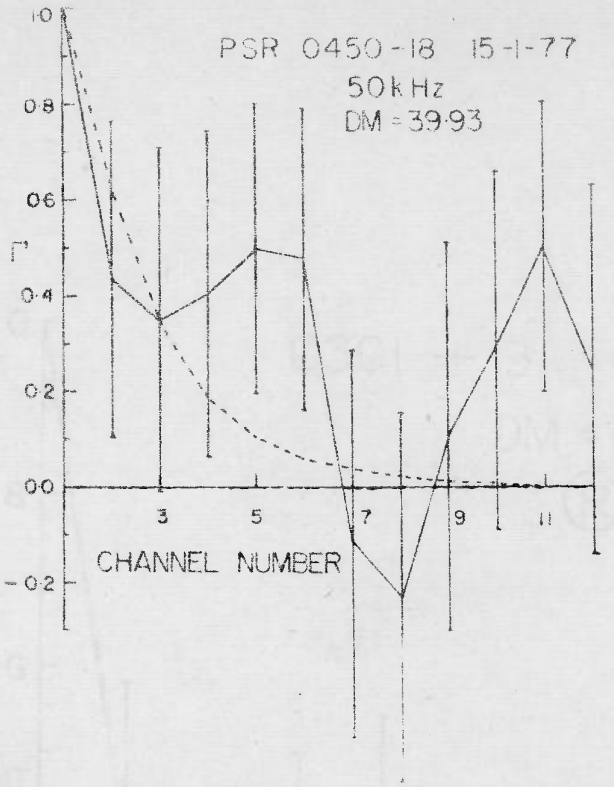

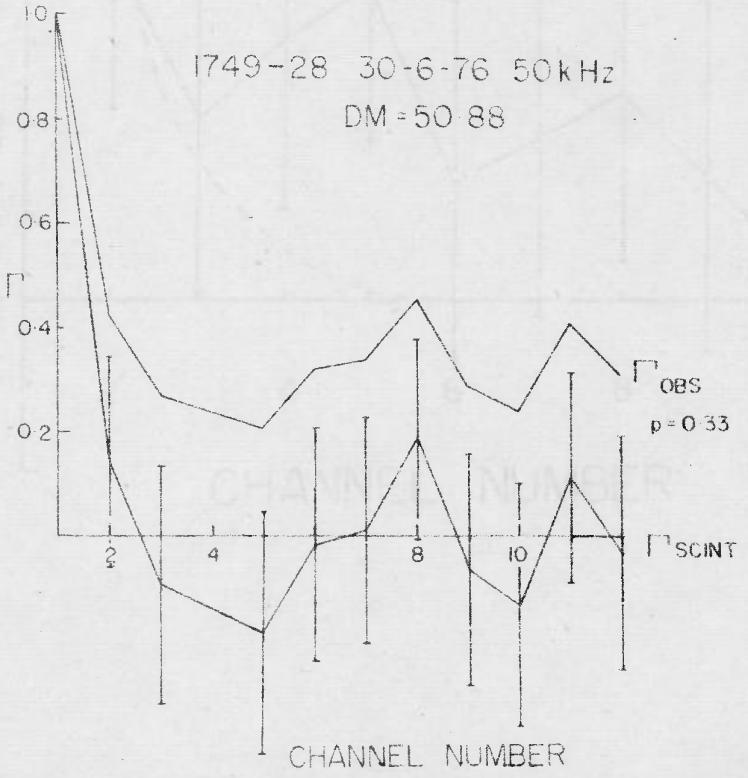

Fig. 5.2ℓ FREQUENCY CROSS-CORRELATION FUNCTIONS $\Gamma_{\Delta\nu}$

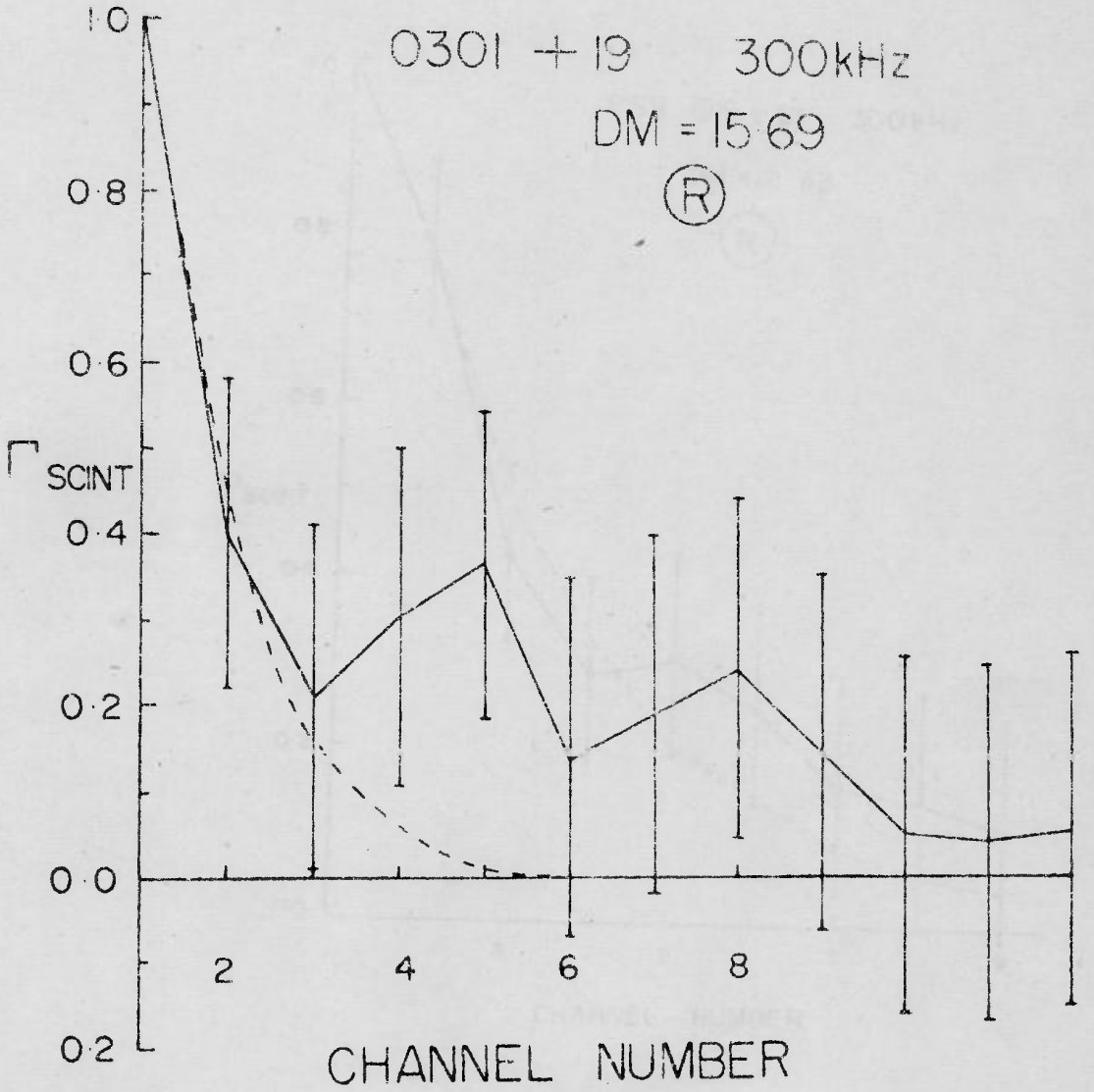

Fig.5.2m FREQUENCY CROSS CORRELATION FUNCTIONS Γ_{1j}

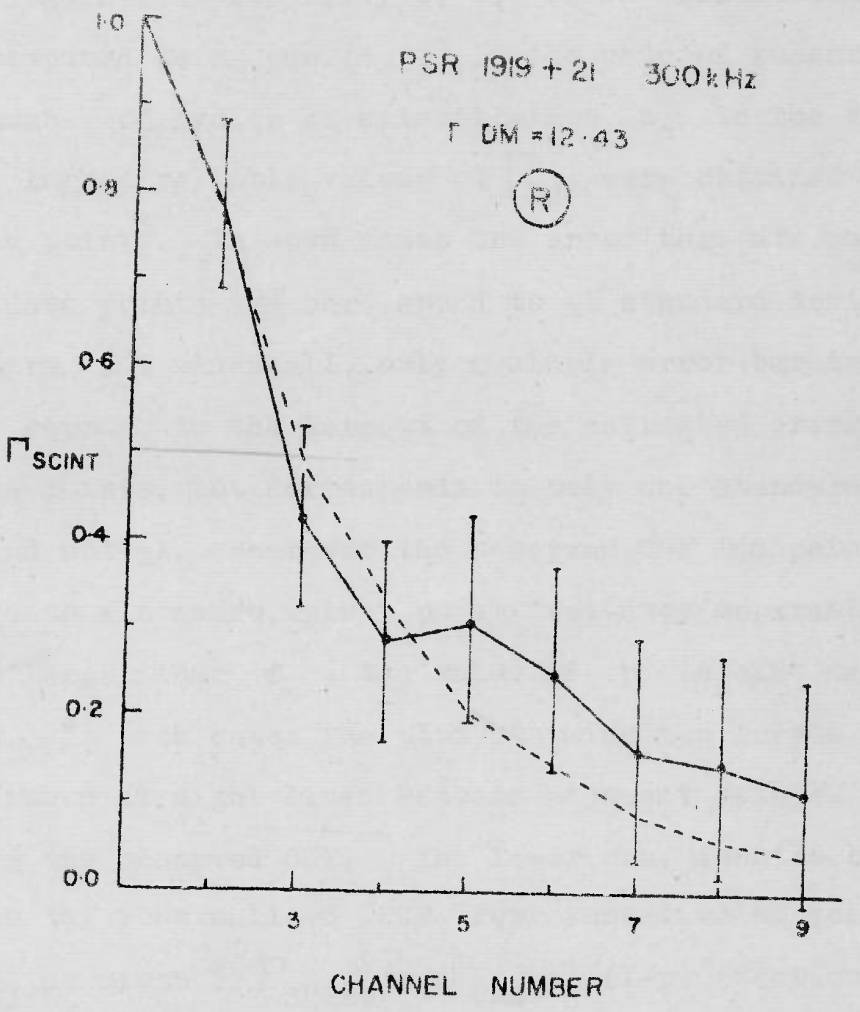

O.K

Fig.5.2n FREQUENCY CROSS CORRELATION FUNCTIONS Γ_{1j}

In the above figures, we have also given relevant observational information such as the frequency separation (either 50 kHz or 300 kHz) between adjacent channels, name of the pulsar, its DM and date of observation. The error bars denote the statistical stability of the cross correlations and have been computed using eqn.(4.3). In the case of pulsars for which the number of cycles of scintillation n_c in the data stretch was large, reliable values of Γ_{1j} were obtained for all the data points. In such cases the error bars are shown on all the data points and correspond to ± 1 standard deviation. In cases where n_c was small, only a single error bar is shown which represents the largest of the estimated errors for all the data points, but corresponds to only one standard deviation and not ± 1. Wherever the observed CCF indicated by Γ_{OBS} decays to a nonzero value p at frequency separations appreciably larger than f_ν, the value of p is also marked in the plot. In such cases the plot contains two curves made up of continuous straight lines between adjacent points. The upper one is the observed CCF. The lower one, denoted by Γ_{SCINT}, is the renormalised CCF representative of scintillations alone, as given by $\Gamma_{SCINT} = (\Gamma_{OBS}-p)/(1-p)$ (Section(4.2)). The figures also show model-based curves which are the best-fit to Γ_{SCINT} curves (Section (4.6.3)). The model-based curves are shown by dashes (------). These are obtained by assuming a Kolmogorov spectrum of irregularities and incorporate finite bandwidth effects.

5.3.2. Case II - Unresolved frequency structures of Scintillation at high DM

For the remaining 18 pulsars the CCF did not contain well-resolved frequency structures at low values of frequency separations. Most of these pulsars have their DM in the range 73.8-231 pc. cm^{-3}. We infer that values of f_ν for these pulsars must be much smaller than the bandwidths and frequency separations of the 12-channel receivers used for observations. It was also noticed that most of these pulsars showed low levels of signal fluctuation, with values of σ_j/σ_{jn} less than 0.3, where σ_j and σ_{jn} are the rms values of signal and receiver noise fluctuations respectively, for the jth channel. The exceptions to this were the pulsars 1857-26, 1818-04, 1911-04, 1933+16 and probably 0611+22 also. The data on these five pulsars are discussed separately later in this section. It may be noted that low values of σ_j/σ_{jn} are expected from the theory, which predicts that the use of observing bandwidths much larger than decorrelation frequency will result in considerable smoothing of the intensity fluctuations due to ISS.

For these 18 pulsars with unresolved frequency structure we present the data on frequency cross correlation of intensity fluctuations in Table (5.2). In this table we give values of (i) $\gamma_{1j\ ON}(j=2,3,...9)$ which is the ONPULSE correlation (eqn.(3.7)) without correction for receiver noise, and (ii) values of $\overline{(\sigma_j/\sigma_{jn})}$ which is the mean value of

TABLE 5.2 : 'ONPULSE' INTENSITY CORRELATIONS FOR THE PULSARS WITH UNRESOLVED FREQUENCY STRUCTURE

Sr. No.	PSR	$\nu_{i+1} - \nu_i$ (kHz)	γ_{12}	γ_{13}	γ_{14}	γ_{15}	γ_{16}	γ_{17}	γ_{18}	γ_{19}	γ_{110}	$\overline{\sigma_{s_i}/\sigma_{n_i}}$
1.	1822-09	300	0.000	0.145	0.045	0.040	-0.022	-0.022	0.016	0.023	0.034	0.29
2.	1857-26	50	0.349	0.218	0.197	0.155	0.204	0.242	0.202	0.166	0.190	0.54
3.	2303+30	50	0.119	0.011	-0.017	0.066	-0.002	0.006	-0.020	-0.036	-0.009	0.16
4.	1831-04	50	0.163	0.107	0.010	0.025	0.028	0.021	0.034	0.025	0.009	0.27
5.	0740-28	50	0.175	0.057	-0.009	0.029	-0.016	-0.012	-0.071	-0.010	0.044	0.19
6.	1818-04	50	0.200	0.123	0.128	0.134	0.079	0.115	0.061	0.092	0.056	0.39
7.	1917+00	50	0.171	0.078	0.008	0.040	0.007	0.078	0.003	0.024	-0.034	0.13
8.	1911-04	50	0.174	0.042	0.054	0.038	0.68	0.072	0.098	0.080	0.091	0.34
9.	0611+22	50	0.178	0.074	0.110	0.069	0.068	0.059	0.063	0.055	0.057	0.19
10.	0907+00	50	0.158	0.102	0.085	0.044	0.024	0.061	0.076	+0.041	0.038	0.17
11.	1700-32	50	0.128	0.069	-0.021	0.086	0.009	-0.043	0.024	0.050	-0.026	0.23
12.	1718-32	50	0.119	0.036	0.065	0.017	0.056	-0.008	0.069	0.061	-0.007	0.28
13.	1845-04	50	0.143	0.005	0.002	-0.008	0.009	-0.012	0.016	0.004	0.007	0.28
14.	1933+16	300	0.357	0.178	0.150	0.159	0.159	0.187	0.115	0.122	0.149	0.82
15.	1845-01	50	0.121	0.043	0.008	0.015	-0.086	0.057	0.055	0.014	-0.031	0.18
16.	1907+02	50	0.167	0.042	0.033	-0.006	0.022	0.051	0.015	-0.031	-0.051	0.13
17.	1900+01	50	0.087	-0.001	0.011	0.006	0.015	-0.033	-0.022	-0.040	0.018	0.27
18.	1831-03	50	0.147	0.031	0.026	0.027	0.002	0.022	0.073	0.003	0.010	0.17

(σ_j/σ_{jn}) averaged over all the channels. We are presenting the values of only the uncorrected correlations because most of these pulsars have $\overline{(\sigma_j/\sigma_{jn})}$ less than 0.3 and at such low values of $\overline{(\sigma_j/\sigma_{jn})}$ the noise-corrected correlation values cannot be relied upon. We have not given the values of correlation for the 10th, 11th and 12th channels as they are not significantly different from those of the nearer channels. Graphical plots of $\gamma_{1j\ ON}$ against channel number j are given for a representative sample of 10 out of the above 18 pulsars in Fig.(5.3a,b,....e) which include the above mentioned pulsars 1857-26, 1818-04, 1911-04, 1933+16 and 0611+22.

For these five pulsars we note that, although their frequency structures of scintillations are unresolved, they differ from the others in the following respects (i) these pulsars have values of R_0 larger than R_c (ii) they have values of $\overline{(\sigma_j/\sigma_{jn})}$ greater than 0.3 and (iii) they show appreciably large positive values of $\gamma_{1j\ ON}$ for all frequency separations, unlike the other 13 pulsars for which $\gamma_{1j\ ON}$ fluctuates on both sides of zero, over a small range. All of these symptoms are consistent with the inference that these five pulsars have intrinsic intensity variations with ISS-like time scales, which aspect is discussed further in Section (5.5).

In the case of the other 13 pulsars with unresolved ISS frequency structure, their broad band power spectra were

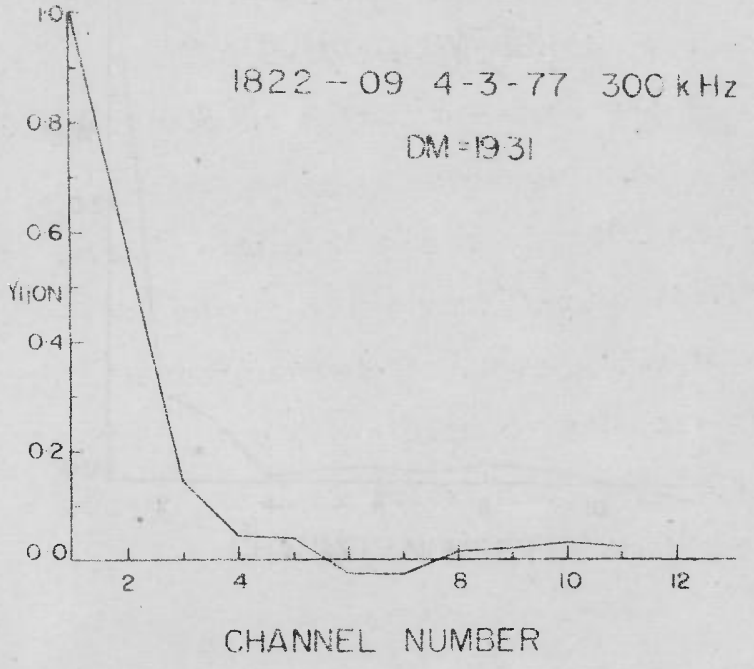

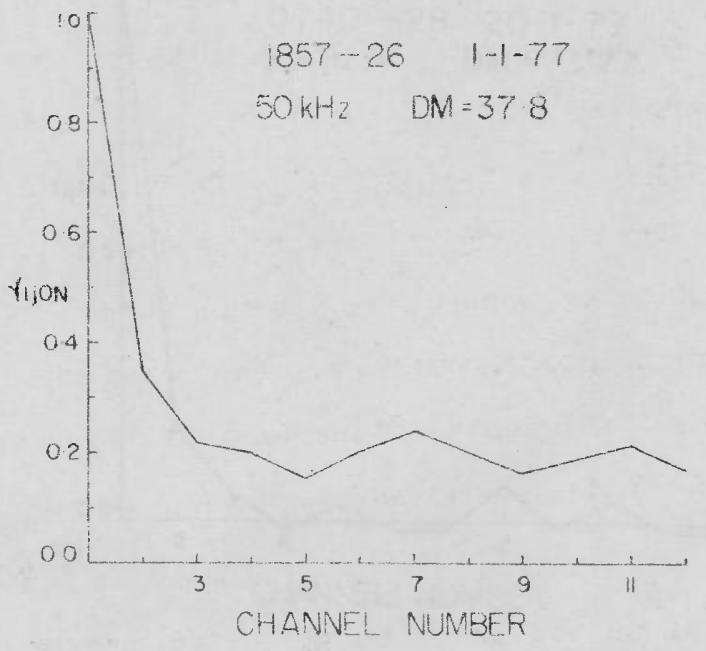

Fig. 5.3a UNCONNECTED CCF Y_{1jON}

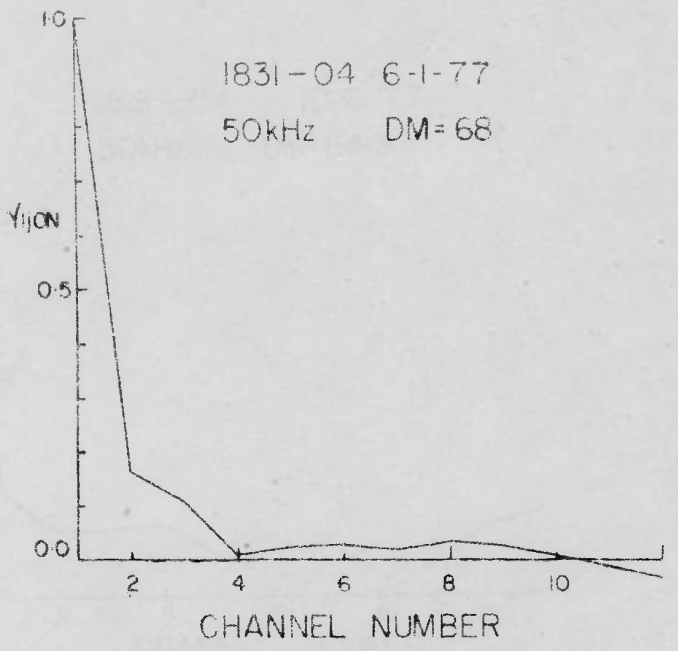

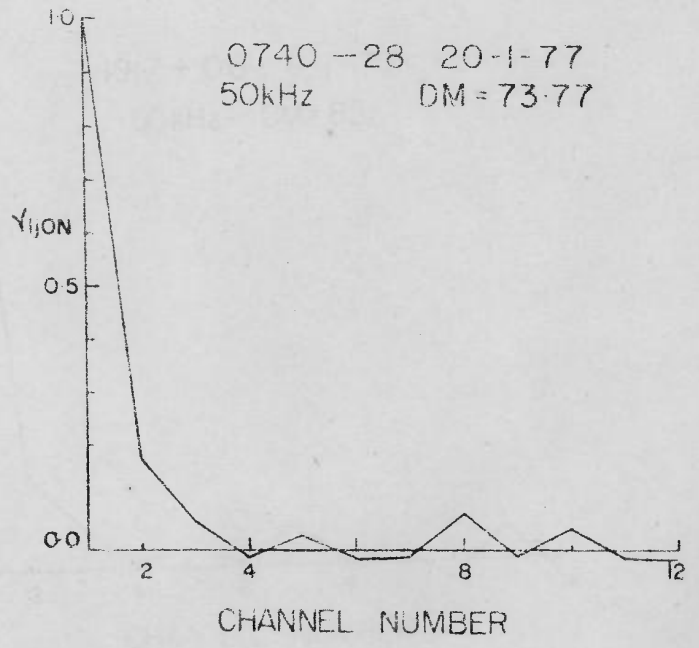

Fig. 5.3b UNCORRECTED COF Y_{1jON}

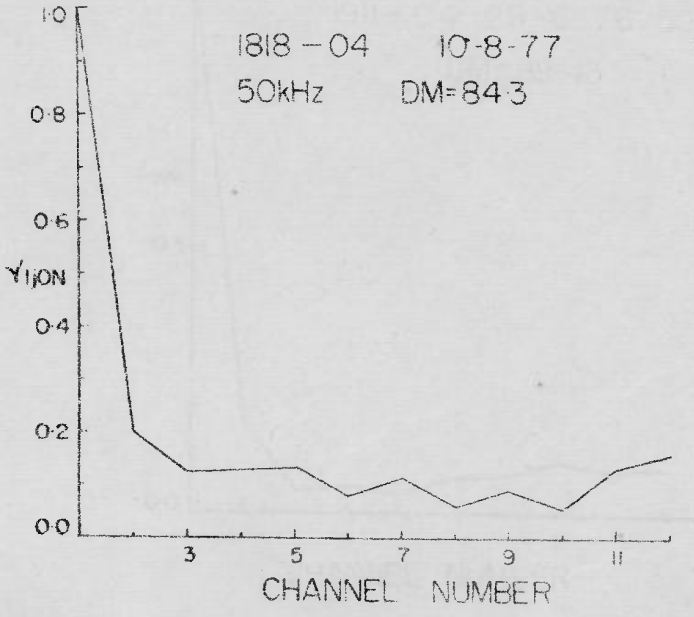

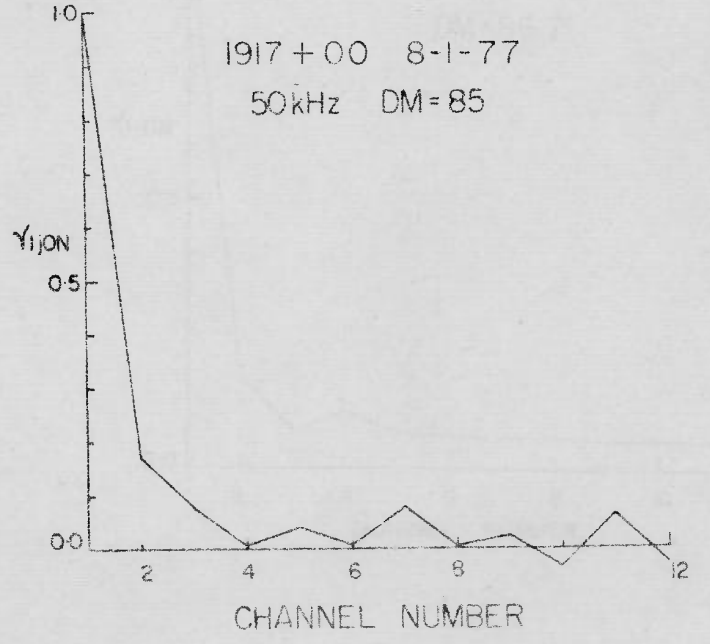

Fig. 5.3c UNCORRECTED CCF γ_{1jON}

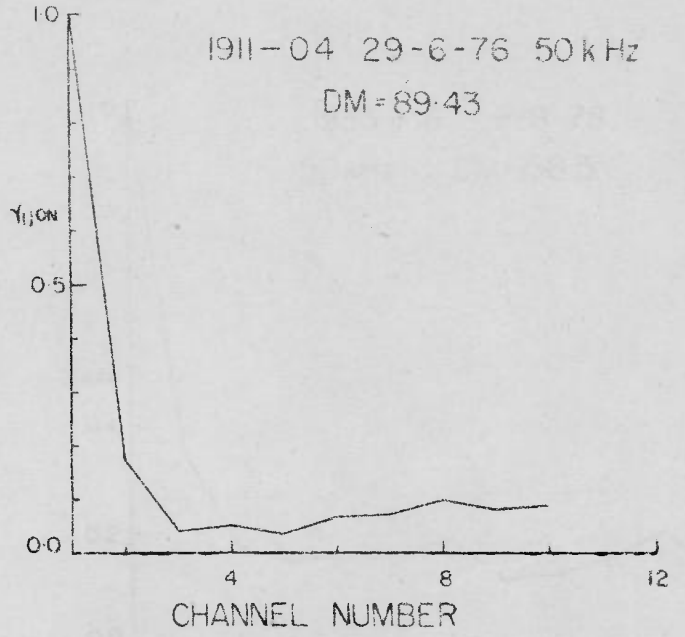

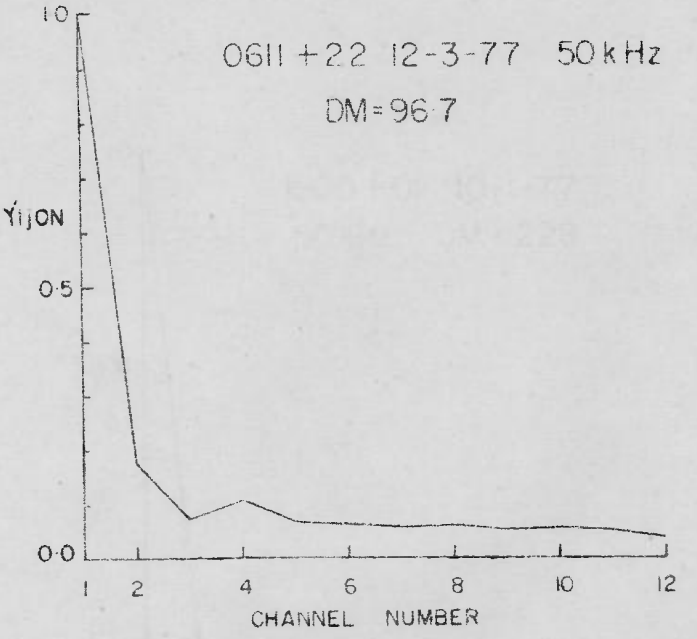

Fig. 5.3d UNCORRECTED CCF $Y_{1,jON}$

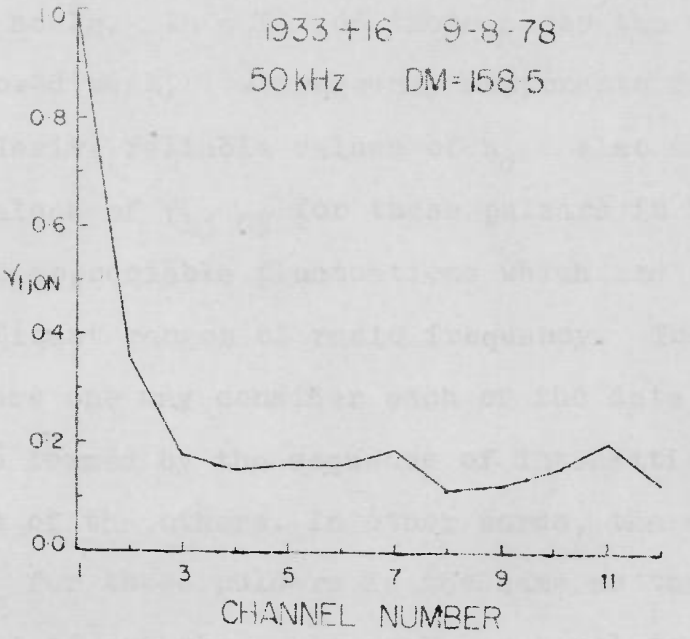

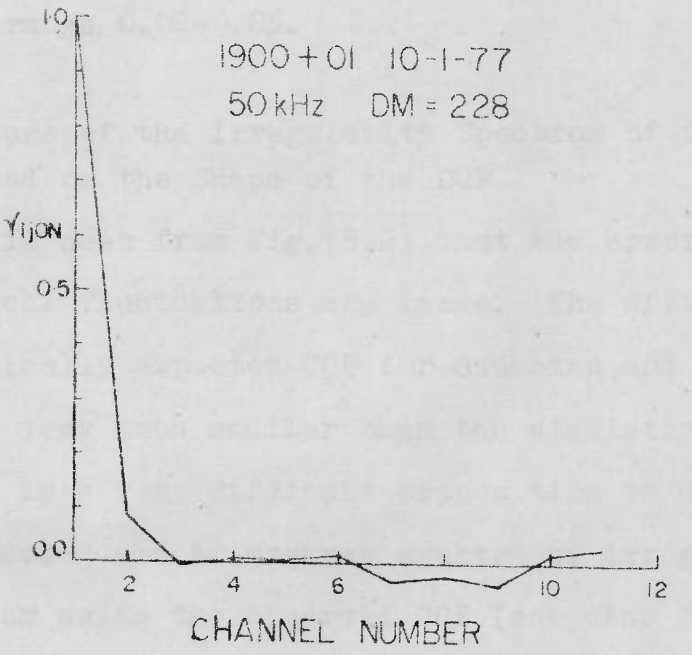

Fig. 5.3e UNCORRECTED OCF Y_{1jON}

practically featureless. This indicates the absence of intensity fluctuations which are correlated over any particular time scale. In a few of these cases the narrow band spectra showed weak, low frequency components from which one could not derive reliable values of n_c. Also as can be seen from the values of $\gamma_{1j\ ON}$ for these pulsars in Table (5.2), there is no appreciable fluctuations which are correlated over significant ranges of radio frequency. Therefore, for these pulsars one may consider each of the data point on the time series formed by the sequence of intensities, to be independent of the others. In other words, the effective value of n_c for these pulsars is the same as the array length M. For most of our observations M was equal to 1024 or 2048. Hence, from eqn.(4.3), the estimated statistical errors on the low values ($\simeq 0$) of intensity correlations for these pulsars, are in the range 0.02-0.03.

5.3.3. Nature of the Irregularity Spectrum of the IS Medium Based on the Shape of the CCF.

It is seen from Fig.(5.2) that the errors on Γ_{OBS} due to statistical fluctuations are large. The differences between the theoretically expected CCF for Gaussian and Kolmogorov spectra are very much smaller than the statistical errors. As a result it is a very difficult proposition to distinguish between Gaussian and Kolmogorov spectra of irregularities in the IS medium using the observed CCF (see also Section 4.6.6)).

A χ^2 goodness of fit test was performed by us on the CCF for PSR-1919+21, on which we had the longest stretch of data in terms of n_c, for the purpose of distinguishing between the two types of spectra. The test yielded an inconclusive result. Still, we note that for several pulsars, in spite of the large errors on Γ_{SCINT}, the shape of the observed CCF seems to be somewhat closer to the theoretically estimated CCF for Kolmogorov spectra than those for the Gaussian spectra.

5.4 ESTIMATED VALUES OF DECORRELATION FREQUENCY

The estimated values of decorrelation frequency f_ν for 23 pulsars are presented in column 3 of Table (5.3). The values are arranged in increasing order of DM. Values of the pedestal P of the frequency cross correlation function Γ_{ij}, at frequency separations which are much larger than f_ν, are given in Column 4. Column 5 gives values of n_c which is the number of cycles of scintillation in the data for narrow bandwidth, as obtained by dividing the total data length by decorrelation time. The values given in Column 6 are of the parameter R_0 which is the ratio of, the variance in the low frequency component of the observed broad band spectrum, to that in the corresponding component of the observed narrow band all channels combined spectrum (Section (2.8.2)). In the last column we list the calculated values of ratio R_c of scintillation variances, for comparison with R_0. R_c values are calculated from eqn. (2.50) using the measured values of f_ν.

TABLE 5.3 : Decorrelation frequencies and ratio of variances in broad and narrow bandwidths for 23 pulsars

Sr. No.	PSR (1)	DM ($pc.cm^{-3}$) (2)	f_ν (kHz) (3)	p (4)	n_c (5)	R_0 (6)	R_c (7)
1.	1133+16	4.85	710^{+380}_{-360}	0.420	32	7.85	6.42
2.	1237+25	9.3	595	0.400	11	8.19	5.92
3.	1604-00	10.72	165	0.0	2	4.69	3.44
4.	2045-16	11.51	400	0.250	20	4.74	4.72
5.	1919+21	12.43	330	0.1-0.4	58(c)	7.82	6.18
6.	0834+06	12.86	495	0.0	17	2.71	2.75
7.	2016+28	14.18	132	0.0	3	2.17a	3.18
8.	0301+19	15.69	$\simeq$ 66	0.275-0.4	21(c)	2.47	$\simeq$ 2.63
9.	1822-09	19.31	$<$ 66	0.0	4	3.26	$<$ 2.63
10.	0823+26	19.46	58	0.250	20	2.40	2.63
11.	2020+28	24.62	150	0.0	13	4.09a	5.06
12.	0628-28	34.36	430	0.0	8	3.74a	5.15
13.	1642-03	35.71	9	0.0	34	1.67	1.50
14.	1857-26	37.8	$<$ 2.5	0.9	6	6.32	$<$ 0.8
15.	0450-18	39.93	47	0.0	6	2.41a	2.74
16.	0818-13	40.99	10	0.300	29	5.40	1.58
17.	2303+30	49.9	$<$ 10	0.0	7	0.44	$<$ 1.58
18.	1749-28	50.88	$\simeq$ 2.5	0.330	17	1.57	$\simeq$ 0.8
19.	0740-28	73.77	$<$ 2.5	0.0	11	4.88	$<$ 0.8
20.	1818-04	84.38	$<$ 2.5	$\simeq$ 0.9	5	9.13	$<$ 0.8
21.	1911-04	89.43	$<$ 2.5	0.300	4	8.62	$<$ 0.8
22.	0611+22	96.7	$<$ 2.5	0.05	13	7.97	$<$ 0.8
23.	1933+16	158.5	$<$ 16	0.35	3	15.45	$<$ 2.63

Inferences are made in the next section by comparing these values of R_o and R_c for 23 pulsars.

It may be noted that the f_ν values listed are obtained by using the procedures described in Section (4.6). These procedures ensure that the f_ν estimate is free from possible intrinsic fluctuations present in the data and also that it would tend to the 'true' value for ideal receivers of zero bandwidth. The methods used by some of the earlier investigators (Lang 1971a; Sutton 1971) incorporated corrections for the effects of intrinsic fluctuations only and not for the finite bandwidth effects. In that sense our measurements are an improvement over the earlier work. Further, in our method of deriving the value of the decorrelation frequency from observations we have given weightage for the expected shape of the CCF also in an attempt to decipher the nature of the spectrum of irregularities (Section (4.6.3)). A comparison of our measurements of f_ν with those by others for a few pulsars which are common to the earlier and the present observations is presented in Section (5.6).

Table (5.3) gives the values of f_ν estimated by assuming a Kolmogorov spectrum of irregularities in interstellar space. f_ν values estimated by assuming a Gaussian spectrum will be only marginally different from the listed values. Errors due to statistical fluctuations on the estimated values of f_ν depend on n_c as described in Section (4.6). For larger values of n_c the errors will be smaller. These errors are

shown in the plot of f_ν vs DM in Section (5.6).

In the case of two pulsars, PSR 1919+21 and PSR 0301+19, the observations on different occasions have been combined to arrive at the estimate of f_ν (Section (4.6.6). This is indicated by a notation '(c)' in the column for n_c. As the observed values of p on different occasions were different we have given only the minimum and maximum of the p values in Table (5.3) for these two pulsars.

5.5 EXISTENCE OF INTRINSIC INTENSITY VARIATIONS WITH TIME SCALES SIMILAR TO THOSE DUE TO ISS

From Table (5.3) we notice that for several pulsars the values of R_0 and R_c are such that $R_0 > R_c$. This implies the existence of intrinsic intensity fluctuations of comparable strength to ISS and with ISS-like time scales in many pulsars. We summarise below the arguments for such a conclusion, and then present results.

As is well known, intrinsic intensity variations of pulsars, such as pulse to pulse variations, are correlated over a large range of radio frequencies. This is in contrast to interstellar scintillations which have narrow correlation bandwidths (Section (1.1)). The existence of intrinsic intensity variations manifests itself as the presence of a nonzero pedestal p in the frequency cross correlation function, at frequency separations which are large compared with f_ν, the decorrelation frequency due to ISS. But, as explained in

Section (2.8.2), the nonzero pedestal in CCF does not give us information on the time scales of the intrinsic intensity fluctuations. Power spectra of fluctuations are needed to infer about the time scales.

As described in Chapter 3, we have determined power spectra of intensity fluctuations of pulsars for narrow as well as wide bandpass of the receiver. From these spectra, we compute variances σ_{SN}^2 for the narrow band and σ_{SB}^2 for the broad band spectra, for the low frequency component typical of ISS. This component can be distinguished clearly in most of the observed power spectra of Fig.(5.1) and is demarcated schematically in Fig.(4.9) by region adb. We then compute the variance ratio $R_0 = (\sigma_{SB}^2/\sigma_{SN}^2)$. Assuming that the low frequency component is only due to ISS with narrow decorrelation frequency as estimated reliably from CCF (See Section (2.8.1)), we can compute the theoretically expected ratio R_c of variances for broad and narrow band (Section (2.8.2)). But in general, a low frequency component of power spectra may also arise due to intrinsic fluctuations with similar time scales as ISS but correlated over large range of radio frequencies. In that case, we expect R_0 to be larger than R_c as explained in Section (2.8.2).

Therefore, if only ISS were present we expect $R_0 = R_c$. On the other hand, in the presence of only intrinsic fluctuations we expect $R_0 = R_p > R_c$. If both are present $R_p > R_0 > R_c$.

We have computed R_0 and R_c for 23 pulsars which showed recognizable components both in their narrow band and broad band spectra. These values of R_0 and R_c are given in Columns 6 and 7 of Table (5.3). As explained in Section (5.3) definite measurements of decorrelation frequency f_ν were possible only for 15 out of the above 23 pulsars. In the other 8 cases the frequency structure due to scintillation was unresolved, leading to estimates of upper limits of f_ν only. Consequently for these 8 pulsars only lower limits on R_c could be calculated.

Fig.(5.4) shows a plot of R_0 against the corresponding R_c for the 23 pulsars. We notice from this plot that the points for several pulsars lie below the straight line at 45° to the axes. This indicates the presence of low frequency fluctuations in intensity with similar time scale and strength as ISS but which are correlated over a large bandwidth for at least 8 cases where $R_0 > R_c$, and possibly for 4 more, out of the 23 pulsars (Table 5.3). The measurements on 4 pulsars are seen to be discrepant with the expectation because their data points lie above the line at 45° to the axes in the R_0 - R_c diagram. These 4 pulsars are marked by the symbol 'a' in Column 6 of Table (5.3). We note from the plot of CCF (Fig.(5.2)) that the observed CCF of these pulsars depart considerably from the model curves leading to large errors in the estimates of their decorrelation frequency. It is likely that the f_ν estimates for the 4 pulsars are on the higher side,

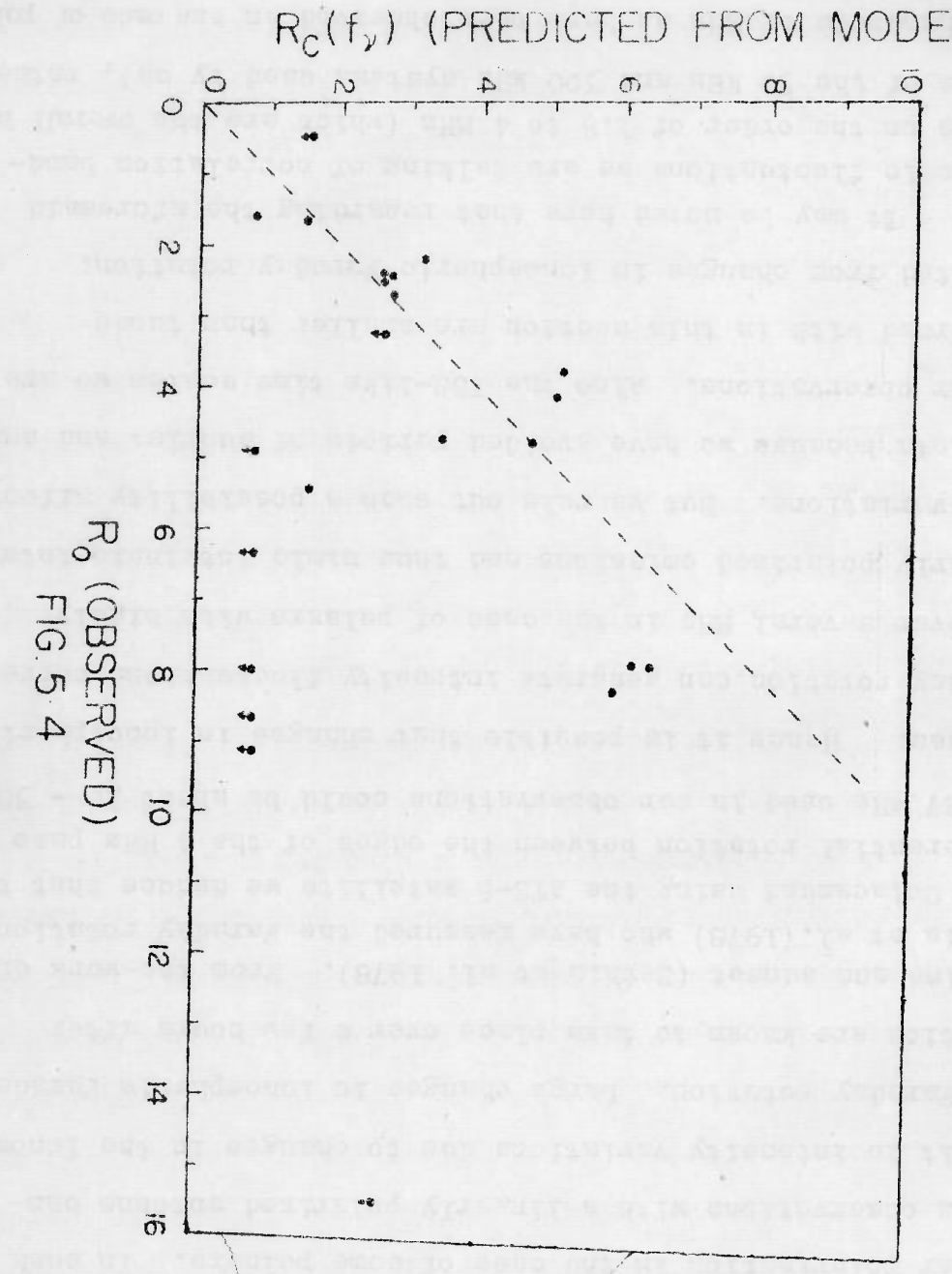

FIG. 5.4

which would explain the discrepancy.

It is known that pulsar pulses exhibit high degree of linear polarization in the case of some pulsars. In such cases observations with a linearly polarized antenna can result in intensity variations due to changes in the ionospheric Faraday rotation. Large changes in ionospheric Faraday rotation are known to take place over a few hours after sunrise and sunset (Sethia et al. 1978). From the work of Sethia et al.(1978) who have measured the Faraday rotation over Ootacamund using the ATS-6 satellite we deduce that the differential rotation between the edges of the 4 MHz pass band at 327 MHz used in our observations could be about 20 - 30 degrees. Hence it is possible that changes in ionospheric Faraday rotation can generate intensity fluctuations correlated over several MHz in the case of pulsars with highly linearly polarized emissions and thus mimic intrinsic intensity variations. But we rule out such a possibility affecting our data because we have avoided periods of sunrise and sunset in our observations. Also the ISS-like time scales we are concerned with in this section are smaller than those expected from changes in ionospheric Faraday rotation.

It may be noted here that regarding the aforesaid intrinsic fluctuations we are talking of correlation bandwidths on the order of 1.5 to 4 MHz (which are the overall bandwidths of the 50 kHz and 300 kHz systems used by us), rather than hundreds of MHz as have been observed in the case of pulse to pulse intensity fluctuations. As such one might attempt to explain the wide band fluctuations observed by us with 1.5

and 4 MHz receivers, with a two region model of the IS medium in which the IS medium between the source and the observer could be composed of two different regions with widely different values of the electron density fluctuations and their scale sizes. Such a model would result in two different correlation frequencies, as shown in Fig.(1) in the paper by Salpeter (1969). Although the possibility of a 2-screen model cannot be ruled out we have not found any observational evidence for it from the pulsars studied by us because no appreciable decline of pedestal p was observed up to 4 MHz. Therefore we prefer to attribute the observed wide band fluctuations discussed above to intrinsic causes.

Pulsars are known to exhibit wide band intrinsic fluctuations from pulse to pulse as well as over days. It is not surprising that they show intrinsic fluctuations with time scales of minutes also. The method used by us has allowed the recognition of this component in many pulsars even in the presence of ISS of similar time scales.

5.6 THE OBSERVED DEPENDENCE OF DECORRELATION FREQUENCY ON DISPERSION MEASURE

In this section we summarise firstly the results on the observed f_ν-DM relationship from the work of earlier investigators. The probable sources of error in the estimates of f_ν (or the equivalent parameter B_h) given by earlier workers are pointed out. In Section (5.6.3) we present our

results which show the genuineness of the steepening of the f_ν-DM dependence at large values of DM which in turn implies inhomogeneity of the IS medium. The implications are discussed in Section 5.5.4.

5.6.1 Earlier Observations

The most convincing observational support for the interstellar scintillation hypothesis of pulsar intensity fluctuations with time scales on the order of a few minutes or more came first from the work of Rickett (1969, 1970). Rickett had measured the scintillation index in each of several bandpass filters with different bandwidths, all centred at the same frequency. The scintillation index was computed after smoothing the intensities for consecutive one minute intervals in order to reduce the fluctuations due to intrinsic causes. The frequency structure seen in pulsar scintillation was parametrised by the half-visibility bandwidth B_h which he defined as the bandwidth at which the scintillation index decreased to half its value for zero bandwidth. B_h was determined by fitting a theoretical curve to the measured values of scintillation index, assuming a rectangular bandpass and a gaussian autocorrelation function for the variations of intensity with frequency. These observations showed that B_h is smaller for pulsars of large dispersion measure, the dependence being given approximately by $B_h \propto (DM)^{-2}$ (See Fig.10 of Rickett 1970). Both thin

screen (Scheuer 1968; Lang 1971a) and extended medium models (Uscinski 1968a, 1968b; Rickett 1970) of the IS medium, with Gaussian spectra of irregularities predict such a dependence of B_h on DM if one assumes that $< \delta N_e^2 >^{\frac{1}{2}}$ is proportional to $< N_e >$ and DM is proportional to the distance to the pulsar. Rickett's data showed considerable scatter in the values of B_h, especially in the range $11.4 \leq DM \leq 14.3$ pc.cm^{-3}. In view of the fact that in our observations many pulsars showed the existence of intrinsic fluctuations with time scales similar to those due to the IS medium, it is possible that Rickett's method of estimating B_h from variation of scintillation index with bandwidth could have resulted in apparently large values of B_h in some cases due to presence of such intrinsic variations.

Most of the other measurements on frequency structure of pulsar intensity fluctuations available in literature were from the work of Lang (1971a). Ewing et al.(1970), Wolzscan et al. (1974) and Backer (1974) had also observed a few pulsars to study the frequency structures. Lang had used multichannel receivers similar to the ones used by us, computed CCF of intensities and then estimated values of f_ν from the computed CCFs after correcting for the nonzero pedestal p . But he had not incorporated corrections to the estimated values of f_ν for finite bandwidth effects. Owing to finite bandwidth effects, the CCF computed from observed pulse intensities gets broadened as compared with

that for the ideal case of zero bandwidth detectors. The half width of the observed curve could be larger than the 'true' f_ν by 25 % or more for cases where the bandwidth is comparable to the true f_ν. This is seen from Figs. (4.1,2,3,4) of this thesis. As such the estimates of f_ν by Lang could have been higher than the actual values. His observations at 318 MHz resulted in measurements of f_ν for 5 pulsars in the DM range 4.9-19.5 pc.cm^{-3}. The relation $f_\nu \propto (DM)^{-2}$ was seen to fit the data on these 5 pulsars. The measurements by Ewing et al. are not very useful as they were only visual estimates of the widths of the frequency structures. The observations at 1420 MHz by Wolzscan et al.(1974) with a correlation spectrometer yielded eye estimate widths of the autocorrelation function of the the spectra for four pulsars. Backer had measured the B_h for PSR 0833-45 at five different frequencies in the range 837 MHz to 8085 MHz. He found that B_h scales as $\nu^{4\pm0.2}$ for this pulsar, in agreement with prediction of scintillation theory.

Sutton (1971) had made a comparative study of the measurements of B_h, B and f_ν by Rickett (1970), Ewing et al. (1970) and Lang (1971a) respectively. He showed that Lang's method of estimating f_ν from the observed CCF by correcting for the nonzero pedestal p, corrects for the effects of intrinsic intensity fluctuations. He also derived the relationship $f_\nu \simeq B_h/9.9 \simeq B/1.5$. Using this relationship, and the measurements by the three authors he determined values of

f_ν at 318 MHz, which were subjective averages of f_ν, $B_h/9.9$ and B/1.5. In Table (5.4) we present a comparison of the values of f_{327} obtained by us with those derived by the above four workers, after scaling to 327 MHz using the ν^{-4} law. The errors for our measurements specify the statistical uncertainties arising from the limited lengths of data (although several hours of stretch !) and correspond to ± 1 standard deviation. Errors of similar magnitude or larger are expected to be associated with the other measurements which were also derived from data streches as long as or less than those of ours. Hence we conclude that the differences amongst the various measurements are mostly within the expected statistical uncertainties

5.6.2. Earlier Results on the Composite f_ν-DM Diagram

Sutton (1971) had attempted to extend the range of the measured values of f_ν (or B_h) beyond DM=50.9 pc.cm^{-3} by invoking the inverse relationship between decorrelation frequency f_ν and the scattered pulse width Δt_s, which was first pointed out by Salpeter (1969). For a thin screen model of the IS medium with the screen located midway between the pulsar and the observer, Sutton showed that the exact form of the inverse relationship is given by

$$2\pi f_\nu \Delta t_s = 1 \qquad (5.1)$$

TABLE 5.4 : DECORRELATION FREQUENCIES f_{327} AT 327 MHZ - COMPARISON OF MEASUREMENTS FOR 8 PULSARS

Sr. No.	PSR	DM ($pc.cm^{-3}$)	(Rickett) (kHz)	(Ewing) (kHz)	(Lang) (kHz)	(Sutton) (kHz)	(Present work) (kHz)
1.	1133+16	4.9	778	289	2223	778	710 ± 430
2.	1237+25	9.3	-	-	778	778	595 ± 375
3.	2045-16	11.5	$\gtrsim 738$	-	-	≥ 778	400 ± 230
4.	1919+21	12.4	123	445	889	333	330 ± 160
5.	0834+06	12.9	226	322	555	333	495 ± 400
6.	2016+28	14.2	29	-	< 555	33	132^{+710}_{-65}
7.	0823+26	19.5	-	-	555	555	58^{+260}_{-26}
8.	1749-28	50.9	6.7	-	-	6.7	2.5^{+13}_{-1}

The above equation was derived under the assumption that both strong and multiple scattering conditions are satisfied. Sutton's model of interstellar scattering further showed that the CCF is the real part of the Fourier transform of the pulse broadening function which leads to the exponential decay of pulse profiles for pulsars with large DM (see also Cronyn 1970). Also he had presented arguments to show that eqn. (5.1) holds good approximately for any screen, thick or thin, and regardless of its location, providing that the strong and multiple scattering conditions are fulfilled.

Using the f_ν-Δt_s relationship (eqn.(5.1)) and the measured values of f_ν(or B_h)and Δt_s for several pulsars available in the literature Sutton constructed a composite f_ν-Δt_s-DM diagram which was a log-log plot of f_ν vs DM. For pulsars with DM > 50.9 pc.cm^{-3}, the f_ν values were derived from the known values of Δt_s using eqn.(5.1). The diagram was for ν = 318 MHz. The relation $\Delta t_s \propto \lambda^4$ was used for scaling the Δt_s values at other frequencies to 318 MHz. He noted from this diagram that for DM $\leq$ 20 pc.cm^{-3} f_ν decreases roughly as $(DM)^{-2}$, but, the dependence steepens considerably, approaching $(DM)^{-4}$ at large dispersion measures particularly for those f_ν values derived from pulse broadening. Such a trend is in disagreement with the predictions of the theoretical models. We discuss this aspect later in the light of the new data obtained from our observations.

In this connection it may be mentioned here that Lang had also constructed a similar diagram in which the f_ν-Δt_s-DM

trend was found to be in fair agreement with theory, i.e. $f_\nu \propto (DM)^{-2}$, especially for 111 MHz, though not for the data at other frequencies namely 40, 318 and 408 MHz (Lang 1971b). But, unlike the relationship given in eqn.(5.1) which was used by Sutton, Lang had used $f_\nu \wedge t_s = 1$ and this has the effect of reducing the deviations from the theoretically expected relationship, $f_\nu \propto (DM)^{-2}$.

5.6.3. Results on f_ν-DM dependance from Our Observations

The values of decorrelation frequencies f_ν derived from our observations are presented as a log-log plot in Fig. (5.5). The error bars shown, represent statistical uncertainties and correspond to ± 1 standard deviations. They were estimated as described in Section (4.6.5). The upper limits for 7 of the pulsars are indicated by downward arrows. The confidence level of the upper limits correspond to two standard deviations or more, except in the case of PSR 1822-09 for which it is about one standard deviation.

As described in Chapter 2, theoretical models of the IS medium predict a linear dependence of log f_ν on log DM, with a slope of -2 in the case of a Gaussian irregularity spectrum and of -2.2 for a Kolmogorov spectrum. In order to compare the observations with the theoretical prediction we tried to fit a straight line to the log f_ν - log DM plot obtained from our measurements using the weighted least squares method. The straight line fit was attempted for two subsets of the data

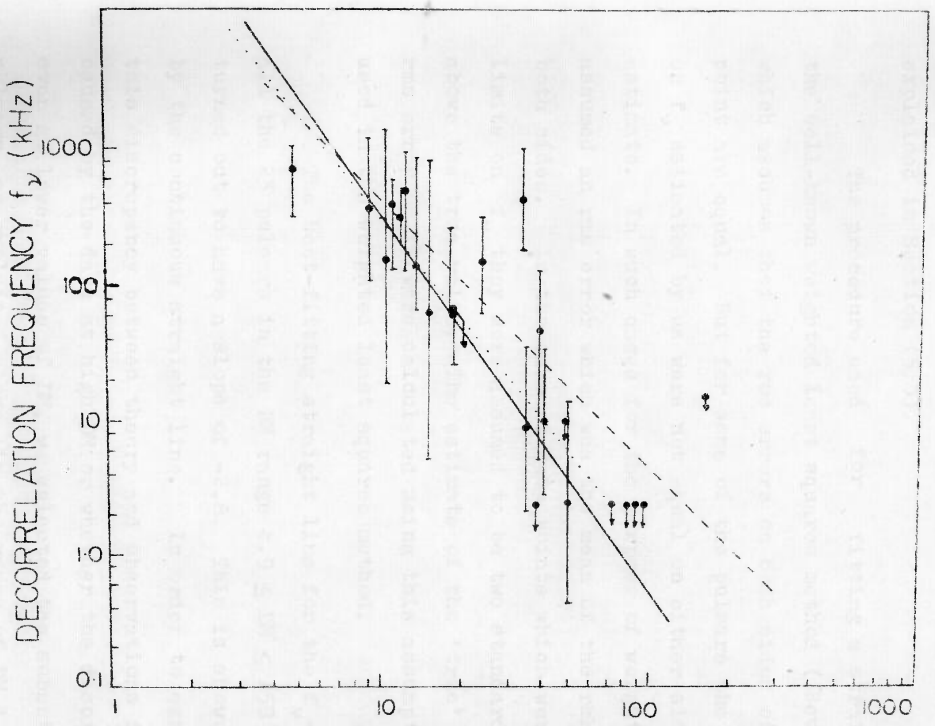

FIG. 5·5 f_ν-DM, DIAGRAM FROM THE PRESENT WORK

as follows: (i) data on all the 23 pulsars in the range $4.9 \leq DM \leq 158$ pc.cm^{-3} and (ii) data on 17 pulsars in the DM range 4.9-50.9 pc.cm^{-3}, and excluding the measurement on PSR 0628-28 the f_ν for which could have been overestimated by us as explained in Section (5.5).

The procedure used for fitting a straight line is the well-known weighted least squares method (Bevington 1969) which assumes that the rms errors on both sides of any data point are equal. But for some of the pulsars the rms errors on f_ν estimated by us were not equal on either side of the f_ν estimate. In such cases for the purpose of weighting, we assumed an rms error which was the mean of the rms errors on both sides. In the case of data points which were upper limits on f_ν they were assumed to be two standard deviations above the true value. The estimate of the 'true' value and rms error on it were calculated using this assumption and then used in the weighted least squares method.

The best-fitting straight line for the f_ν-DM data on all the 23 pulsars in the DM range $4.9 \leq DM \leq 158$ pc.cm^{-3} turned out to have a slope of -2.8. This is shown in Fig.(5.5) by the continuous straight line. In order to examine whether this discrepancy between theory and observations is mostly caused by the data at high DM or whether the discrepancy exists even at lower values of DM, we selected the subset of 17 pulsars, as explained above, in the range of DM 4.9-50.9 pc. cm^{-3}. These 17 data points were separately subjected to the

least squares method. The best-fitting straight line obtained from this procedure had a slope of -2.5. This line is shown in Fig.(5.5) by dots (.....). A straight line with slope of -2 is also given in the figure.

It should be noted here that the slope of -2.8 (or -2.5) derived from our observations could not be a consequence of the particular method used by us to choose the best-fitting model curve of CCF to the observed CCF (Section (4.6.3)). The weighting procedure used by us for CCF fits tends to increase the f_ν estimates, especially from CCF with narrow frequency structures of ISS. This has the effect of reducing the deviations of measured values of f_ν from the $(DM)^{-2}$ slope at large DM. Therefore we conclude that the deviation of the observed log f_ν-log DM slope from the theoretical prediction, is significant even though the departure is apparently small.

5.6.4. Implications of the Observed f_ν-DM Trend

In order to explain the observed steepening of the composite f_ν-Δt_s-DM diagram at large dispersion measures, Sutton had considered the possibility that the conditions necessary for the validity of the inverse relationship between f_ν and Δt_s (eqn.(5.1)) may not hold good in the interstellar medium. Our results described in the previous section rule out this possibility because they are based on measurements of f_ν only and do not invoke the inverse relationship between f_ν and Δt_s derived from theory of scattering. We conclude that the discrepancy between observations and theory regarding the f_ν-DM

dependence, reflects the lack of validity of some assumption on which the theoretical model of the IS medium is based so as to arrive at the predicted f_ν-DM slope of -2.

As has been pointed out by Rickett (1977) the steep slope at large DM cannot be explained by postulating a power law spectrum of irregularities in the IS medium such that the index α of the spectrum has a value of about 2.7. Such a value of α will match the observed steep slope of -4 for the f_ν-DM diagram but will predict $f_\nu \propto \lambda^{-8}$ or $\Delta t_s \propto \lambda^{8}$. Such a steep λ dependence for f_ν has not been observed so far. On the contrary Backer (1974) has observed $B_h \propto \lambda^{-4\pm0.5}$ for PSR 0833-45 and there exist in literature several measurements of Δt_s at several radio frequencies for quite a few pulsars which show that $\Delta t_s \propto \lambda^{4\pm0.5}$.

From the above considerations it is clear that the assumption of homogeneity of the IS medium may not be valid i.e. the assumption that the rms electron density fluctuation $< \delta N_e^2 >^{\frac{1}{2}}$ is proportional to the mean electron density may not hold good everywhere in the IS medium of our galaxy. We discuss this aspect in the next section.

5.6.5. Inhomogeneity of the Interstellar Medium

The f_ν-Δt_s-DM diagram is essentially a comparison of the scattering and dispersive properties of the IS medium. The conclusion one draws from the observed f_ν-DM trend is that the scattering properties of the IS medium become more pronounced

in comparison with the dispersive properties at larger values of DM. Larger values of DM imply larger distances, at least on a statistical average. Therefore one infers that the rate at which scattering properties of the IS medium become accentuated with distance, is more than that for the dispersive property. The scattering property which is represented by a combination of the rms fluctuation in electron density $\langle \delta N_e^2 \rangle^{\frac{1}{2}}$ and its scale size L can be characterised by the parameter $[\langle \delta N_e^2 \rangle / L]^{\frac{1}{2}}$. The dispersion in the IS medium is represented by the mean electron density $\langle N_e \rangle$. The inference one draws from observations, therefore, is that the conditions for the validity of the relationship $\langle \delta N_e^2 \rangle / L \propto \langle N_e \rangle^2$ may not hold good in the IS medium, over all the regions of our galaxy. In other words, the IS medium does not have a homogeneous character throughout our galaxy with regard to $\langle \delta N_e^2 \rangle^{\frac{1}{2}}$, L and $\langle N_e \rangle$.

A possible reason for this could be that with increasing distance from the Sun there is higher probability for the line of sight to a pulsar intersecting H II regions. Further, it would be interesting to investigate whether there is any systematic variation of $\langle \delta N_e^2 \rangle^{\frac{1}{2}} / L$ and $\langle N_e \rangle$ with distance of the pulsar from the galactic centre. With the data available on a limited number of pulsars there are indications that such a systematic variation of scattering and dispersive properties of the IS medium in our galaxy could be present. This is seen from the composite $f_\nu - \Delta t_s$-DM diagram for 327 MHz shown in

Fig.(5.6). In this diagram we present the data available in literature along with our measurements of f_ν for 15 pulsars. Our measurements are shown as filled circles. Filled circles with downward arrows indicate upper limits on f_ν estimated by us. The ν^4 scaling law was used in converting the measurements of f_ν at other frequencies to values at 327 MHz. These values are shown by filled squares. The open circles are values of f_ν derived from measurements of Δt_s available in literature, using the λ^4 scaling law and the relationship $2\pi f_\nu \Delta t_s = 1$. The derived values of f_ν used in constructing the diagram in Fig.(5.6) are given in Table (5.5). The diagram contains the f_ν values of a total of 35 pulsars over a DM range 3-450 pc.cm^{-3}. From Fig.(5.6) we see that it may not be possible to fit a linear relationship between log f_ν and log (DM) over the entire range of dispersion measures. The best-fit to the diagram would be a nonlinear curve whose slope would steepen continually from about -2 to -4 as the DM increases from low to high values. Such a continual change of slope reflects a continual increase of $\langle \delta N_e^2 \rangle^{\frac{1}{2}}/L$ with dispersion measure. From the values of galactic longitude and latitude for the 35 pulsars given in Table (5.5) we find that pulsars with high DM tend to lie in the direction towards galactic centre. Hence it seems likely that $\langle \delta N_e^2 \rangle^{\frac{1}{2}}/L$ decreases with galactocentric distance of the pulsars.

To confirm the existence of such a systematic variation of the scattering property of the IS medium with

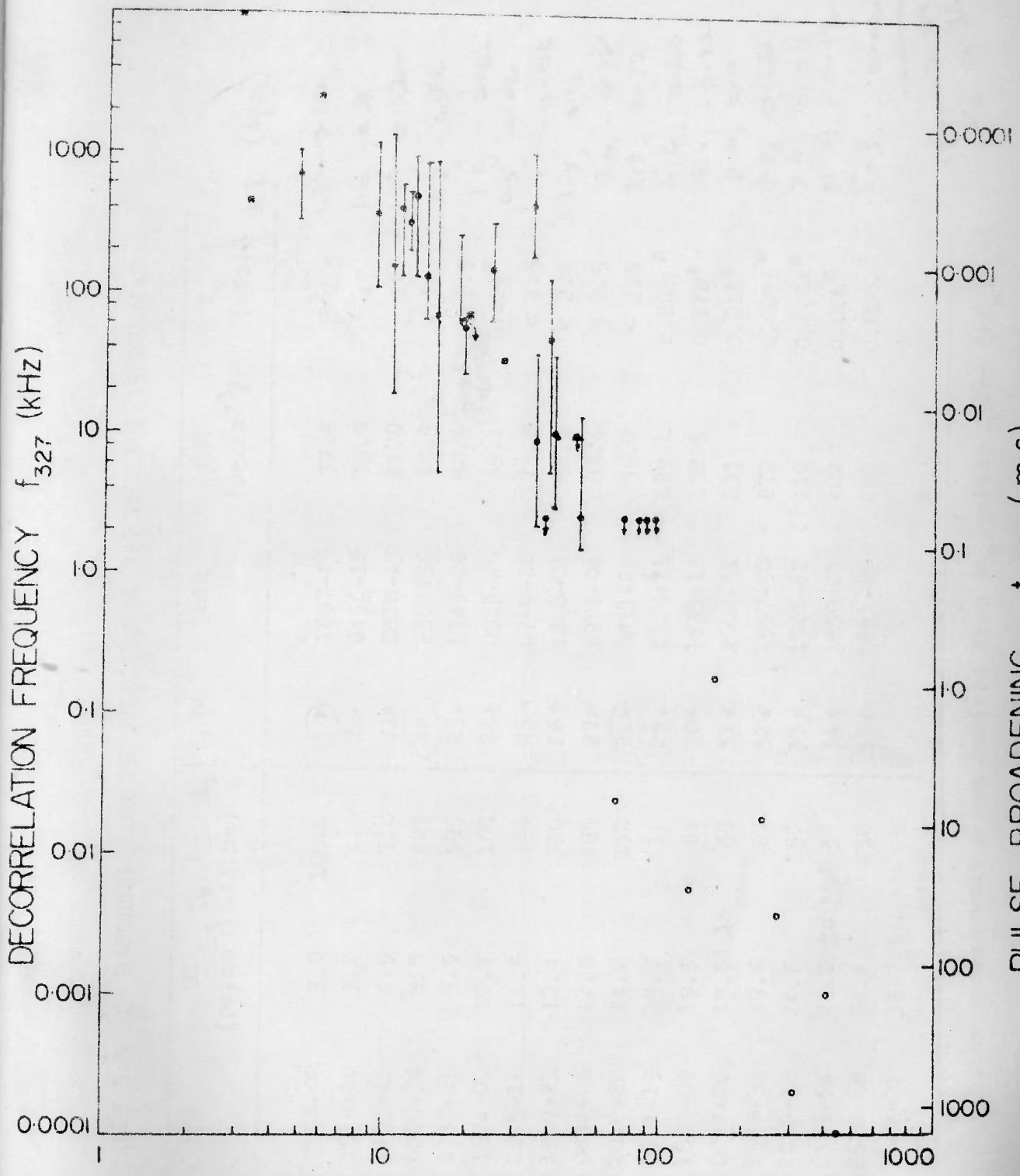

FIG.5·6 $f_\nu - \Delta t_s$ – DM DIAGRAM FOR 35 PULSARS

TABLE 5.5 : DECORRELATION FREQUENCIES AT 327 MHZ FOR 35 PULSARS

S.No.	PSR	DM ($pc.cm^{-3}$)	f_ν (kHz)	S.No.	PSR	DM ($pc.cm^{-3}$)	f_ν (kHz)
1.	0950+08	3.0	10000	19.	1857-26	37.8	< 2.5
2.	1929+10	3.2	445	20.	0450-18	39.9	47
3.	1133+16	4.9	710	21.	0818-13	41.0	10
4.	0809+74	5.8	2623	22.	2303+30	49.9	< 10
5.	1237+25	9.3	595	23.	1749-28	50.9	2.5
6.	1604-00	10.7	165	24.	0833-45	69.1	0.024*
7.	2045-16	11.5	400	25.	0740-28	73.8	< 2.5
8.	1919+21	12.4	330	26.	1818-04	84.4	< 2.5
9.	0834+06	12.9	495	27.	1911-04	89.4	< 2.5
10.	2016+28	14.2	132	28.	0611+22	96.7	< 2.5
11.	0301+19	15.7	$\simeq$ 16	29.	1946+35	129.1	0.0055*
12.	1822-09	19.3	< 66	30.	1933+16	158.5	0.188*
13.	0823+26	19.5	58	31.	2002+31	233	0.018*
14.	1508+55	19.6	67	32.	1557-50	270	0.0036*
15.	2020+28	24.6	150	33.	1323-62	310	0.0008*
16.	0329+54	26.8	33	34.	1859+03	402	0.001*
17.	0628-28	34.4	430	35.	1641-45	450	0.0001*
18.	1642-03	35.7	9				

Note: f_ν values marked with * are derived from Δt_s values using $2\pi f_\nu \Delta t_s = 1$

distance from the galactic centre, data on f_ν and Δt_s for more number of pulsars will be necessary, with the pulsars selected for observations such that they are more or less uniformly distributed over the range of galactocentric distances. Such studies could be compared with the galactic distribution of the sources of ionisation of the IS medium, such as supernova remnants and O,B stars. These investigations may lead to an understanding of the possible mechanisms which produce systematic variations in $\langle \delta N_e^2 \rangle^{\frac{1}{2}}$, L and $\langle N_e \rangle$ so as to result in the observed f_ν-DM trend.

5.7 OBSERVED RELATIONSHIP BETWEEN WIDTHS OF INTENSITY FLUCTUATION SPECTRA AND DISPERSION MEASURES

In the subsequent sections we describe the observed dependence of f_e on DM, summarising both earlier results available from published literature as well as those from the present observations. We deal with the implications of the results in Section (5.7.3).

5.7.1. Results from Earlier Work

The earliest attempt by Rickett (1970) at elucidating the dependence of time scales of pulsar scintillations did not yield very definitive results except that the characteristic time scale of scintillations tended to be larger for pulsars of lower dispersion measure. His observations at 408 MHz of 10 pulsars with DM $\leq$ 50.88 pc.cm^{-3} are summarised in Fig.(9) of his paper. The next major attempt at understanding temporal behaviour of ISS was done by Backer (1975).

He had observed 28 pulsars ($3.0 \leq DM \leq 158.5$) and computed the temporal spectra of intensity fluctuations, with degrees of freedom ranging from 1 to 50. In 25 cases low frequency components in the spectra were recognised which he ascribed to scintillation due to IS medium. Assuming ISS spectra to be Gaussian in shape and scintillation index of unity, Backer obtained e^{-1} widths f_e of the ISS components in the spectra. He found that f_e increases linearly with dispersion measure though there was a scatter by a factor of 3 in the values of f_e for comparable values of DM. One may note that the scatter could be explained by differing values of the relative velocity of the IS medium with respect to the Earth-based observer, in different regions and directions. Further, pulsars themselves have different proper motions.

5.7.2. Results from the Present Observations

Results from our observations of 23 pulsars are summarised in Fig.(5.7) which is a plot of f_e against DM. The notable difference between this plot and the corresponding one from Backer's measurements (Fig.(6) of Backer 1975) is that our measurements of f_e do not show any correlation with DM. The statistical stability of the spectra obtained by us are much better than those of Backer as could be seen by comparing the values of the quality factor Q ($Q = f_e T$ = number of degrees of freedom), for the two sets of observations. In Table (5.6) we list for comparison values of f_e for pulsars common to ours and Backer's observations. Backer's

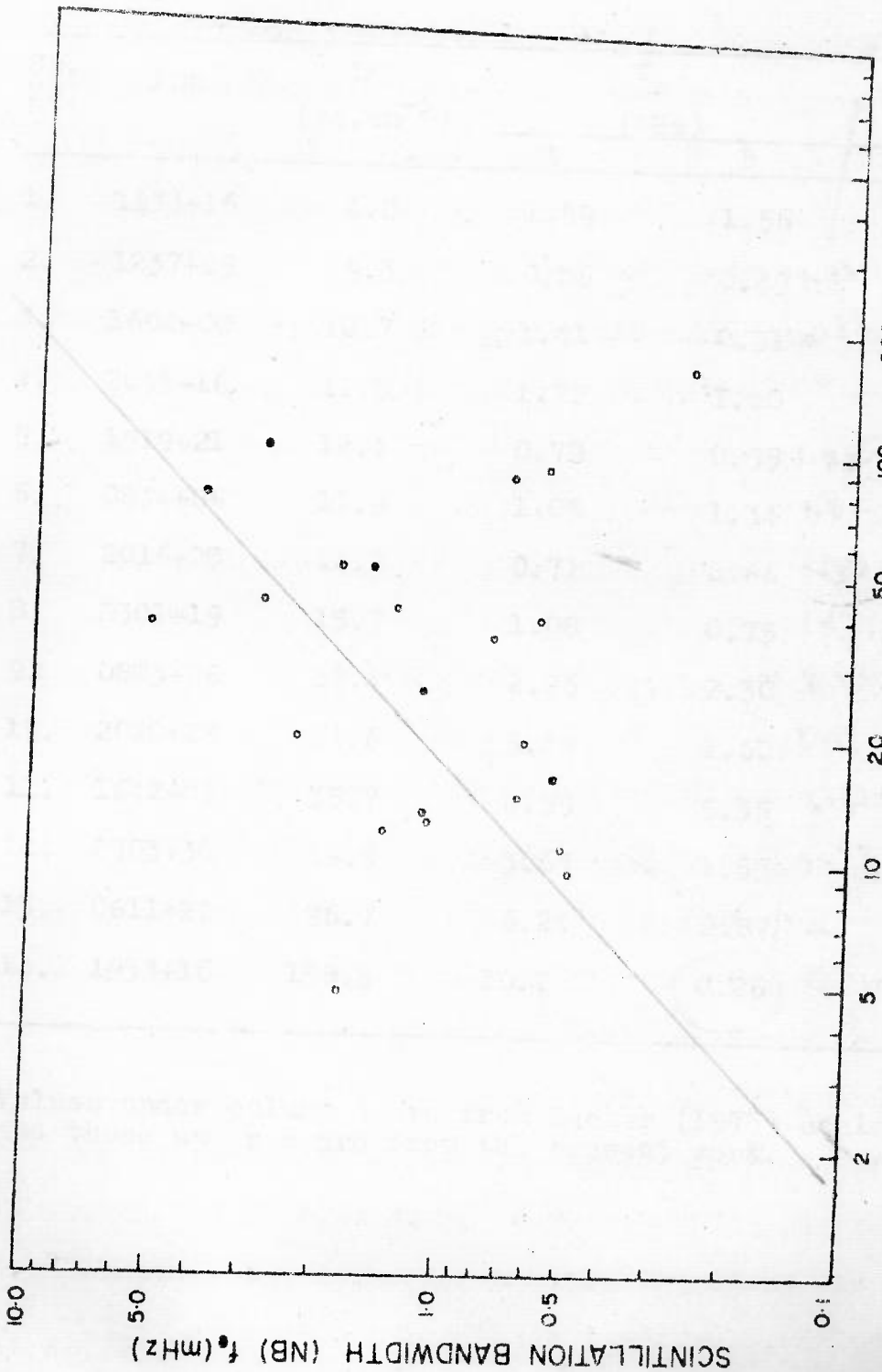

FIG. 5·7 f_e-DM DIAGRAM FROM THE PRESENT WORK

TABLE 5.6 : COMPARISON OF MEASUREMENTS OF ISS SPECTRAL WIDTHS

Sr. No.	PSR	DM ($pc.cm^{-3}$)	f_e (mHz)		Q	
			A	B	A	B
1.	1133+16	4.8	1.59	1.56	17	96
2.	1237+25	9.3	0.86	0.49	2	44
3.	1604-00	10.7	$\leq$ 1.41	0.51	1	14
4.	2045-16	11.5	1.22	1.40	11	100
5.	1919+21	12.4	0.78	0.55	7	33
6.	0834+06	12.9	1.05	1.34	6	63
7.	2016+28	14.2	0.71	0.66	16	20
8.	0301+19	15.7	1.08	0.75	10	170
9.	0823+26	19.4	2.26	2.30	30	200
10.	2020+28	24.6	3.49	1.60	3	72
11.	1642-03	35.7	4.59	5.35	48	340
12.	2303+30	49.9	3.67	1.55	1	46
13.	0611+22	96.7	6.24	2.87	24	160
14.	1933+16	158.5	10.2	0.26	3	30

Values under column A are from Backer (1975) scaled to 327 MHz and those under B are from the present work.

observations have been scaled from 408 MHz to 327 MHz assuming $f_e \propto \lambda^{-1}$. Values of Q are also listed. Q ranges from 1 to 58 for Backer's data compared with a range of 14 to 340 for our data.

5.7.3. Discussion

Theoretical models of the IS medium predict a dependence of the spatial correlation scale $\rho_{c.s.}$ on dispersion measure and wavelength of the form

$$\rho_{c.s.} \propto (DM)^{-\frac{1}{2}} \lambda^{-1} \qquad (5.2a)$$

for Gaussian spectra of irregularities, and

$$\rho_{c.s.} \propto (DM)^{-1/(\alpha-2)} \lambda^{-2/(\alpha-2)} \qquad (5.2b)$$

for power law spectra, if one makes the usual assumption of DM proportional to the pulsar distance z and $\langle \delta N_e^2 \rangle^{\frac{1}{2}} \propto \langle N_e \rangle$. A frozen-in scintillation pattern - the so called Taylor hypothesis - gives a direct relation between spatial and temporal spectra (Tatarskii 1971) through the velocity V_m of the medium with respect to the observer.

The discrepancy between the theoretical predictions embodied in equations (5.2a,b) and the observed f_e-DM plot (Fig.(5.7)) could be due to any one or all of the following reasons

i) The estimates of f_e could be confused by intrinsic variations. The evidence for the existence of such variations

has been presented in Section (5.5). This may also lead to differing values of f_e measured at different epochs, owing to variability of intrinsic fluctuations, which may partly explain difference between ours and Backer's values.

ii) The assumption of frozen pattern may not be valid as is shown by sudden reversals of the pattern velocity during spaced receiver observations (Rickett and Lang 1973; Slee et al. 1974 and Uscinski 1975).

iii) Inhomogeneity of the medium. From our discussion of the steepening of the dependence of f_ν on DM at large values of DM it is clear that the IS medium cannot be considered to be homogeneous.

iv) Further, as noted above, scatter arises due to differing values of the velocities of the medium and pulsars with respect to observer.

As pointed out by Rickett (1977) the linear dependence of f_e on DM as inferred by Backer demands $\alpha = 3$ for power law models. But, then the predicted λ dependence (for $\alpha = 3$) turns out to be $f_e \propto \lambda^2$ which is discrepant with observations of PSR 0329+54 by Rickett (1970) and that by Backer (1974) of PSR 0833-45. As in the case of the observed f_ν-DM relationship, the linear f_e-DM dependence is also at odds with both Gaussian and Kolmogorov spectral models of the IS medium.

In this connection we would like to mention that the linear f_e-DM relationship observed by Backer could be an

artifact due to the presence of intrinsic intensity variations with time scales comparable to those due to ISS. It could also arise if data lengths were not long enough so as to contain many cycles of scintillation. In such a case the statistical errors on the estimates could be very large. It may be pointed out that in Fig.(5.7) which gives our measurements of f_e, if we remove four points corresponding to DM $\gtrsim$ 80 pc.cm^{-3} and $f_e \lesssim 1$ m Hz, a linear dependence of log f_e on log(DM) could be inferred. A similar reasoning may be responsible for the observed $f_e \propto$ DM trend by Backer. It seems important to extend the measurements of f_e for high DM pulsars. This would require a multichannel receiver with several narrow bandwidths spread over a wide band so that observations with good signal to noise ratio can be made, because many of the high DM pulsars are weak.

5.8. NONUNIFORM SPATIAL DISTRIBUTION OF FLUCTUATIONS IN ELECTRON DENSITY

In the forthcoming sections we describe the method adopted to estimate the magnitude of rms fluctuations in electron density using the observed values of decorrelation frequencies, present these estimates and briefly discuss the implications of these results.

5.8.1. Estimation of ΔN and L from observed values of f_ν

From the observational determination of ISS of a pulsar one would like to calculate the values of the rms

fluctuation of electron density ΔN ($=<\delta N_e^2>^{\frac{1}{2}}$) and the scale size L of the fluctuations. The method for estimation of ΔN and L was established first by Scheuer (1968), for a thin screen model of the IS medium. It involves the use of the two conditions for strong scattering and the dependence of decorrelation frequency f_ν on the mean square scattering angle θ_s. These three conditions impose constraints on the range of permissible values of ΔN and L. Lee and Jokipii (1975c and 1976) have derived these conditions as applicable to an extended medium for both forms of spectra - Gaussian and Kolmogorov of irregularities. These constraints are given in eqns.(6), (7a), (7b), (8a), (8b), (9a) and (9b) of their paper (1976). These contraints at 327 MHz, for a Gaussian spectrum are given by:

$$\frac{(\Delta N)^2}{L} = \frac{7.5319 \times 10^{28}}{z^2 f_\nu} \qquad (5.3a)$$

$$\frac{(\Delta N)^{2/3}}{L} > \frac{1.2540 \times 10^{6}}{z} \qquad (5.3b)$$

$$(\Delta N)^2 L > \frac{4.2094 \times 10^{20}}{z} \qquad (5.3c)$$

where z is the distance, in cm., to the pulsar, L is in cm and f_ν is in Hz. These conditions are indicated by the three straight lines in the logarithmic plot of ΔN vs L in Fig.(5.8). The constraints imply that the point representing the medium must lie above lines (b) and (c), and on the line (a). The

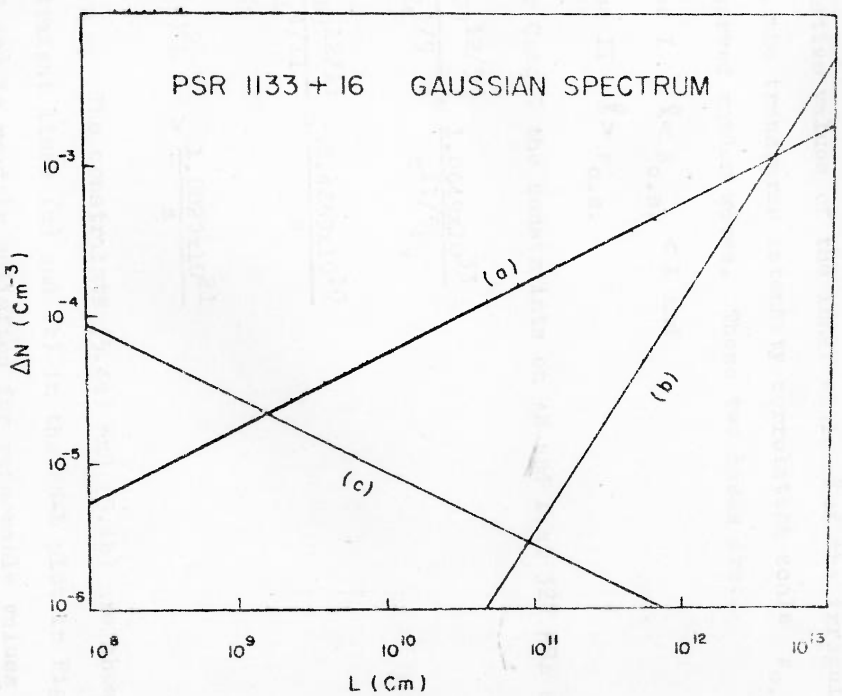

Fig.5.8 CONSTRAINTS ON ▲N AND L

segment of the line (a) between lines (b) and (c) specifies the range of permissible values of ΔN and L. Hence these values are easily evaluated.

For the extended medium with Kolmogorov spectrum of irregularities two situations are possible depending on the relative values of the inner scale ℓ of the irregularities and the transverse intensity correlation scale $\rho_{c.s.}$ of the observed random waves. These two cases are:

Case I $\ell < \rho_{c.s.} < L$ and

Case II $\ell > \rho_{c.s.}$

For Case I the constraints on ΔN and L at 327 MHz are given by

$$\frac{(\Delta N)^{12/5}}{L^{4/5}} = \frac{1.0649 \times 10^{33}}{z^{11/5} f_\nu} \qquad (5.4a)$$

$$\frac{(\Delta N)^{12/11}}{L^{4/11}} > \frac{8.4269 \times 10^{10}}{z} \qquad (5.4b)$$

$$(\Delta N)^2 L > \frac{1.0022 \times 10^{21}}{z} \qquad (5.4c)$$

The constraints (5.4a) and (5.4b) are shown by the straight lines (a) and (b) in the ΔN-L plot in Fig.(5.9). (5.4c) is readily satisfied for reasonable values of the parameters and is not shown. We note that unlike the case of the Gaussian spectrum the lines (a) and (b) are parallel implying that the condition (5.4b) has no constraint on the values of

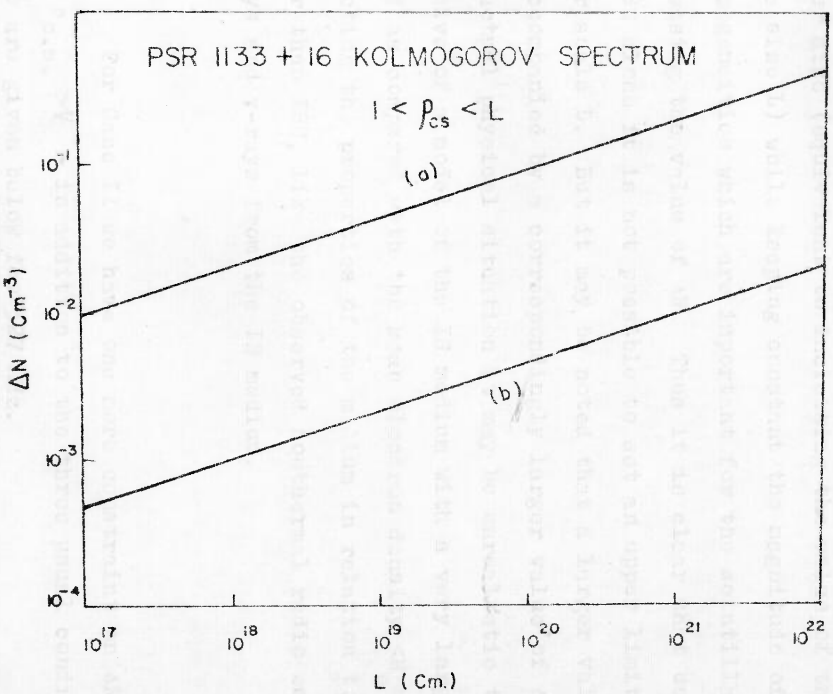

Fig.5.9 CONSTRAINTS ON ΔN AND L

ΔN and L. This is understandable from the following physical aspects: Inhomogeneities with scales much greater than the Fresnel scale $\rho_f=(z/k)^{\frac{1}{2}}$ have hardly any effect on the scintillations of radio waves. Therefore the scintillation pattern will be unaffected if one introduces inhomogeneities of larger size (equivalent to increasing the value of the largest scale size L) while keeping constant the magnitude of the i homogeneities which are important for the scintillations, by increasing the value of ΔN. Thus it is clear that using data on ISS alone it is not possible to set an upper limit on the outer scale L. But it may be noted that a larger value of L is accompanied by a correspondingly larger value of ΔN and in the actual physical situation it may be unrealistic to conceive of a model of the IS medium with a very large value of ΔN as compared with the mean electron density $\langle N_e \rangle$, without affecting the properties of the medium in relation to aspects other than ISS, like the observed nonthermal radio emission, X-rays and γ-rays from the IS medium.

For Case II we have one more constraint on ΔN and - that $\rho_{c.s.} > \ell$ - in addition to the three usual conditions. These are given below for 327 MHz.

$$\frac{(\Delta N)^2}{\ell^{1/3} L^{2/3}} = \frac{3.8662 \times 10^{28}}{z^2 f_\nu} \qquad (5.5a)$$

$$\frac{(\Delta N)^{2/3}}{\ell^{7/9} L^{2/9}} > \frac{7.2982 \times 10^{6}}{z} \qquad (5.5b)$$

$$(\Delta N)^{2} L > \frac{1.0022 \times 10^{21}}{z} \qquad (5.5c)$$

$$\frac{(\Delta N)^{2} \ell^{5/3}}{L^{2/3}} > \frac{4.3213 \times 10^{20}}{z} \qquad (5.5d)$$

The constraints embodied in eqns.((5.5a),(b),(d)) are shown by the straight lines (1a), (1b) and (1c) in Fig.(5.10) for a particular value of L and by (2a), (2b) and (2c) for a smaller value of L. The constraint in eqn.(5.5c) is well-satisfied for reasonable values of ΔN and L, and is not shown in Fig.(5.10)

5.8.2. Results Obtained from the Present Observations

In Table (5.7) we summarise the estimates of ΔN and scale sizes, for both Gaussian and Kolmogorov spectra, derived from our measurements of decorrelation frequency f_ν for 15 pulsars at 327 MHz. The distances z were taken from the table of properties of pulsars compiled by Taylor and Manchester (1975). We have assumed a value of 0.03 cm^{-3} for the mean electron density $< N_e >$. As pointed out earlier, one is unable to set a limit on the value of the outer scale of Kolmogorov type of turbulence from ISS data alone. Hence we have drawn on the work of other investigators to assign a reasonable value to the outer scale L as described below.

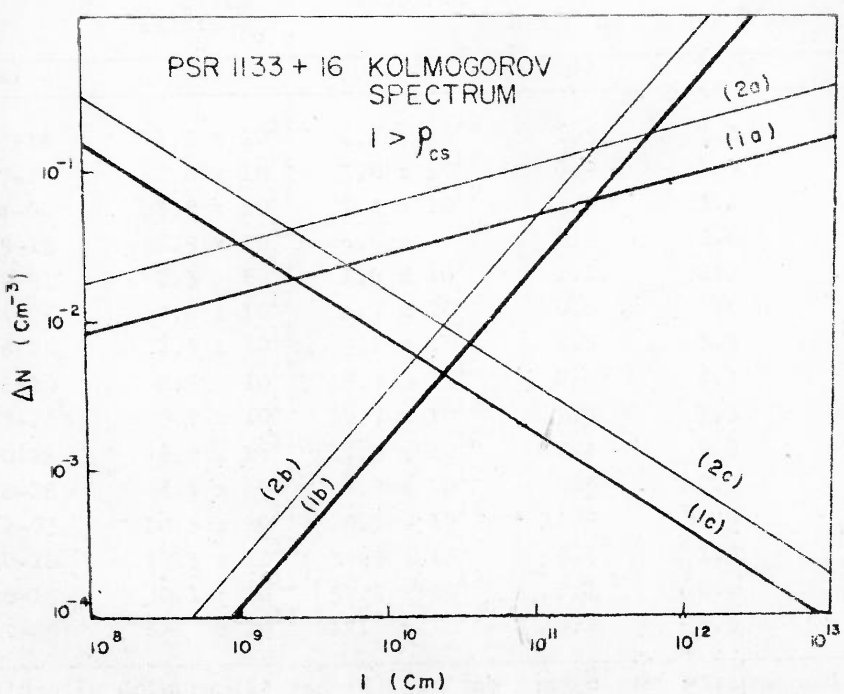

Fig. 5.10 CONSTRAINTS ON ΔN AND ℓ

TABLE 5.7 : ESTIMATES OF ΔN AND SCALE SIZES

S.No.	PSR	ℓ (cm) Kolmogorov spectrum with $\ell > \rho_{c.s}$	L(cm) Gaussian spectrum	$\Delta N/\langle N_e \rangle$ KOLMOGOROV SPECTRUM $L=10^{19}$cm	$L = 10^{20}$cm	$\Delta N/\langle N_e \rangle$ Gaussian Spectrum
	(1)	(2)	(3)	(4)	(5)	(6)
1	1133+16	1.2×10^{11}	2.4×10^{12}	1.5	3.3	0.19
2	1237+25	2.0×10^{11}	3.8×10^{12}	0.9	1.9	0.13
3	1604-00	3.8×10^{11}	7.4×10^{12}	1.6	3.4	0.31
4	2045-16	2.5×10^{11}	5.0×10^{12}	0.9	2.0	0.15
5	1919+21	2.3×10^{11}	1.7×10^{12}	1.1	2.3	0.03
6	0834+06	2.4×10^{11}	4.7×10^{12}	0.8	1.6	0.12
7	2016+28	4.7×10^{11}	9.1×10^{12}	1.5	3.3	0.32
8	0301+19	8.5×10^{11}	15.3×10^{12}	2.0	4.4	0.05
9	0823+26	9.1×10^{11}	17.7×10^{12}	1.5	3.3	0.41
10	2020+28	8.9×10^{11}	17.3×10^{12}	0.4	0.8	0.10
11	0628-28	4.4×10^{11}	8.7×10^{12}	0.3	0.7	0.06
12	1642-03	10.5×10^{11}	20.3×10^{12}	18.5	39.8	5.53
13	0450-18	17.3×10^{11}	34.5×10^{12}	0.6	1.3	0.21
14	0818-13	30.1×10^{11}	53.7×10^{12}	2.1	4.4	0.86
15	1749-28	62×10^{11}	121×10^{12}	4.1	8.9	0.23

Note: a) Values in Columns (2) and (3) are the mean of the maximum and minimum values permissible for the parameter

b) Values in Columns (4), (5) and (6) are obtained by using $\langle N_e \rangle = 0.03$ cm^{-3} and the mean value of ΔN

The importance of turbulent stochastic fluctuations in the galactic magnetic field for explaining the observed life times of cosmic rays in the Galaxy was pointed out by Jokipii and Parker (1969a,b). Subsequently Jokipii and Lerche (1969) applied this theory to explain the observed dependence on galactic latitude of Faraday rotation of extragalactic radio sources and of pulsar dispersion measures. They found that a correlation length L on the order of 250 pc ($=8\times10^{20}$cm) for the fluctuations in magnetic field and electron density, fits the observed data reasonably well and also that the fluctuations could be as large as the mean value of the quantities. Also investigations on the observed fluctuations in the polarization of starlight (Jokipii et al. 1969) yielded a value of 150 pc ($=5\times10^{20}$cm) for the correlation length of the inhomogeneities responsible for the polarization fluctuations, presumably produced by alignment of dust grains by the galactic magnetic field. It may be noted, however, that the estimated value, $\sim$ 100 pc., for the scale size of the fluctuations cannot be treated as precise, owing to the large uncertainties in the observational data on Faraday rotation and starlight polarization. We have evaluated the range of permissible values of ΔN, in the case of Kolmogorov spectrum for two values of the outer scale - $L = 10^{19}$ cm (3.2 p.c) and $L = 10^{20}$ cm (=32 p.c).

From Table (5.7) we see that the range of scale sizes estimated for a Gaussian spectrum are on the order of 10^{11} cm, similar to the estimates by Rickett (1970). The values of the ratio $\Delta N/N_e$ for the Gaussian spectrum are consistently smaller

than those for the Kolmogorov spectrum. This is because the value of ΔN in the Gaussian spectrum corresponds to the density fluctuations of only those inhomogeneities which are important in causing scintillations, unlike the case with the Kolmogorov spectrum. PSR 1642-03 stands out in Table (5.7), by its large value of ΔN. This is easily explained along the lines adopted by Lee and Jokipii (1976) to explain similar observations in the cases of the Vela and the Crab pulsars. The inference is that the line of sight to PSR 1642-03 intercepts an ionized 'thin' region with strong electron density fluctuations. This inference is confirmed by the observations of Prentice and ter Haar (1969) that the line of sight to this pulsar hits the H II region of the $O_{9.5}$ star ζ Ophiuchi.

Apart from the specific case of PSR 1642-03, the general range of values of $\Delta N/\langle N_e \rangle$ for the other pulsars is itself interesting from the aspect of the structure of the general IS medium. For a Kolmogorov spectrum of irregularities we find that the range of values of $\Delta N/\langle N_e \rangle$ is 2-3 for outer scale sizes on the order of 10^{20} cm (32 p.c.). If one were to use a value of 150 p.c. for the outer scale size - as indicated by data on Faraday rotation of extragalactic radio sources and starlight polarization - this ratio will tend to be larger than 3. Such a value, larger than unity, of the ratio of the rms to the mean of electron density fluctuations implies a highly nonuniform distribution of electrons along the line of sight to pulsars. The picture one gets of the

general IS medium is one with clumpy aggregates of electrons. It may be noted that this description of the IS medium agrees well with the clumpy distribution of H II regions, deduced from data on interstellar optical lines and other observations (Kaplan and Pikelner 1970; Spitzer 1978). It may be noted here that a Gaussian spectrum of irregularities does not lead to such large values of $\Delta N/\langle N_e \rangle$ as is the case with Kolmogorov turbulence spectra, although the assumption of Gaussian spectrum is capable of explaining the other observed features of ISS of pulsars such as CCF and scintillation indices. This is because of the fact that the Gaussian spectrum emphasises those scale sizes important to scintillation very much more than the others, unlike the Kolmogorov spectrum which incorporates effects of all scale sizes over a very large range.

CHAPTER 6

SUMMARY AND DISCUSSION

In this chapter we summarise the principal results obtained from our detailed studies of the interstellar scintillations of 33 pulsars. These results pertain to intrinsic intensity fluctuations of pulsars with time scales similar to those due to ISS, comparison of observed values of ISS parameters with predictions of theory, and estimates of rms electron density fluctuations and their scale sizes in the IS medium.

Measurements by earlier workers have shown that there is considerable scatter in the dependence on DM of the ISS parameters such as decorrelation frequency f_ν and scintillation bandwidth f_e . Also the mean trends of DM vs f_ν or f_e have not been in agreement with theoretical predictions. The aim of our studies was to investigate possible reasons for these discrepancies. We have, therefore, carried out long stretches of observations with the Ooty Radio Telescope using multichannel receivers and also made careful estimates of various observational errors on the measured values of the ISS parameters. In derivation of these parameters, especially f_ν , corrections have been made for the effects due to finite bandwidths of the receivers, using the theory of ISS by Lee and Jokipii. It may be noted that the observed intensity fluctuations of pulsars are produced by both ISS and intrinsic

causes. As intrinsic fluctuations are already known to have time scales of seconds as well as days, it is reasonable to expect that they may have time scales in the intermediate range of several minutes also. Such intrinsic intensity variations with ISS-like time scales could interfere with the accurate determination of ISS parameters and thus give rise to scatter in the values of the parameters. Hence we have attempted to detect the existence of intrinsic intensity fluctuations with ISS-like time scales.

The 33 pulsars selected for our observations are among the brightest of the 102 pulsars in the declination range of the Ooty telescope, out of the 157 pulsars which were known at that time (1976-78). The DM of the 33 pulsars are in the range $4.8 \leq DM \leq 231$ pc.cm^{-3}. Good power spectra of the intensity fluctuations were obtained for 23 of the pulsars. Useful frequency cross correlation functions for zero temporal lags (CCF) were obtained for 15 of them. The results are discussed below.

a) Intrinsic Intensity Fluctuations with ISS-like Time Scales

We have developed a method for detecting the presence of intrinsic intensity variations with time scales similar to those due to ISS. It may be noted that ISS is correlated over a narrow range of frequencies in contrast to intrinsic variations such as pulse to pulse or day to day variations which are known to be correlated over a wide bandwidth. Hence

a wide band pedestal in the CCF for zero time lag indicates the presence of intrinsic variations, but their time scales cannot be distinguished unless we determine CCF with different time lags. Our method is based on determination of variance of intensity fluctuations of ISS-like time scales for two different receiver bandwidths. The variance is found from the power spectrum over ISS-like fluctuation frequencies. The variance ratio will be proportional to the square of the ratio of the receiver bandwidths for the case of fluctuations with wide correlation bandwidths. On the other hand the variance ratio will be approximately proportional only to the ratio of the receiver bandwidths if the decorrelation frequency of the intensity fluctuations is narrower than the smaller of the two receiver bandwidths. Thus, by determining the ratio of variances for the two receiver bandwidths and comparing its value with the theoretically expected value based on measurements of ISS decorrelation frequency, we can recognize the presence of any intrinsic variations with ISS-like time scales (Sec.2.8.2))

Of the 23 pulsars for which the power spectra of intensity fluctuations were measured reliably, intrinsic variations with ISS-like time scales and comparable strength seem to be present for at least 8 and possibly for 4 more cases.

b) f_ν-DM Relationship

Decorrelation frequencies f_ν have been determined for 15 pulsars in the DM range of about 5 to 50 pc.cm^{-3}, from the observed CCF after correcting for the intrinsic variations

(using the method by Sutton (1971)), the finite bandwidth effects and instrumental characteristics following a procedure described in Chapter 4. Upper limits were obtained for 7 more pulsars in the DM range 50 to 158 pc.cm^{-3}. We have determined the rms errors for the above values.

A weighted least squares straight line fit to the plot of the observed log f_ν against log (DM) for the 23 pulsars shows a slope of at least -2.8 in the DM range 5 to 158 pc.cm^{-3}. This is appreciably steeper than the predicted slope of -2 from theoretical models of irregularities in the IS medium, in which it is assumed that $\langle \delta N_e^2 \rangle^{\frac{1}{2}} / L^{\frac{1}{2}} \propto \langle N_e \rangle$. By including estimates of f_ν derived from measurements of pulse broadening for pulsars in the DM range 3.0 - 450 pc.cm^{-3} by other workers, it is clear that the slope of the f_ν-DM plot changes continually from about -2.5 at low DM to about -4 at high DM. Earlier workers could note the steepening of the slope only in the high DM range.

A steeper-than-minus-two slope of f_ν-DM plot can be explained by assuming that the ratio $\langle \delta N_e^2 \rangle^{\frac{1}{2}} / (L^{\frac{1}{2}} \langle N_e \rangle)$ increases with DM. Since the high DM pulsars are mostly located closer to the galactic centre, this implies that either electron density fluctuations increase or scale size decreases or both vary with increasing distance from the solar system towards the central regions of our Galaxy.

Our observations showed a slight tendency to fit a Kolmogorov model of irregularities in the IS medium better

than the Gaussian model. However, as shown in Sections(4.6) and (5.3.3) statistical uncertainties on the estimates of f_ν are quite large unless stretches of tens of hours of data on intensity fluctuations are obtained. Therefore, it is difficult to distinguish between Gaussian and Kolmogorov spectra of irregularities in the IS medium using our CCF measurements obtained with data lengths of 2 to 6 hours.

c) Nonuniform Distribution of Electron Density in the IS Medium

From the definite measurements of f_ν for 15 pulsars, we have estimated the values of the rms electron density fluctuations $< \delta N_e^2 >^{\frac{1}{2}}$ under the framework of the Kolmogorov model for different values of the outer scale L. From the analysis of data on Faraday rotation of extragalactic radio sources and starlight polarization by other investigators, we note that the typical value of the scale size of the irregularities in the IS medium in our Galaxy is about 150 pc. For such values of L and mean electron density $< N_e > = 0.03$ cm^{-3}, using our measurements of f_ν for the 15 pulsars, we find that $< \delta N_e^2 >^{\frac{1}{2}} / < N_e > > 3$ for most of the pulsars. Such large values of the ratio of rms electron density deviation to the mean electron density, imply that the degree of ionisation of the IS medium along the line of sight to a pulsar is highly variable. Hence one pictures the IS medium as one with clumpy aggregates of electrons. We note that such a description of the structure of the IS medium derived from observations of ISS

of pulsars is in agreement with the results obtained from optical observations of interstellar lines.

In the specific case of PSR 1642-03 we infer from the large value of $<\delta N_e^2>^{\frac{1}{2}}/<N_e>$ derived from ISS observations that the line of sight to this pulsar passes through an ionized 'thin' region with strong electron density fluctuations. This region is identified with the H II region of the $O_{9.5}$ star ζ Ophiuchi.

The above results show the usefulness of the observations of interstellar scintillations of pulsars in probing the structure of the IS medium of our Galaxy. Particularly they show that the value of $< \delta N_e^2 >^{\frac{1}{2}}/< N_e >$ and scale size vary with galactocentric distance. Also, since information about electron density irregularities are not easily obtainable by other astrophysical observations, it is desirable to extend studies of ISS to pulsars of higher DM.

APPENDIX A

We describe below the method of theoretically estimating the variances, scintillation indices and the CCF of intensities due to ISS. The formulae which are derived below express the relevant ISS parameters as functions of the intensity response of the receiver channels and Γ_D. They are based on the theory of ISS developed by Lee and Jokipii and incorporate the effects on ISS parameters due to the finite bandwidth of the receivers.

A.1. VARIANCES AND SCINTILLATION INDICES DUE TO ISS FOR NARROW AND BROAD BANDWIDTHS OF THE 12-CHANNEL DATA

A.1.1 Case I - Narrow band data

Let $G_i(\nu)$ be the intensity response of the ith channel of the 12 channel receiver system. If $A(\nu,t)$ is the electric field at the radio frequency ν, then the intensity registered by the ith channel at time t is given by

$$\mathcal{I}_i(t) = \int_i G_i(\nu) A(\nu,t) A^*(\nu,t) d\nu \qquad \text{(A.1a)}$$

where A^* indicates the complex conjugate of A. The time-averaged mean intensity $\langle \mathcal{I}_i \rangle$ is given by

$$\langle \mathcal{I}_i \rangle = \int_i G_i(\nu) \langle A(\nu,t) A^*(\nu,t) \rangle d\nu \qquad \text{(A.1b)}$$

Pulsar emission is of a broad band nature with a spectral index of about 1. Over the 4 MHz bandwidth of the 12-channel receiver system, the mean intensity $\bar{\mathcal{I}}$ at any

Fourier component ν is independent of ν', if fluctuations caused by ISS are smoothed out by averaging over time i.e.

$$< A(\nu,t)A^{*}(\nu,t) > = < A(\nu',t)A^{*}(\nu',t) > = \bar{\vartheta} \qquad (A.2)$$

Therefore, we have

$$<\vartheta_i> = \bar{\vartheta} \int_i G_i(\nu)d\nu \qquad (A.3)$$

The mean-subtracted variance σ_i^2 of intensity fluctuations due to ISS for the ith channel is given by

$$\sigma_i^2 = <[\vartheta_i(t)-<\vartheta_i(t)>]^2> = <\vartheta_i^2(t)>-<\vartheta_i(t)>^2 \qquad (A.4)$$

We can express $<\vartheta_i^2(t)>$ as

$$<\vartheta_i^2(t)> = < \int_i G_i(\nu)A(\nu)A^{*}(\nu,t)\,d\nu \int_i G_i(\nu')A(\nu',t)A^{*}(\nu',t)d\nu' >$$

$$= \iint_{ii} G_i(\nu)G_i(\nu')<A(\nu,t)A^{*}(\nu,t)A(\nu',t)A^{*}(\nu',t)>d\nu d\nu' \qquad (A.5)$$

Now,

$$<A(\nu,t)A^{*}(\nu,t)A(\nu',t)A^{*}(\nu',t)> = \Gamma_{2,2}(|\nu-\nu'|/f_\nu)x\bar{\vartheta}^2 \qquad (A.6)$$

From eqn.(2.24) we have,

$$\Gamma_{2,2} = 1+|\Gamma_{1,1}|^2 \qquad (A.7)$$

Therefore, we get

$$\langle \vartheta_i^2(t) \rangle = \bar{\vartheta}^2 \iint_{ii} G_i(\nu) G_i(\nu') [1 + |\Gamma_{1,1}|^2] \, d\nu d\nu' \qquad (A.8)$$

It may be remembered that $\Gamma_{1,1}$ is a function of the frequency separation $|\nu - \nu'|$ only and can be expressed as a function of $(|\nu - \nu'| / f_\nu)$ where f_ν is the decorrelation frequency.

i.e. $$\Gamma_{1,1} = \Gamma_{1,1}(|\nu - \nu'| / f_\nu)$$

Hence, we can express σ_i^2 as,

$$\sigma_i^2 = \bar{\vartheta}^2 \iint_{ii} G_i(\nu) G_i(\nu') [1 + |\Gamma_{1,1}|^2] \, d\nu d\nu'$$

$$- \bar{\vartheta}^2 \iint_{ii} G_i(\nu) G_i(\nu') \, d\nu d\nu'$$

$$= \bar{\vartheta}^2 \iint_{ii} G_i(\nu) G_i(\nu') |\Gamma_{1,1}|^2 \, d\nu d\nu' \qquad (A.8)$$

From eqn.(2.18) $\Gamma_{1,1} = \Gamma_R \Gamma_D$. But in the above formulae $\Gamma_{1,1}$ can be replaced by Γ_D, as explained in Section(2.3.1), because the refraction effect due to Γ_R is negligible for observations lasting several hours only.

Therefore, we have

$$\sigma_i^2 = \bar{\vartheta}^2 \iint_{ii} G_i(\nu) G_i(\nu') |\Gamma_D|^2 \, d\nu d\nu' \qquad (A.9)$$

The scintillation index m_i for the ith channel is given by

$$m_i^2 = \sigma_i^2 / \langle \vartheta_i \rangle^2$$

i.e.
$$m_i^2 = \frac{\iint_{ii} G_i(\nu) G_i(\nu') |\Gamma_D|^2 d\nu d\nu'}{\iint_{ii} G_i(\nu) G_i(\nu') d\nu d\nu'} \qquad (A.10)$$

A.1.2. Case II - Broad band data, obtained by combining the intensities in all the 12 channels

The intensity $\vartheta_B(t)$ obtained by combining the intensities in all the 12 narrow band channels can be written as

$$\vartheta_B(t) = \sum_{i=1}^{12} \vartheta_i(t) \qquad (A.11)$$

The mean-subtracted variance σ_B^2 of the intensity fluctuations caused by ISS, for the broad band data, can be derived by proceeding along lines similar to those in Section (A.1.1) and is given by,

$$\sigma_B^2 = \vartheta^2 \sum_{i=1}^{12} \sum_{j=1}^{12} \left[\iint_{ij} G_i(\nu) G_j(\nu') |\Gamma_D|^2 d\nu d\nu' \right] \qquad (A.12)$$

Similarly, the scintillation index m_M for the broad band data can be expressed by

$$m_M^2 = \frac{\sum_{i=1}^{12} \sum_{j=1}^{12} \left[\iint_{ij} G_i(\nu) G_j(\nu') |\Gamma_D|^2 d\nu d\nu' \right]}{\sum_{i=1}^{12} \sum_{j=1}^{12} G_i(\nu) G_j(\nu') d\nu d\nu'} \qquad (A.13)$$

From eqns.(A.9) and (A.12) we can compute the value of the parameter R_c (Section (2.8.2)) which is the ratio of the scintillation variance in the broad band to the sum of the scintillation variances in all the 12 channels i.e. R_c is given by,

$$R_c = \frac{\sigma_B^2}{\sum_{i=1}^{12} \sigma_i^2} = \frac{\sum_{i=1}^{12}\sum_{j=1}^{12} \left[\iint_{ij} G_i(\nu) G_j(\nu') \left|\Gamma_D\right|^2 d\nu d\nu'\right]}{\sum_{i=1}^{12} \left[\iint_{ii} G_i(\nu) G_i(\nu') \left|\Gamma_D\right|^2 d\nu d\nu'\right]} \qquad (A.14)$$

A.2 THE CROSS CORRELATION Γ_{ij} OF INTENSITY FLUCTUATIONS DUE TO ISS IN THE iTH AND jTH CHANNELS

Γ_{ij} is defined by

$$\Gamma_{ij} = \frac{\langle [\vartheta_i(t) - \langle \vartheta_i(t) \rangle][\vartheta_j(t) - \langle \vartheta_j(t) \rangle] \rangle}{\sigma_i \sigma_j} \qquad (A.15a)$$

$$\text{i.e.} \quad \Gamma_{ij} = \frac{\langle \vartheta_i(t)\vartheta_j(t) \rangle - \langle \vartheta_i(t) \rangle \langle \vartheta_j(t) \rangle}{\sigma_i \sigma_j} \qquad (A.15b)$$

Now, $$\vartheta_i(t) = \int_i G_i(\nu) A(\nu,t) A^*(\nu,t) d\nu$$

and $$\vartheta_j(t) = \int_i G_i(\nu') A(\nu',t) A^*(\nu',t) d\nu'$$

Therefore, we have

$$\langle \vartheta_i(t)\vartheta_j(t) \rangle = \iint_{ij} G_i(\nu) G_j(\nu) \langle A(\nu,t) A^*(\nu,t) A(\nu',t) A^*(\nu',t) \rangle d\nu d\nu'$$

$$= \bar{\vartheta}^2 \iint_{ij} G_i(\nu) G_j(\nu') \left[1 + \left|\Gamma_D\right|^2\right] d\nu d\nu' \qquad (A.16a)$$

Also, we have

$$\langle \vartheta_i(t) \rangle \langle \vartheta_j(t) \rangle = \bar{\vartheta}^2 \iint_{ij} G_i(\nu) G_j(\nu') d\nu d\nu' \qquad \text{(A.16b)}$$

Therefore Γ_{ij} can be written as

$$\Gamma_{ij} = \frac{\iint_{ij} G_i(\nu) G_j(\nu') |\Gamma_D|^2 d\nu d\nu'}{\left[\iint_{ii} G_i(\nu) G_i(\nu') |\Gamma_D|^2 d\nu d\nu'\right]^{\frac{1}{2}} \left[\iint_{jj} G_j(\nu) G_j(\nu') |\Gamma_D|^2 d\nu d\nu'\right]^{\frac{1}{2}}} \qquad \text{(A.17)}$$

It may be noted that the above formulae take into account the partial overlap of the intensity response of the different receiver channels also. For example, we can compute values of Γ_{ijOFF} which is the cross correlation of OFFPULSE intensities between the ith and the jth channels i.e. the correlation of receiver noise between the channels. For this purpose we use eqn.(A.17) with $|\Gamma_D|^2 = \delta_{\nu\nu'}$ where $\delta_{\nu\nu'}$ is Kronecker's delta function, i.e.

$$\delta_{\nu\nu'} = 1 \text{ if } \nu = \nu'$$

$$= 0 \text{ if } \nu \neq \nu'$$

Values of Γ_{ijOFF} were computed by us using this method for the various receiver channels and they were found to agree with the values determined from observations, which are given in Table (3.1).

APPENDIX B

ESTIMATION OF THE CORRECTION FACTOR a

As described in Chapter 3, each of the pair of ONPULSE and OFFPULSE data points obtained from PULSCINT condensation are the result of summation of consecutive k number of samples over the pulsar pulse and ℓ consecutive samples over the off-pulse receiver noise, k and ℓ are not equal, in general. When $k \neq \ell$ comparison of the fluctuation power at different frequencies of the ONPULSE and OFFPULSE power spectra is possible only if the OFFPULSE spectral power (or variance) is multiplied by a factor 'a'. The correction factor 'a' is a function of the R-C time constant τ of the receiver, the sampling interval t and the parameters k and ℓ. We derive below an expression for 'a' in terms of the above parameters.

Let n(t') be the receiver noise output at the instant of time t' for $\tau=0$. In this case the outputs at different instants will be independent of one another, i.e.

$$< n(t')\ n(t'+\ell t) > = 0 \text{ for } \ell \neq 0 \qquad \text{(B.1)}$$

If s is the variance of the fluctuations obtained from a sequence of data points, then s is independent of the value of ℓ for $\tau = 0$.

If $\tau \neq 0$ then each of the samples would contain contributions from the samples at earlier instants. For $\tau > t$ we can express the ith sample $n_i'(t')$ at the instant t' by the

approximate relation

$$n_i' = n_i + n_{i-1}\, e^{-t/\tau} + n_{i-2}\, e^{-2t/\tau} + \ldots\ldots\ldots\ldots \qquad (B.2)$$

If ℓ number of consecutive samples of the receiver noise were added to yield a data point, the variance s obtained from a sequence of such data points is given by

$$s_\ell = \left\langle \left[\sum_{i=1}^{\ell} n_i' \right]^2 \right\rangle = \left\langle \sum_{i=1}^{\ell} \sum_{j=1}^{\ell} n_i'\, n_j' \right\rangle \qquad (B.3)$$

Substituting for n_i' and n_j' in terms of n_i, n_{i-1}, ... from eqn.(B.2) and by using the relationship (B.1) we can write,

$$s_\ell = s\left[\ell + 2(\ell-1)e^{-t/\tau} + 2(\ell-2)e^{-2t/\tau} + \ldots\ldots\ldots + 2e^{-(\ell-1)t/\tau}\right] \qquad (B.4)$$

For k number of consecutive ONPULSE samples added to get an ONPULSE data point, the OFFPULSE variance to be used for comparison with the ONPULSE variance is s_k . s_k is given by

$$s_k = s\left[k + 2(k-1)e^{-t/\tau} + 2(k-2)e^{-2t/\tau} + \ldots\ldots\ldots + 2e^{-(k-1)t/\tau}\right] \qquad (B.5)$$

Therefore we can write $s_k = a\, s$ where a is given by

$$a = \frac{k + 2(k-1)e^{-t/\tau} + 2(k-2)e^{-2t/\tau} + \ldots\ldots\ldots + 2e^{-(k-1)t/\tau}}{\ell + 2(\ell-1)e^{-t/\tau} + 2(\ell-2)e^{-2/\tau} + \ldots\ldots\ldots + 2e^{-(\ell-1)t/\tau}} \qquad (B.6)$$

LIST OF REFERENCES

Ables,J.G., Komesaroff,M.M. and Hamilton,P.A., 1970, Astrophys. Lett., 6, 147.

Armstrong,J.W., Spangler,S.R. and Hardee,P.E., 1977, Astron.J., 82, 785.

Backer,D.C., 1970a, Nature, 228, 42.

Backer,D.C., 1970b, Nature, 228, 1297.

Backer,D.C., 1974, Astrophys. J., 190, 667.

Backer,D.C., 1975, Astron. Astrophys., 43, 395.

Backer,D.C., Rankin,J.M. and Campbell,D.B., 1975, Astrophys.J., 197, 481.

Bevington,P.R., 1969, Data Reduction and Error Analysis for the Physical Sciences, McGraw-Hill Book Co., N.Y.

Blackman,R.B. and Tukey,J.W., 1959, Measurement of Power Spectra, Dover Publications, N.Y.

Brown Jr.,W.P., 1972a, J. Opt. Soc. Amer., 62, 45.

Brown Jr.,W.P., 1972b, J. Opt. Soc. Amer., 62, 966.

Cohen,M.H., 1969, Ann. Rev. Astron. Astrophys., 7, 619.

Coles,W.A., Rickett,B.J. and Rumsey,V.H., 1974, Solar Wind, Proc. Asilomar.Conf., Calif.

Condon,J.J. and Backer,D.C., 1975, Astrophys. J., 197, 31.

Cronyn,W.M., 1970, Science, 168, 1453.

Damashek,M., Taylor,J.H. and Hulse,R.A., 1978, Astrophys.J(Letters), 225, L31.

Davies,J.G., Lyne,A.G. and Seiradakis,J.H., 1972, Nature, 240, 229.

Drake,F.D. and Craft Jr., H.D., 1968, Nature, 220, 231.

Ewing,M.S., Batchelor,R.A., Friefeld,R.D., Price,R.M. and Staelin,D.H., 1970, Astrophys. J. (Letters), 162,L169.

Galt,J. and Lyne,A.G., 1972, Mon. Not. R. astr. Soc., 158, 281.

Gurvich,A.S. and Tatarskii,V.H., 1975, Rad. Sci., 10, 3.

Hanbury Brown,R., 1974, The Intensity Interferometer, Taylor and Francis Ltd., London.

Hueguenin,G.R., Taylor,J.H. and Troland,T.H., 1970, Astrophys. J, 162, 727.

Isaacman,R. and Rankin,J.M., 1977, Astrophys.J., 214, 214.

Johnson,N.L. and Kotz,S., 1970, Cointinuous Univariate Distributions-2, Houghton Mifflin Co., Boston

Jokipii,J.R. and Parker,E.N., 1969a, Astrophys.J., 155, 777.

Jokipii,J.R. and Parker,E.N., 1969b, Astrophys.J., 155, 799.

Jokipii,J.R. and Lerche,I., 1969, Astrophys.J., 157, 1137.

Jokipii,J.R., Lerche,I. and Schommer,R.A., 1969, Astrophys.J. (Letters), 157, L119.

Jokipii,J.R., 1973, Ann. Rev. Astron. Astrophys., 11, 1.

Kapahi,V.K., Damle,S.H., Balasubramanian,V. and Swarup,G.,1975, J. Inst. Elec. Telecom. Engg., 21, 117.

Kaplan,S.A. and Pikelner,S.B., 1970, The Interstellar Medium, Harward University Press, Mass.

Lang,K.R., Astrophys.J. Letters), 158, L175.

Lang,K.R. and Rickett,B.J., 1970, Nature, 225, 528.

Lang,K.R., 1971a, Astrophys. J., 164, 249.

Lang,K.R., 1971b, Astrophys. Letters, 7, 175.

Lee, L.C., 1974, J. Math. Phys., 15, 1431.

Lee, L.C., 1976, Astrophys. J., 206, 744.

Lee, L.C. and Jokipii,J.R., 1975a, Astrophys. J., 196, 695.

Lee, L.C. and Jokipii,J.R., 1975b, Astrophys. J., 201, 532.

Lee, L.C. and Jokipii,J.R., 1975c, Astrophys. J., 202, 439.

Lee, L.C. and Jokipii,J.R., 1976, Astrophys. J., 206, 735.

Little,L.T., 1968, Plan. Space Sci.,16, 749.

Little,L.T., 1976, Methods of Experimental Physics, 12, Part C, 118.

Lyne,A.G., 1971, Mon. Not. R. astr. Soc., 153, 27P

Lyne,A.G. and Rickett,B.J., 1968a, Nature, 218, 326.

Lyne,A.G. and Rickett,B.J., 1968b, Nature, 219, 1339.

Lyne,A.G. and Smith,F.G., 1972, Mon. Not. R. astr. Soc.157,15P

Manchester,R.N., Lyne,A.G., Taylor,J.H., Durdin,J.M., Large,M.I. and Little,A.G., 1978, Mon. Not. R. astr. Soc.,185, 409.

McLean,A.I.O., 1973, Mon. Not. R. astr. Soc., 165, 133.

Mutel,R.L., Broderick,J.J., Carr,T.D., Lynch,M., Desch,M., Warnock,W.W. and Klemperer,W.K., 1974, Astrophys.J., 193, 279.

Otnes,R.K. and Enochson,L., 1972, Digital Time Series Analysis John Wiley and Sons Inc., N.Y.

Prentice,A.J.R. and ter Haar,D., 1969, Mon. Not. R. astr. Soc., 146, 423.

Rankin,J.M., Comella,J.M., Craft,H.D., Richards,D.W., Campbell, D.B. and Counselmann,C.C., 1970, Astron.Astrophys.4,357.

Ratcliffe,J.A., 1956, Rep. Prog. Phys., 19, 188.

Readhead,A.C.S. and Hewish,A., 1972, Nature, 236, 440

Rickett,B.J., 1969, Nature 221, 158.

Rickett,B.J., 1970, Mon. Not. R. astr. Soc., 150, 67.

Rickett,B.J., 1977, Ann.Rev. Astr. Astrophys., 15, 479.

Rickett,B.J. and Lang,K.R., 1973, Astrophys. J., 185, 945.

Salpeter,E.E., 1967, Astrophys. J., 147, 433.

Salpeter,E.E., 1969, Nature, 221, 31.

Sarma,N.V.G., Joshi,M.N. and Ananthakrishnan,S., 1975a, J. Inst. Elec. Telecom. Engg., 21, 107.

Sarma,N.V.G., Joshi,M.N., Bagri,D.S. and Ananthakrishnan,S., 1975b, J. Inst. Elec. Telecom. Engg., 21, 110.

Scheuer,P.A.G., 1968, Nature, 218, 920.

Sethia,G., Chandra,H., Deshpande,M.R. and Rastogi,R.G., 1978, Ind. J. Rad. Space. Phys., 7, 153.

Slee,O.B., Ables,J.G., Batchelor,R.A., Krishnamohan,S., Venugopal,V.R. and Swarup,G., 1974, Mon. Not. R. astr. Soc., 167, 31.

Spitzer Jr.,L., 1978, Physical Processes in the Interstellar Medium, John Wiley and Sons, N.Y.

Staelin,D.H. and Sutton,J.M., 1970, Nature, 226, 69.

Sutton,J.M., 1971, Mon. Not. R. astr. Soc., 155, 51.

Sutton,J.M., Staelin,D.H., Price,R.M., Weimar,R., 1970, Astrophys. J. (Letters), 159,L89.

Swarup,G., Sarma,N.V.G., Joshi,M.N., Kapahi,V.K., Bagri,D.S., Damle,S.H., Ananthakrishnan,S., Balasubramanian,V., Bhave,S.S. and Sinha,R.P., 1971, Nature Phys. Sci., 230, 185.

Tatarskii,V.I., 1971, The Effects of the Turbulent Atmosphere on Wave Propagation, NTIS, Springfield.

Taylor,J.H. and Manchester,R.N., 1975, Astron. J., 80, 794.

Uscinski,B.J., 1968a, Phil. Trans. R. Soc., A262, 609.

Uscinski,B.J., 1968b, Proc. R. Soc., A307, 471.

Uscinski,B.J., 1975, Mon. Not. R. astr. Soc., 172, 117.

Wolszczan,A., Hesse,K.H. and Sieber,W., 1974, Astron. Astrophys. 37, 285.